Investigating the Contribution of Iron Acquisition to *Serratia marcescens* Pathogenesis during Bloodstream Infection

by

Danelle Rae Weakland

A dissertation submitted in partial fulfillment
of the requirements for the degree of
Doctor of Philosophy
(Microbiology and Immunology)
in the University of Michigan
2020

Doctoral Committee:

Frederick G. Novy Professor Harry L. T. Mobley, Chair
Assistant Professor Christopher Alteri
Associate Professor Michael Bachman
Professor Philip Hanna
Associate Professor Nicole Koropatkin

Danelle Weakland

danraewe@umich.edu

ORCID iD: 0000-0002-2245-1385

Dedication

This dissertation is dedicated to me—may this degree open the doors leading to the career I've been dreaming of.

And to my parents, who believe in me more than I believe in myself.

Acknowledgements

I first acknowledge my advisor, Dr. Harry Mobley for providing not only the resources, tools, and space that have set up my success, but also a positive environment and optimistic outlook. I thank my undergraduate research advisor, Dr. Andy Stephenson, for igniting my scientific curiosity. I also acknowledge my thesis committee, Dr. Chris Alteri, Dr. Nicole Koropatkin, Dr. Phil Hanna, and Dr. Mike Bachman, for the thoughtful scientific discussions and guidance.

I must especially thank Chris Alteri for all of his input regarding my project and for the hours-long discussions on not just science, but also life. Thank you, Chris, for the encouragement and reassurance. You were instrumental to this process.

I'd like to thank all of the Mobley lab members who I've had the pleasure to work with during my graduate studies—you all made the lab an enjoyable place to spend these five years. I'd especially like to acknowledge Sara Smith, Dr. Anna Sintsova, Dr. Laura Mike, Stephanie Himpsl, and Dr. Melanie Pearson. I also thank my collaborator, Dr. Ashu Tripathi for his contribution to my research.

I thank the Cellular Biotechnology Training Program (CBTP) for partially funding the work presented here and for giving me exposure to non-traditional career paths that I am excited to pursue.

I thank the wonderful people of the Infectious Disease department at Genentech where I completed my CBTP internship in 2018. I thank my manager, Dr. Peter Smith, who took a chance on a young graduate student and taught me how to be a better scientist. This opportunity was truly transformative to my professional development and no doubt my future career, and for that I am very grateful.

I've met some truly amazing friends in graduate school who have supported me and contributed significantly to my personal happiness throughout this process. They include: Dr. Hayley Warsinske, Dr. Courtney Luterbach, Dr. Matt Foley, Dr. Zack Abbott, Dr. Travis Kochan, and Sadie Marlow.

I also want to especially thank Dr. Arwen Frick Cheng, Dr. Allyson Shea, and Dr. Jay Vornhagen who are not only superb scientists but fantastic people. They have selflessly lent scientific support but, more importantly, been incredible friends to me. I can't thank them enough for what they've done to help me.

Finally, I lovingly thank my family—Mom, Dad, Devin, and Thomas. I struggle to find the words to express my gratitude for the encouragement and love they have given me. Mom, Dad—thank you for all of the sacrifices you've made, the countless pep-talks, and for always reminding me of what I'm capable of.

Table of Contents

List of Tables

List of Figures

List of Appendices

Abstract

Although largely considered an environmental pathogen given its ability to infect insects and survive in nature, *Serratia marcescens* is an important cause of multi-drug resistant bloodstream infections with increasing prevalence. With its current status as an emerging pathogen, little is known about factors contributing to *S. marcescens* infection specifically regarding those that aid in iron acquisition. Iron uptake is well established in the field as being crucial for bacterial colonization and pathogenesis since it is an essential protein co-factor in many cellular functions. However, mammalian hosts tightly regulate iron, making it difficult for pathogens to access. Therefore, bacteria employ specialized systems to gather iron, including the use of siderophores, heme uptake, ferrous iron receptors, and others. The overarching goal of this dissertation was to comprehensively characterize the iron-uptake systems in a bloodstream isolate of *S. marcescens,* UMH9. In Chapter II, iron-depleted RNA-sequencing was used to identify all the genes regulated by iron concentration in UMH9. Through these experiments, I identified seven independent iron acquisition systems, including two siderophore loci and two previously described heme uptake systems. Seven additional orphan transporters were also identified. Further studies in this dissertation focused on characterizing the siderophore and heme uptake loci.

In Chapters III and IV, I describe my work characterizing the two siderophore systems, *cbs* and *sch*, identified by RNA-seq in UMH9 and named after previously described siderophore loci to which they have similarity. In Chapter III, deletions were made in the non-ribosomal

peptide synthetase (NRPS) machinery in each siderophore locus as well as together in a double mutant. *In vitro* growth in iron-poor conditions revealed that the double NRPS mutant in both siderophore loci had defective growth, but still produced siderophore by chrome azurol S (CAS) and mass spectrometry. The single NRPS mutants behaved similarly to the wild type strain, suggesting that the deleted NRPS genes potentially have redundant roles in siderophore transport. These findings challenge the traditional exclusive role of NRPSs in siderophore biosynthesis. Chapter IV examines the siderophores from a pathogenesis perspective. Mutations were made deleting the entire siderophore loci individually and in combination. Mutants lacking the full *sch* locus lost their ability to chelate iron as quantified by the CAS assay, while the *cbs* single mutant retained wild-type activity. Using mass spectrometry, the chelating siderophore was found to be serratiochelin (*sch*) while the other was chrysobactin (*cbs*). *Sch*-mutants had defective growth in iron-limited conditions and deletion of the *sch* gene cluster resulted in attenuation of UMH9 in the mouse bacteria model. Therefore, serratiochelin is necessary for full virulence during bloodstream infection. Chapter V examines the *S. marcescens* heme uptake systems, *hem* and *has*. Deletion mutants were made in each system individually and together in a double mutant. Growth conditions supplemented with heme revealed that mutants with intact *hem* system experienced an abnormally long lag phase before reaching exponential growth and saturation. This suggests that the *hem* system may contribute to heme toxicity. Whole genome sequencing revealed new insights into potential heme detoxification mechanisms. Interestingly, the double heme uptake mutant did not display any *in vivo* fitness defects or attenuation, suggesting a nonsignificant contribution of heme uptake to UMH9 pathogenesis during bacteremia. Altogether, these studies provide an in-depth characterization of two major classes of iron acquisition, siderophore and heme uptake, and their contribution to pathogenesis in *Serratia*

marcescens. This work challenges canonical understandings of Gram-negative iron acquisition and provides new insights into the virulence of emerging pathogens.

Chapter I

An Introduction to Bacterial Iron Acquisition and *Serratia marcescens*

Notes. A portion of this chapter was published in the Encyclopedia of Microbiology:

Weakland DR, and Hammer ND. Bacterial Iron Acquisition Strategies. Editor: Thomas M. Schmidt, *Encyclopedia of Microbiology,* Ed. 4. Academic Press-Elsevier, 2019, Pg. 410-417.

This chapter provides a review of the literature describing what is known in the field of bacterial iron acquisition more generally pertaining to Gram-negative microbes, and then specifically focusing on iron systems in *Serratia marcescens*, the bacterium of interest for the remainder of this dissertation excluding Appendix C.

Iron: why it's important

Iron is a fundamental building block for life. The dynamic oxidation states of this transition metal are required for the catalysis of many essential biochemical reactions. Consistent with this, iron typically exists in the ferric (+3) state or ferrous (+2) oxidation states. However, the ease with which iron transitions between these oxidation states and its low solubility at neutral pH are two problems organisms must solve. The solution is to complex iron within cofactors or bound to proteins. Thus, this highly reactive atom is rarely "freely" available to react

with sensitive molecules within organisms. Iron-containing cofactors and proteins allow cells to harness the chemical dynamism of iron without the associated toxicity or insolubility. Numerous chemical reactions involved in central metabolism, nucleotide synthesis, and the detoxification of reactive oxygen and nitrogen species are catalyzed by enzymes that contain one or more iron atom, highlighting the essentiality of iron to cellular physiology.

In eukaryotes, an additional benefit of maintaining low levels of "free" iron is the challenge that the limitation imposes on invading bacterial pathogens. Most pathogens, like their hosts, require iron to perform essential biochemical reactions, but pathogens are completely dependent on sources of iron present within the host environment to fulfill this requirement. The host exploits this requirement and utilizes multiple mechanisms to impede pathogen iron procurement. The process of inhibiting the proliferation of invading bacteria by obstructing access to essential nutrients, such as iron, is called "nutritional immunity" [1, 2]. To overcome nutritional immunity, bacterial pathogens have evolved sophisticated systems to procure iron from the host environment.

Iron sources in the host

Low solubility at physiological pH and a high propensity for oxidation necessitates that iron be complexed to another molecule. Numerous, iron-binding molecules present in the host achieve this goal. In vertebrates, iron is predominantly bound to proteins or the tetrapyrrole heme. Iron-binding and heme-binding proteins also function to impair the availability of iron from invading pathogens. Additionally, iron is principally contained within host cells, further obstructing the accessibility of this metal to invading pathogens. Extracellular iron is bound by high-affinity iron-binding proteins such as ferritin, transferrin, and lactoferrin [3]. Extracellular

heme is sequestered by hemopexin [4]. Together, these mechanisms of iron sequestration ensure that the host environment is a "free" iron-deplete environment. These iron-binding proteins act as additional barriers to pathogen iron acquisition. However, pathogens have evolved elegant systems to extract iron from these proteins.

The most abundant iron-containing molecule in vertebrates is the tetrapyrrole heme. Consequently, many pathogens encode heme acquisition systems to steal heme-iron from the host. Heme is predominantly complexed to the protein, hemoglobin within erythrocytes. In this context, heme functions to transport oxygen to, and carbon dioxide away from host tissues. Consistent with this, erythrocyte lysis is a virulence trait associated with many bacterial pathogens, and this trait functions to liberate a great deal of iron in the form of heme-bound hemoglobin [5]. However, through the Fenton reaction, iron can yield highly reactive hydroxyl radicals, which are toxic at high concentrations; therefore, the systems that function to scavenge iron or heme from the host environment are under strict transcriptional control. As such, pathogens express iron acquisition systems only when the cell resides within iron depleted environments. In most bacteria this transcriptional control is achieved by the **f**erric **u**ptake **r**egulator Fur (Figure 1.1) [6].

Transcriptional control of iron acquisition systems

Despite the abundance of iron within vertebrates, iron-binding proteins and the vast intracellular reservoirs are not readily available to invading pathogens. Therefore, upon breach of protective barriers and invasion into tissues the pathogen enters an iron-deplete environment. Concomitantly, the microbial invaders upregulate genes encoding iron acquisition systems. Fur (monomer molecular weight: 17-21 kDa) is the master transcriptional regulator of iron

acquisition systems and Fur-dependent transcriptional control is achieved via a canonical mechanism of repression (Figure 1.1) [7]. Within the bacterial cytoplasm, Fur dimerizes and binds excess iron. It then represses the expression of iron acquisition systems. Repression of target transcripts is mediated by the high affinity of ferric iron-bound Fur for consensus DNA sequences present within the promoter sequences of genes encoding iron acquisition systems. Fur binding blocks RNA polymerase, resulting in transcriptional repression. When iron becomes limiting, the amount of intracellular iron decreases. This causes the release of iron from Fur and the DNA-binding affinity of Fur for the consensus sequence is significantly reduced [8]. Consequently, the freed target promoter is accessible to RNA polymerase that in turn transcribes iron acquisition genes. Fur is conserved in Gram-negative pathogens, and locating the Fur consensus sequences within bacterial genomes has led to the identification of many of the iron acquisition systems discussed below [6]. The importance of this transcriptional regulator is demonstrated by the profound virulence defects of *fur* mutants [9-12]. Additionally, Fur activity ensures that iron acquisition systems are expressed exclusively in iron-depleted environments. Unregulated expression of these systems is energetically costly to the bacterium in iron-replete conditions when iron import is not needed. Constitutive import of iron is also detrimental to bacterial cells as excessively high levels of iron can lead to production of damaging reactive oxygen species through the Fenton reaction. Therefore, while iron is crucial to bacterial survival, regulation of these systems is equally as important.

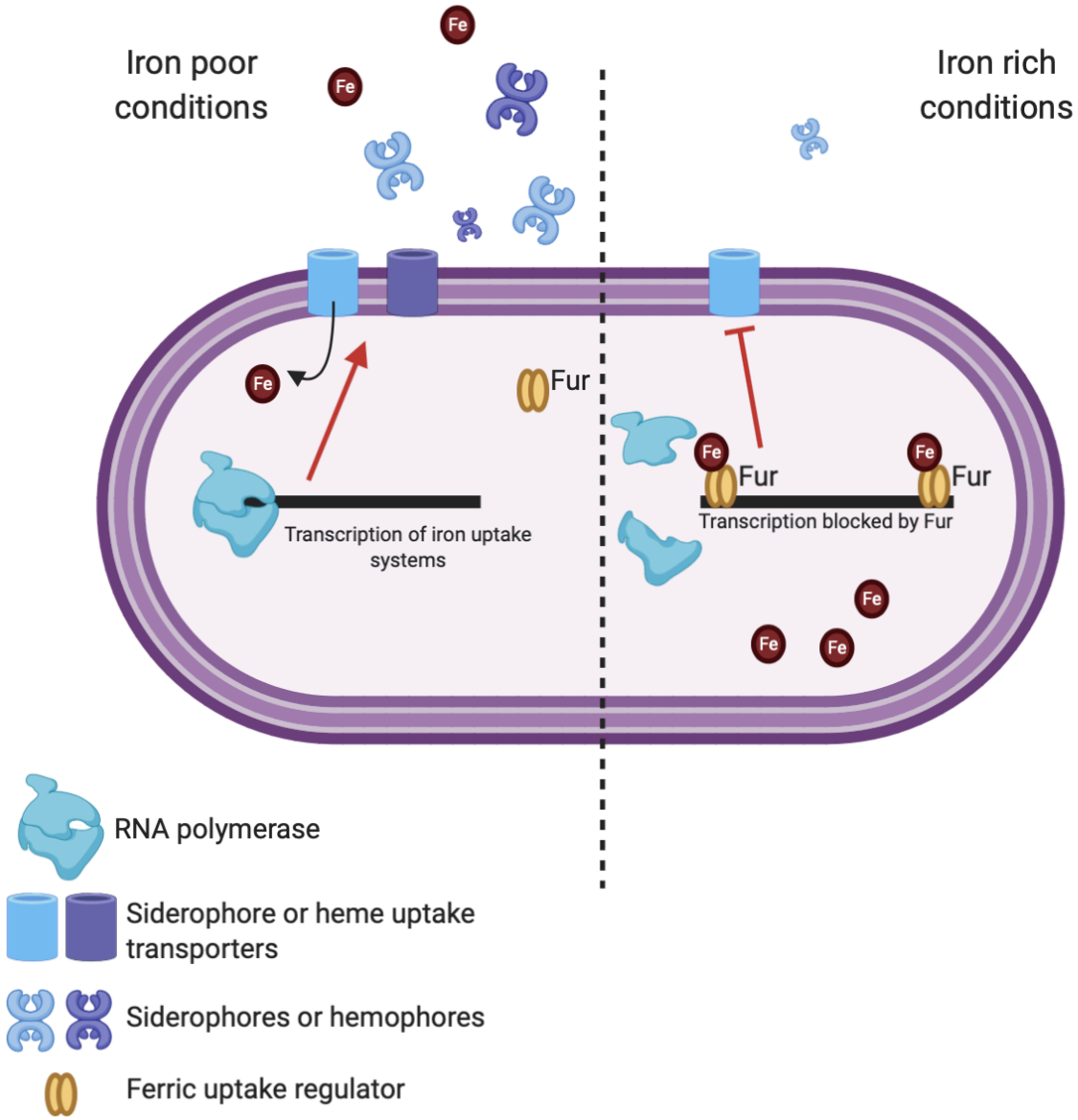

Figure 1.1. Iron uptake gene regulation by Fur.

Iron systems are regulated by intracellular iron concentrations. In iron-poor conditions, uptake systems are highly expressed in order to import iron. However, when iron levels are sufficient, iron molecules bind the ferric uptake regulator (Fur), which then binds to Fur-box consensus sequences on the genome. The Fur-iron complex displaces RNA polymerase to repress iron-uptake system gene expression.

Bacterial strategies to acquire iron

Due to the aforementioned low levels of iron in the body, Gram-negative pathogens use several mechanisms to acquire iron. Because ferrous iron is soluble, bacterial transporters can easily take it up. Ferric iron is insoluble and requires active transport across bacterial membranes. Citrate can act as a low-affinity siderophore and bind ferric iron for import. However, bacteria primarily employ two mechanisms to acquire ferric iron, using siderophores and heme uptake.

Iron acquisition via siderophores

A major class of Fur-regulated genes encode enzymes that synthesize low molecular weight (500-1500 Da), ferrous iron-binding compounds called siderophores [13]. The high affinity siderophores have for iron allows these molecules to outcompete most host proteins for iron. For example, the ferric binding constants of siderophores is typically $K_f > 10^{-30}$ M, with enterobactin having the highest reported affinity at 10^{-52} M. This is much greater than the binding constant of transferrin, 10^{-23} M [13, 14]. Siderophore-mediated iron acquisition is a common iron procurement strategy that is widely conserved among pathogenic and non-pathogenic bacteria but also fungi, yeast, and animals. Consistent with this, over 500 different siderophores have been described [15]. Often, different species of bacteria produce identical siderophores; however, some pathogens produce novel siderophores to prevent competing microbes from stealing their siderophore. In bacteria, the genes involved in siderophore biosynthesis and import are typically present within a single operon [16]. Specifically, these operons usually consist of biosynthesis enzymes, siderophore efflux pumps, siderophore-iron complex importers, and accessory proteins that aid in siderophore function. The operons present in Gram-negative bacteria also contain outer membrane-localized receptors specific to a particular siderophore (Figure 1.2) [17]. The

importance of siderophores to bacterial pathogenesis has been established in numerous studies demonstrating that mutant strains devoid of siderophore production are severely attenuated in many different models of infection [17-19]. Additionally, numerous strains of pathogenic bacteria, including *Escherichia coli* and *Klebsiella. pneumoniae*, synthesize more than one siderophore and mutant strains that are restricted to the synthesis of a single siderophore often demonstrate organ-specific virulence defects [19]. These findings demonstrate the temporal and spatial specificity between different siderophores and have prompted investigators to evaluate the potential of siderophores as vaccine candidates. Thus far, two reports demonstrate that immunization with siderophores mounts an effective host immune response that reduces bacterial burdens within the vaccinated host [20, 21]. Thus, host antibodies that bind the siderophore can be generated that obstruct siderophore-mediated import of host iron into the pathogen.

Types of siderophores and biosynthesis

Siderophores are classified into five different families based on the chemical signature of the iron-binding moiety. Catecholate, phenolate, hydroxamate, and α-hydroxycarboxylate represent four of the five classifications. The fifth classification represents mixed siderophores that contain more than one iron-binding moiety [22].

Siderophore synthesis occurs via one of two mechanisms. The first mechanism is dependent on large multi-enzyme complexes called non-ribosomal peptide synthetases (NRPSs) that bind precursor molecules and catalyze the synthesis of the siderophore synthesis using energy generated from ATP hydrolysis. Specific genes within the siderophore operon create the prerequisite precursors molecule needed for the NRPS. Next, the precursor molecules are

assembled into the siderophore product with the aid of other enzymes present within the NRPS complex. NRPSs are composed of multiple large enzymes working in an assembly line to incorporate the needed amino acid into the growing polypeptide chain that will make up the siderophore. These NRPSs have three main domains; however, they can have more depending on the structure of the siderophore. First, the adenylation domain recognizes the incoming amino acid that will be incorporated. Next, the growing chain is covalently tethered to the peptidyl carrier protein (PCP) domain, sometimes referred to as the thiolation domain. Finally, the condensation domain incorporates the amino acid into the product. Condensation reactions can occur multiple times until the chain is cyclized by the thioesterase domain, also called the termination domain [16].

Alternatively, siderophore biosynthesis can occur independently of the NRPS using NRPS-independent synthetases (NIS). The NRPS-independent pathways are not as well studied; however, recent reports have shown that NRPS-independent siderophores contain their own synthetases within the siderophore operon that catalyze various condensation reactions that form amide or ester bonds between the precursor molecules [23]. In both systems, the final product is then effluxed from the bacterium using dedicated, membrane-bound exporters.

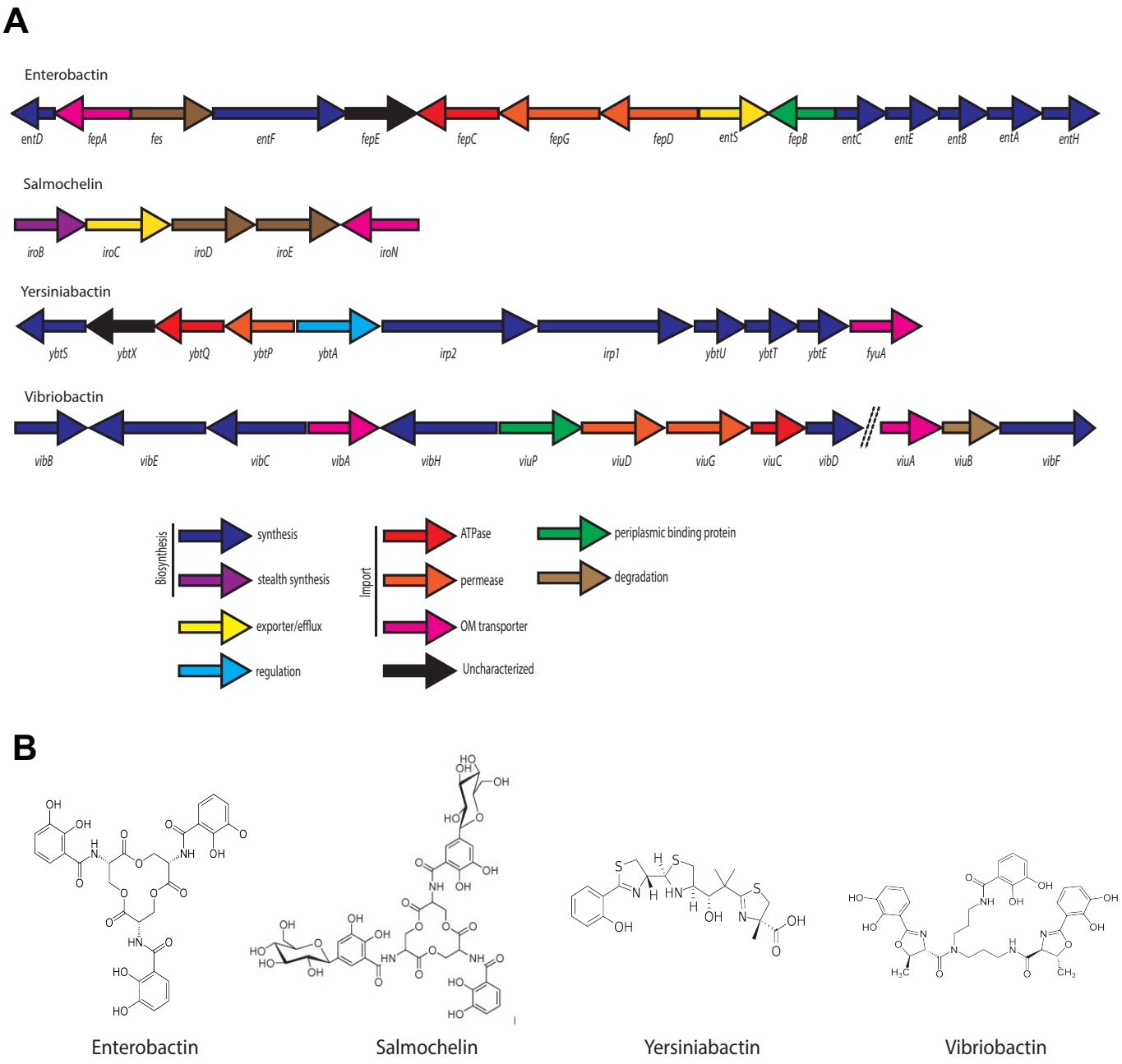

Figure 1.2. Siderophore loci and structure.

(A) The loci for enterobactin, salmochelin, yersiniabactin, and vibriobactin are depicted with biosynthetic, transport, and accessory genes annotated. (B) The corresponding siderophore structures are shown.

Siderophore transport

Upon siderophore binding of iron in the extra-cellular space, the molecule undergoes a conformational change, allowing the iron-siderophore complex to be recognized by specific bacterial cell surface receptors expressed within the outer membrane of Gram-negative bacteria. This interaction facilitates import. The outer membrane-localized receptors typically consist of a beta-barrel structure with a domain inside the barrel that creates a "plug" [24]. Studies have shown that reconfiguration of the "plug" domain allows for the passage of the siderophore-iron complex through the barrel [25]. The TonB complex, consisting of three proteins, TonB, ExbB, and ExbD, utilizes the proton motive force (PMF) to couple energy from the inner membrane to drive import of the substrate across the outer membrane [26]. Once the iron-siderophore complex is transported into the periplasm, transporters of the ATP-binding cassette (ABC) superfamily are responsible for passage of the complex across the inner membrane and into the cytoplasm. The energy required for this transport is generated via ATP hydrolysis. ABC transporters typically consist of three distinct functional units: a lipoprotein that binds the siderophore-iron substrate in the periplasm, a permease composed of two proteins located within the cytoplasmic membrane and that function as the channel through which the siderophore-iron complex traverses, and a cytoplasmic ATP hydrolysis enzyme (Figure 1.3). Typically, the genes encoding a siderophore ABC transporter are located in close proximity within the genome to the genes encoding the siderophore biosynthesis enzymes. However, some pathogens express orphan ABC transporters that promiscuously import siderophores produced by other bacteria [27]. The most well-known and best-characterized ABC transporter is found in *E. coli* and consists of FhuBCD proteins.

Once in the cytoplasm, iron must be liberated from the siderophore for it to be utilized in various enzymatic processes. Two unique mechanisms facilitate the release of iron from the siderophore. The first mechanism is mediated by an enzyme called ferrisiderophore reductases that catalyzes the reduction of Fe^{3+} to Fe^{2+}. Because siderophores bind Fe^{2+} with a lower affinity than Fe^{3+}, the Fe^{2+} is easily released. Alternatively, some bacteria release iron through enzymatic hydrolysis of the siderophore; however, this disrupts the integrity of the complex and is costly because the siderophore is unable to be recycled. Therefore, an advantage of the reductase-mediated strategy of iron release is that the siderophore can be recycled to retrieve another Fe^{+3} atom [22].

Stealth siderophores that evade the immune response

In the continuous evolutionary battle between host and pathogen, vertebrates are equipped to impede siderophore-mediated iron acquisition. The lipocalin family of proteins bind a diverse set of small molecules with a subset sequestering catecholate- and phenolate-type siderophores. For instance, lipocalin 2 (also referred to as 24p3, NGAL, or siderocalin) binds enterobactin, a siderophore commonly produced by the *Enterobacteriaceae* [28]. The importance of this siderophore countermeasure is demonstrated by the observation that lipocalin 2-deficient mice are more susceptible to Gram-negative infections [29]. In response to the selective pressure applied by the lipocalin family of proteins, pathogens adapted by evolving mechanisms to chemically modify their siderophores, blocking recognition by host siderophore-binding proteins. These so-called stealth siderophores contain slight chemical modifications to an existing siderophore, maintaining the high affinity for iron but abolish binding of the lipocalin family of host proteins. For example, *E. coli* synthesizes the siderophore enterobactin, which is

bound by host immune protein, lipocalin 2. However, some strains of *E. coli* also encode the enzyme, *iroB*, which glycosylates enterobactin, resulting in a modified enterobactin called salmochelin (Figure 1.2). Lipocalin 2 fails to bind salmochelin, allowing the stealth siderophore to bypass host sequestration of enterobactin such that *E. coli* can achieve unperturbed acquisition of host iron [30]. Enterobactin is also found in many commensal strains of *E. coli* while stealth siderophores are much more common in pathogenic strains [31]. In addition to the synthesis of stealth siderophores, many pathogens are also equipped with the capacity to scavenge siderophores produced by other bacterial species [32]. Together these mechanisms enhance the iron acquisition strategies of invading pathogens ensuring that the requirement for iron is satisfied during infection.

Iron acquisition via heme uptake

Heme represents the most abundant iron-containing molecule in vertebrates. Not surprisingly, many pathogens, especially those that proliferate within the vasculature, target host heme to fulfill the iron requirement. Heme acquisition begins with the lysis of erythrocytes, liberating the enclosed hemoglobin. Each hemoglobin contains four heme molecules and each erythrocyte contains approximately 270 million hemoglobins [33]. Therefore, lysis of one erythrocyte results in a tremendous yield of iron for the pathogen. Hemolytic activity is a virulence trait associated with many Gram-negative pathogens [34].

Some pathogens are equipped with additional mechanisms that facilitate acquisition of heme from reservoirs less abundant than hemoglobin. One example is the heme-binding protein hemopexin that functions to alleviate heme-mediated damage to host tissues [4]. The high reactivity of heme requires that the molecule be complexed to proteins to prevent illicit damage

to other host molecules. Consequently, the amount of 'free' heme is kept low in order to protect tissues from heme-induced redox damage. Hemopexin functions in this capacity and is a viable source of heme-iron for Gram-negative pathogens, such as *Serratia marcescens*, but not all pathogens are capable of stealing heme from hemopexin. A common strategy is to procure the hemopexin heme using a siderophore-like mechanism that outcompetes hemopexin for heme. This is the case for *S. marcescens*, which will be discussed later in this chapter.

Gram-negative heme acquisition systems

Enterobacterales also target heme-containing hemoglobin as a source of iron. But first, the pathogen must lyse erythrocytes to liberate hemoglobin from these cells and initiate heme acquisition. To accomplish this, *S. marcescens* and *E. coli* rely on the hemolysins ShlA and HlyA, respectively [35, 36]. Gram-negative bacteria capture the heme liberated via hemolysis utilizing two distinct mechanisms: direct heme binding to outer membrane receptors or secretion of hemophores that scavenge the heme, subsequently passing the heme to their cognate receptor (Figure 1.3). Some Gram-negative bacteria possess both hemophore-mediated and receptor-mediated systems, such as *Serratia marcescens*; however, it is more common for the pathogens to employ one or the other. Two heme receptors have been extensively characterized in uropathogenic *E. coli,* ChuA and Hma; however, more than 30 heme receptors have been described in Gram-negative species [37]. Outer membrane heme receptors are similar to the iron-siderophore complex receptors described above both in terms of structure and the utilization of the PMF to drive import [38]. Heme receptors are β-barrels that encode specific residues within extracellular domains that bind heme. Two of these domains, FRAP and NPNL, contain conserved amino acid motifs in the extracellular loops of outer membrane receptors that are critical for heme import. These domains function to bind heme and transport it through the outer

membrane. The β-barrel heme receptors rely on the TonB protein complex to couple energy from the inner membrane to power heme import [39]. Gram-negative pathogens also utilize hemophores to scavenge heme. One of the best-described hemophores is HasA produced by *S. marcescens* which will be discussed later in this chapter [40].

Periplasmic binding proteins (PBPs) are responsible for shuttling heme from the outer membrane through the periplasm to the inner membrane. PBPs that bind heme have been identified in *Pseudomonas aeruginosa*, *Shigella dysenteriae* [41], and *Yersinia pestis*. PBPs coordinate heme binding using a conserved tyrosine residue within a cleft connected via the N and C termini [42]. The heme-binding PBPs then pass the heme to dedicated ABC transporters. Analogous to siderophores, ABC transporters hydrolyze ATP to mediate heme delivery to the cytoplasm. While the outer membrane receptors for both siderophores and heme are incredibly substrate-specific, the ABC transporters do not seem to be. For example, *P. aeruginosa* encodes approximately 34 TonB-dependent outer membrane receptors, but only four ABC transporters function in iron import [43]. Therefore, it is likely that the same ABC transporters used for siderophore-iron import are also used to import heme.

Gram-negative bacteria employ heme oxygenases to degrade heme. In addition to iron, biliverdin and carbon monoxide are products of heme degradation in these organisms. A new mechanism of heme degradation has recently been reported in the Gram-negative pathogen, enterohemorrhagic *E. coli* O157:H7. In aerobic environments canonical heme oxygenases catalyze the release of iron from heme, using oxygen as a cofactor. However, bacteria capable of growing in anaerobic environments, such as the gut, must have alternative mechanisms to liberate iron from heme without oxygen. *E. coli* O157:H7 encodes an operon for heme uptake that includes three additional uncharacterized genes, *chuW*, *chuX*, and *chuY*. Elegant biochemical

experiments demonstrated that ChuW uses the oxidizing potential of a carbon radical to free heme-bound-iron through a methyl transfer reaction leading to the rearrangement of the heme porphyrin ring. The complete mechanism of this reaction is currently not known; however, ChuW catabolizes the porphyrin ring of heme yielding free iron and a tetrapyrrole called anaerobilin (Fig. 2B) [44]. ChuY breaks down and reduces anaerobilin, a potentially toxic product of heme degradation. *chuW* and *chuY* are co-transcribed, suggesting a comprehensive mechanism of anaerobilin synthesis by ChuW after iron liberation from heme followed by anaerobilin reduction by ChuY [45]. Results from LaMattina *et al.* show that anaerobic bacteria have systems to extract iron from heme without using oxygen as a substrate. Heme oxygenase reduces the bound ferric iron to ferrous iron through a series of steps to break bonds within the heme-binding pocket to release the iron [46]. The freed iron can then be used in various cellular processes.

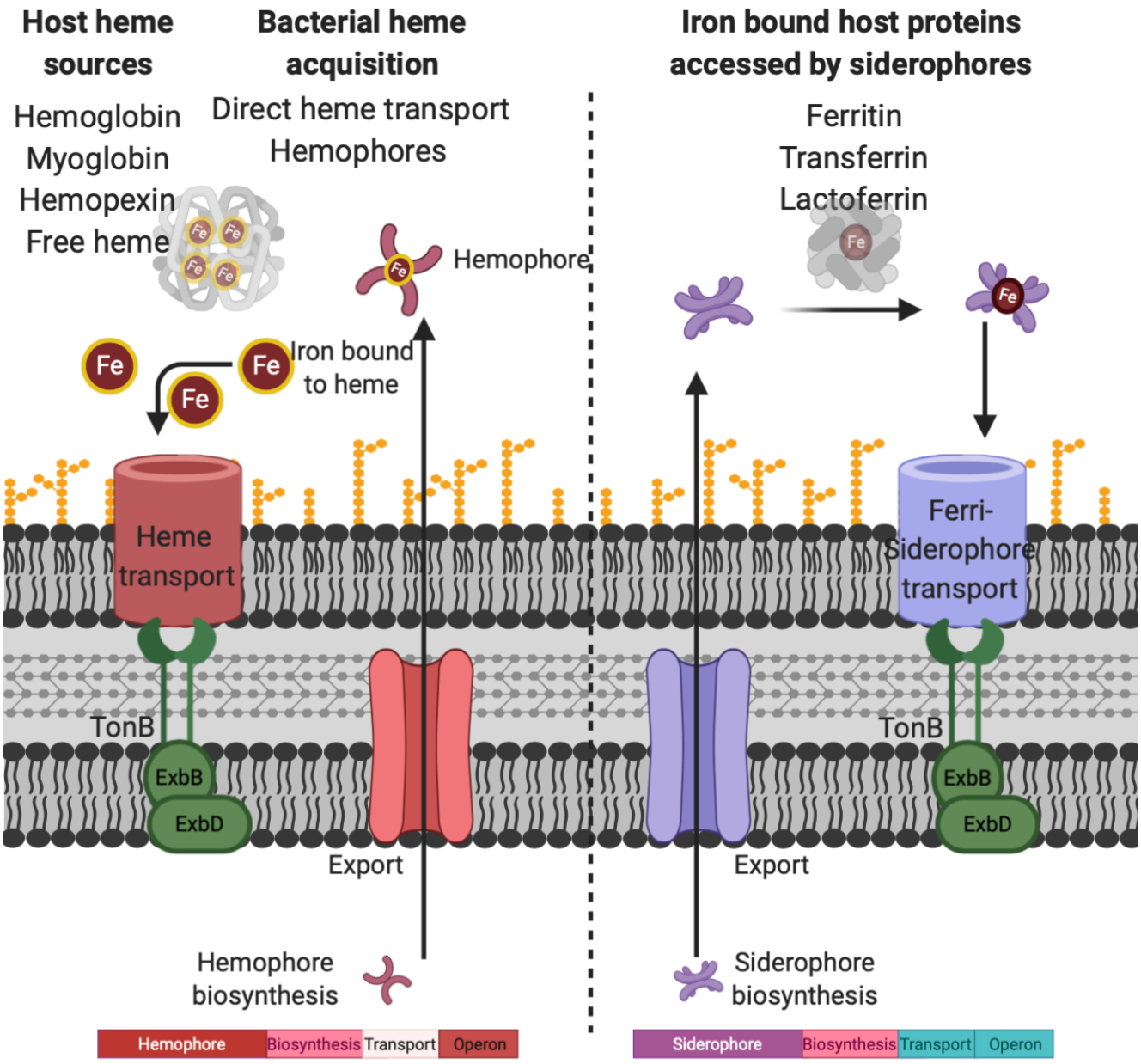

Figure 1.3. Bacterial heme and siderophore uptake strategies.

The host heme sources that are targeted by bacterial heme transporters and hemophores are described. Hemophores are synthesized by the bacterium and exported to scavenge for heme. Membrane transporters interact with hemophores or take up heme independently. Siderophores target iron bound to the host proteins described. Siderophores are produced intracellularly, exported, and then transported back into the bacterium after binding iron.

Coordinating the iron acquisition systems

Heme and iron are exceedingly toxic at high levels. Therefore, bacteria that target both iron and heme reservoirs within the host must coordinate expression of the acquisition systems to maintain iron homeostasis without corresponding toxicity. It is likely that the host contains niches where the abundance of the various iron sources may dramatically change depending on the tissue being colonized. In keeping with this paradigm, siderophore-mediated iron acquisition may be better suited for colonization of distinct organs or tissues compared to heme-mediate acquisition systems or vice versa. Thus, bacteria must coordinate the expression of the acquisition systems to maximize fitness during infection of distinct niches. We are just beginning to understand the interplay between the iron acquisition systems but a recently described transcriptional regulator expressed in *Staphylococcus aureus*, a Gram-positive pathogen, has emerged that serves as a coordinator of iron acquisition systems.

SbnI is a transcriptional regulator encoded within one of the *S. aureus* siderophore synthesis operons. *S. aureus* produces three siderophores, a nicotinamine-like broad spectrum metallophore called staphylopine and two α-hydroxycarboxylate siderophores: Staphyloferrin A and Staphyloferrin B. The *sbn* operon encodes the genes required for Staphyloferrin B synthesis. *sbnI* is the terminal gene of a nine gene operon. The function of SbnI remained elusive as the other genes, *sbnA-H*, emerged as enzymes encoding the siderophore synthesis or efflux proteins. Recent work demonstrated that SbnI enhanced the expression of *sbnD-H* in conditions of low iron. Notably, SbnI-dependent expression of *sbnD-H* is dependent on the presence of heme. SbnI is capable of binding heme and this reduces the affinity SbnI has for its DNA promoter sequence within the *sbnD* gene. In the presence of heme the expression of sbnD-H is decreased, reducing the production of Staphyloferrin B. Therefore, SbnI coordinates the production of Staphyloferrin

B in iron deplete environments devoid of heme. However, in iron depleted environments containing heme, Staphyloferrin B is not produced [47, 48]. This elegant coordination of heme and siderophore iron acquisition maximizes *S. aureus* iron acquisition and ensures that the bacterium maintains sufficient iron during pathogenesis.

Introduction to *Serratia marcescens*

Serratia marcescens (referred to as Sm throughout this dissertation) is a Gram-negative, facultative anaerobic bacillus within the *Enterobacterales* order that is frequently found in environmental settings. It infects plants and insects, and due to its low nutritional needs, is able to survive in soil and aquatic reservoirs such as drinking water [49]. For many years, *S. marcescens* was thought of as a nuisance as it is also commonly found in the grout of tiling as well as being a common bathroom contaminant, and generally was not considered pathogenic. However, only over the last four decades has *S. marcescens* been appreciated for the clinical threat it poses. *S. marcescens* infection prevalence is increasing in hospitals worldwide, and is now recognized as an important opportunistic pathogen associated with nosocomial infections and alarming rates of antibiotic resistance. In fact, a study in Poland revealed *S. marcescens* to be the fifth most commonly isolated bacterium from the Enterobacterales order nationwide from 2003-2004 [50]. Another study in Japan implicated *S. marcescens* as the fifth most common cause of UTIs in 2008 [51]. Additionally, *S. marcescens* outbreaks in hospitals have been on the rise since the 1960s. By 1977, over 100 *S. marcescens* outbreaks were described [52], occurring in ICUs [53-60], surgery units [61-63], obstetric wards [64], and outpatient clinics [65] as well as more. Finally, in 2011, six patients were diagnosed with *S. marcescens* infections that were

traced back to a soap dispenser in an ICU in India [66]. These studies reflect the importance of *S. marcescens* as an emerging pathogen.

S. marcescens causes many types of infections such as meningitis [67, 68], urinary tract infections [69-72], pneumonia [73, 74], bacteremia, and endocarditis [72, 75, 76]among others. It can also colonize indwelling catheters and medical devices. Mortality rates among these infections vary depending on the type of infection and the underlying condition of the patient. Because *S. marcescens* is an opportunist, immunocompromised patients including neonates are at high risk with mortality rates above 40% [77]. Treating *S. marcescens* infections is extremely difficult because of its antibiotic resistance profile. *S. marcescens* isolates can be resistant to a wide range of antibiotics including ampicillin, amoxicillin, cephalosporins, cephamycins, colistin, and several others [78-80]. Intrinsic resistance to colistin is especially concerning as this is typically a last-resort antibiotic. The presence of a chromosomal *ampC* confers resistance to β-lactams, as well. It is also common for *S. marcescens* to have low level resistance to aminoglycosides, as many strains weakly express AAC(6')-Ic, an aminoglycoside-modifying enzyme [81]. Some *Serratia* sp. strains are resistant to all clinically used aminoglycosides by expressing both 6'-*N*-acetyltransferase and the ANT(2") enzyme [82]. Carbapenem resistance is uncommon in *Serratia spp*.; however, *S. marcescens* strains producing SME, a carbapenemase, as well as plasmids with carbapenemases have been found sporadically, which is highly concerning given that carbapenems are used to treat severe infections [83].

Bacteremia and Virulence Factors

S. marcescens is in the top 10 of pathogens that cause hospital acquired bloodstream infections [84]. Typically, the pathogen gains access to the bloodstream via the urinary tract,

respiratory system, or an open wound. If these infections are uncontrolled bacteria reach the bloodstream and the infection may quickly become systemic, resulting in septicemia with strikingly high mortality rate ranging from 23-52%. A study of European ICU-acquired infections in 2008 showed that *Serratia* caused 2.0% of all bloodstream infections, ranking it among the top frequently isolated organisms from bacteremia cases in the ICU [85]. Furthermore, a 2007 outbreak related to contaminated heparin syringes spread across nine states and resulted in 162 bacteremia cases with four deaths [86, 87].

These *Serratia* outbreaks are becoming more common as *S. marcescens* finds its niche in the human host. The increase in outbreaks could be due to the previous dismissal of *S. marcescens* as a commensal or the genetic diversity seen between environmental isolates and clinical isolates particularly within virulence loci such as fimbriae, capsule, O-antigen, and toxins [88]. With the rise of *Serratia* infections, research interest examining virulence factors contributing to *S. marcescens* pathogenesis has also risen over the last ten years, giving the field some understanding of this otherwise uncharacterized emerging pathogen.

A pore-forming toxin called ShlA is a common virulence factor associated with *S. marcescens*. Together with ShlB, ShlA destroys red blood cells as well as epithelial cells and fibroblasts [89]. ShlB is found in the outer membrane where it activates and secretes ShlA; however, these proteins are not released extracellularly and are contact-dependent. Therefore, the action of these proteins is dependent on the bacterium attaching to the cell to be lysed. Due to the cytotoxicity of this system and its ability to mediate inflammatory molecule release, it appears to be important to pathogenesis during UTI [90, 91]. Additionally, a regulatory pathway, called RssAB, regulating swarming and biofilm formation also regulates hemolysin production and seems to be important to virulence [92, 93]. Because *S. marcescens* is frequently found on

catheters and indwelling devices, its ability to quorum sense and produce biofilm is clinically important as this contributes to its resistance to antibiotics and evasion of the immune system [94-97]. *S. marcescens* also produces a capsule composed of acidic polysaccharides which aids in resisting opsonophagocytosis and complement-mediated killing [98]. Several other virulence factors of *S. marcescens* include secreted proteases, an extracellular phospholipase, as well as iron acquisition systems [99]. With *S. marcescens* emerging as a prevalent pathogen of concern, the field has recognized this bacterium's clinical importance, but the understanding of its virulence is lagging. While literature for *S. marcescens* various virulence factors exists, significantly more work is required to advance our understanding of *S. marcescens* pathogenesis, particularly with respect to its iron acquisition systems.

Iron in *Serratia marcescens*

The importance of iron in the context of Gram-negative pathogens has been extensively studied especially in *E. coli*. Studies have found iron uptake systems, including siderophores and heme uptake, in uropathogenic *E. coli* to have redundant but also hierarchical roles during infection [19]. Additionally, expression of particular siderophores in *Klebsiella* have been associated with hypervirulence [18, 100]. Because *E. coli*, *K. pneumoniae*, and *S. marcescens* are all members of the *Enterobacterales* order, it would not be surprising for them to produce similar iron acquisition systems; however, much less is known about how iron acquisition systems contribute to *S. marcescens* pathogenesis and if *Serratia*-specific systems exist.

Heme uptake in *Serratia marcescens*

Some studies of heme acquisition systems in *S. marcescens* have been completed. *S. marcescens* typically encodes two heme uptake systems, referred to as Hem and Has. The Hem system is composed of a TonB-dependent outer-membrane receptor and transports heme at concentrations above 10^{-6} M [101]. It functions by stripping iron directly from the heme molecule. The **h**eme **a**cquisition **s**ystem or Has takes up heme at even lower concentrations (2.5 x 10^{-8} M) by utilizing a secreted hemophore that scavenges for iron bound to heme. *hasA* encodes this hemophore, and in its proteinaceous form has a higher affinity for heme than hemopexin. This allows HasA to retrieve heme from host hemopexin. Has consists of the hemophore itself as well as an outer membrane receptor, HasR. HasR is structurally similar to the β-barrel heme receptors but HasR heme binding is significantly enhanced when it functions in concert with HasA [102]. HasA is secreted as a dimer and conserved tyrosine and histidine residues coordinate within a pocket to facilitate heme binding. These residues are critical for heme binding. HasR recognizes monomeric HasA; therefore, the function of the HasA dimer is not well understood. Once HasR binds HasA, both proteins undergo conformational changes leading to the exchange of heme from HasA to HasR [102]. The has system can function with a variety of heme sources [103, 104]; however, the same is not true for the Hem system, as it cannot strip heme from hemopexin [101]. Studies have shown that Hem and Has are not redundant, since each is individually favored at high and low heme concentrations, respectively [101]. However, expression of the Has system may be advantageous during infection, since extracellular heme concentrations are extremely low and the heme is typically bound to either hemopexin or hemoglobin. Although this has not been empirically tested, it suggests that the hemophore-dependent has system may contribute more to virulence in this environment (Figure 1.4).

Serratia marcescens siderophores

Most studies on *Serratia* species siderophores have been largely biochemical, identifying secreted siderophores using mass spectrometry or other methodologies, or clinical case studies, and not necessarily examining their contribution to pathogenesis. As a result, we know relatively little about *Serratia marcescens* siderophores. Previous work has shown *Serratia liquefaciens* and *Serratia ficaria* to encode the aerobactin biosynthesis locus, while *S. marcescens* typically encodes just the receptor [105, 106]. Enterobactin and ferric citrate have also reportedly been found in some *S. marcescens* strains [106]. However, a novel siderophore, first identified by Ehlert *et al* in 1994, called serratiochelin has been associated with *S. marcescens* [107]. This siderophore is predicted to be a result of the evolutionary mixing and matching of the enterobactin and vibriobactin synthesis pathways to produce it [108] (Figure 1.4).

Serratiochelin

Even though the initial identification of serratiochelin was in 1994, it has largely been overlooked in scientific literature since that time. However, with increasing *S. marcescens* prevalence in the clinic, studies on serratiochelin are becoming more common. A thorough characterization of serratiochelin which was purified from *Serratia plymuthica* sp. V4 was performed by Seyedsayamdost *et al*. This study identified three serratiochelin variances (A, B, and C), consistent in their molecular formula but differing in their structure. Although, serratiochelin C was not naturally occurring and was a hydrolytic product of A occurring during purification. Serratiochelin A coordinates iron using one of its catechols as one pair of ligands and the oxazoline N and one hydroxyl group as the second pair of ligands, complexing the iron ion with four ligands as a tetradentate [108].

The full serratiochelin gene cluster contains 21 open reading frames, involving both enterobactin and vibriobactin homologs. Within the enterobactin-related cluster, there are eight genes (*schI-schP*) for siderophore export and reuptake of the ferri-siderophore complex. The six remaining genes (*schG, F0, C, E, B, A*) are involved in synthesizing the serratiochelin molecule itself. SchG is highly similar to an enzyme called acetolactate synthase, which activates the first step in branched-chain amino acid biosynthesis. The remaining biosynthesis genes share homology to genes within the enterobactin biosynthesis operon in *E. coli*, with SchC, B, E, and A being involved in precursor molecule production and F0 acting as part of the NRPS machinery. Chorismate is the starting molecule to serratiochelin synthesis. Through a series of reactions involving SchC, B, and A, 2,3-dihydroxybenzoate (DHB) is produced and then handed off to SchE which adenylates DHB and passes it to SchB. Once tethered to SchB, the biosynthesis reaction proceeds in two directions, with the products of both reactions being combined to create serratiochelin A and B. The first direction involves SchH from the vibriobactin cluster. It attaches a nontethered propane-1,3-diamine to the SchB-tethered DHB. This propane-1,3-diamine is a unique backbone for a siderophore. The second direction involves incorporation of L-Thr into the SchB-tethered DHB. The peptide chain is handed off to enzymes within the vibriobactin-related gene cluster where the action of several NRPSs finish building the siderophore by incorporation of amino acids. This is an iterative process until the products of the two pathways are joined by amide bond formation [108].

Serratiochelin is an interesting and unique siderophore because it has structural similarity to two separate siderophores, enterobactin and vibriobactin. This suggests the evolution of a new biosynthetic pathway through the combination and altering of these two clusters, resulting in a new siderophore. It is particularly advantageous for microbes to produce novel siderophores that

competing bacteria are unable to take up. Therefore, the evolutionary agility of siderophore clusters give bacteria a competitive advantage especially in polymicrobial environments.

Chrysobactin

In addition to serratiochelin, *S. marcescens* has been reported to also produce a lower affinity siderophore called chrysobactin. Chrysobactin was initially isolated in the plant pathogen *Dickeya chrysanthemi* and was essential for pathogen dissemination in the host plant [109]. Because of *S. marcescens'* environmental niche and ability to infect plants, identification of chrysobactin in the *S. marcescens* genome is not entirely surprising; however, the role it plays in human infection is unclear.

Chrysobactin is a catecholate siderophore and, in the case of *Dickeya chrysanthemi*, can have mono-, di-, tri-metric forms, as well as cyclized structures [109]. It is an NRPS-dependent siderophore that incorporates L-serine and D-lysine into the 2,3-dihydroxybenzoic acid backbone. CsbABCE produces 2,3-DHB which is passed to the NRPS protein, CbsF, where the amino acids are added to the growing chain. CbsF, contains eight NRPS domains to synthesize the final chrysobactin molecule [110]. Outside of plant pathogenesis, chrysobactin has not been studied in the context of mammalian disease.

Siderophore transport in *S. marcescens*

Siderophore export is an ongoing area of study and is not fully understood in most gram-negatives. For example, enterobactin is one of the most well characterized siderophores in terms of its production and reuptake [111]; however, its export is still under scrutiny. EntS, an ABC-type transporter is involved in enterobactin export [112], but additional studies have suggested

resistance-nodule-division (RND) family efflux pumps to also play a role in enterobactin export [113]. Therefore, these studies indicate that siderophore export is complicated, potentially involving several proteins and enzymes. More is known with respect to enterobactin reuptake and transport back into the bacterium. Enterobactin has several dedicated cell surface receptors dependent on the TonB complex. It traverses the periplasm using periplasmic binding proteins and crosses the inner membrane with the ABC transporter consisting of permease and ATPase proteins, called FepBCDE [111] (Figure 1.4). Much less is understood with siderophore export and reuptake in *S. marcescens*, but is most likely similar to other gram-negatives. Within both the chrysobactin and serratiochelin loci, there are putative exporters; however, their role in export has not been empirically tested. A study identified the efflux pump, MacAB, to possibly be involved in siderophore export in *S. marcescens* strain SR41-8000, but did not contribute to export in strain SM6 [114]. Like enterobactin, this suggests S. *marcescens* siderophore export is also complicated. Additionally, while receptors and *fepBCDE*-like genes are found within the *S. marcescens* chromosome, transport of serratiochelin has not been extensively studied and the mechanism behind the transportation pathway has not been characterized. While it is hypothesized to function similarly to other gram-negative pathways, the results in Chapter III potentially suggest otherwise.

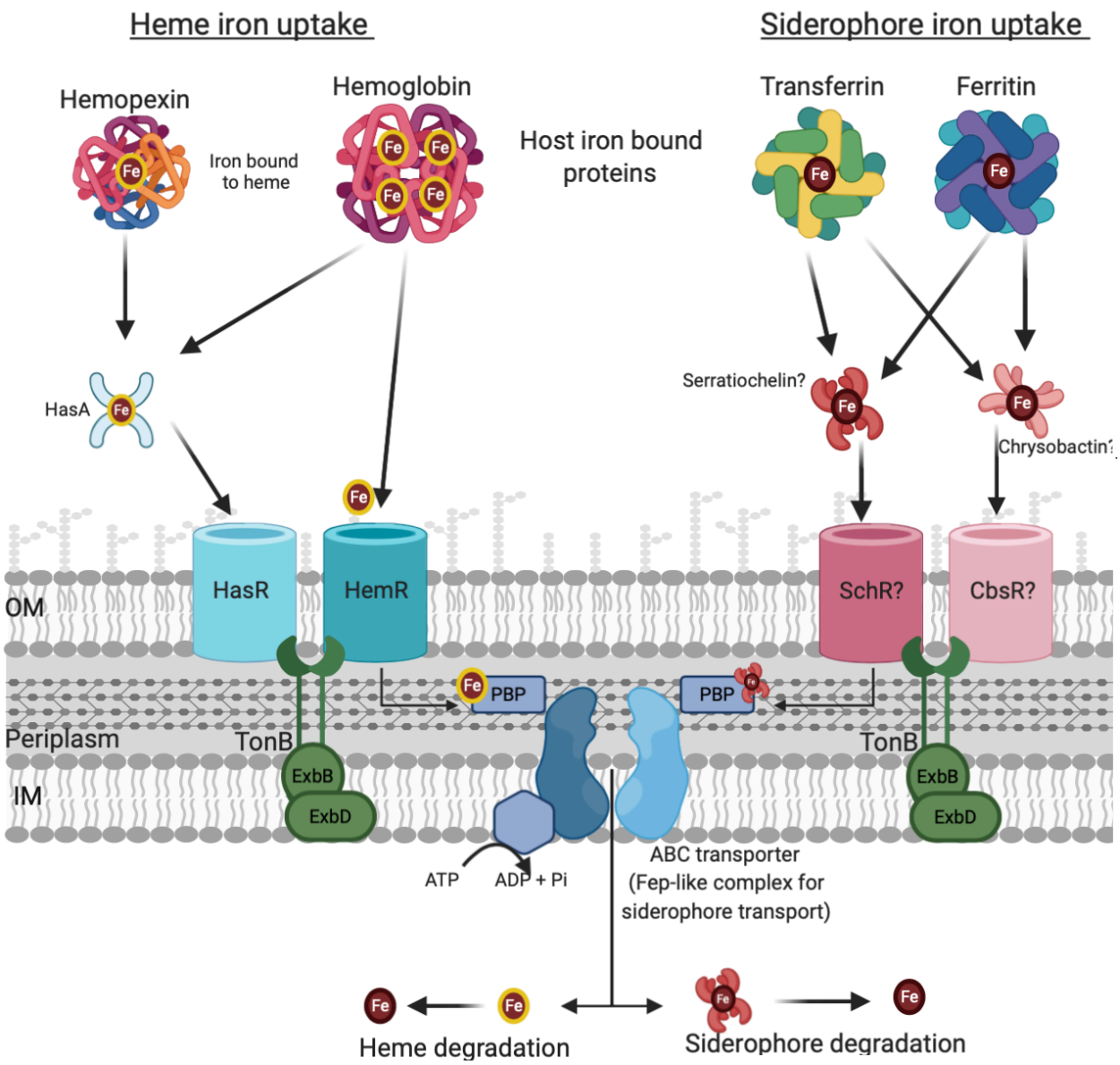

Figure 1.4. Predicted heme and siderophore systems in Serratia marcescens.

S. marcescens has two previously described heme uptake systems, Hem and Has. The has system encodes a hemophore, HasA. Has brings in heme from hemopexin or hemoglobin while Hem targets only iron from hemoglobin. Chrysobactin and serratiochelin are two predicted siderophores of *S. marcescens* with corresponding outer membrane receptors. Heme and siderophore receptors are TonB-dependent and are internalized using a periplasmic binding

protein (PBP), which then interacts with an ABC transporter. For siderophore transport, this is most likely a Fep-like complex as described in *E. coli*. Once the heme or siderophore iron complex reaches the cytoplasm, the heme and siderophore are degraded to release the bound iron.

Siderophores and Pathogenesis

There have been few studies examining how the siderophores found in *S. marcescens* actually contribute to pathogenesis and none that have looked at virulence in a mammalian host. In a *Caenorhabditis elegans* infection model, one study identified mutants with reduced virulence using a transposon library constructed in *S. marcescens* Db11. A mutation within a predicted siderophore biosynthesis gene conferred attenuated virulence within this model [91]. To date, the connection between *S. marcescens* siderophores and mammalian infection is unknown.

Regulation of Iron Systems in *S. marcescens*

I speculate that the regulation of *S. marcescens* iron systems parallels those of other Gram-negative species. Fur boxes are present upstream of the known siderophore biosynthesis operons as well as the Hem and Has heme uptake operons, suggesting that these operons are repressed by Fur when iron levels are adequate [17]. In other microbes, siderophore expression is sometimes influenced by temperature and oxidative stress [115-117]; however, iron system expression under these conditions in *S. marcescens* has not been examined. Since *S. marcescens* is found in diverse ecological niches, additional environmental cues may also regulate its iron systems.

Summary and Chapter Outline

This chapter summarized the current knowledge of iron acquisition systems in the context of *Serratia marcescens*. Because *S. marcescens* has a history of infecting plants, insects, and surviving in a variety of environmental settings, some features of its pathogenesis may

potentially be unique when compared to other gram-negative microbes, and should not be assumed to follow typically understood mechanisms of pathogenesis specifically related to iron acquisition. The following chapters aim to elucidate some of these mechanisms. Chapter II identifies the iron-regulated transcriptome of *Serratia marcescens* isolate UMH9 using RNA-sequencing to provide a complete outline of all genes involved in iron uptake. Interesting systems that were identified by RNA-seq and hypothesized to contribute to UMH9 pathogenesis guided the questions addressed in subsequent chapters. Chapters III and IV home in on putative siderophore systems that were identified in Chapter II. Chapter III describes interesting findings suggesting how Sm NRPS machinery may be involved in siderophore transport. Chapter IV defines the contribution of Sm siderophores to mammalian pathogenesis. Finally, Chapter V outlines preliminary conclusions on Sm heme acquisition systems and their potential involvement in heme toxicity. Together, the findings presented herein provide novel insights into iron acquisition in the broader context of Gram-negative infection as well as to *S. marcescens* pathogenesis specifically.

Chapter II

Identification of the Iron-Regulated Transcriptome of *Serratia marcescens* Clinical Isolate UMH9

Notes. The results presented in this chapter were adapted from the following article:

Weakland DR, Smith SN, Bell B, Tripathi A, Mobley HLT. The *Serratia marcescens* Siderophore Serratiochelin Is Necessary for Full Virulence during Bloodstream Infection. *Infect Immun*. 2020; 88(8): e00117-20. Published 2020 Jul 21. doi:10.1128/IAI.00117-20

Abstract.

Serratia marcescens is an emerging infectious pathogen; however relatively little is known regarding its pathogenesis and virulence factors, particularly with respect to iron acquisition systems. Therefore, addressing this knowledge gap was the overarching goal of my dissertation. By taking a global transcriptomic approach to identify all genes regulated by iron concentration, the results of this chapter provide the foundational work to describing how iron acquisition contributes to virulence in Sm. RNA-sequencing in iron-depleted conditions on a clinical isolate of Sm called UMH9, revealed two previously identified heme uptake systems called *hem* and *has* as well as two putative siderophore loci. In addition to heme and siderophore uptake, ferrous iron transporters and ferric citrate transporters were upregulated under iron-limited conditions.

Finally, seven orphan transporters that were located outside of dedicated iron transport loci were identified by RNA-seq, suggesting UMH9's ability to import siderophores from other microbes or additional transporters for its own siderophores. The results of this RNA-seq experiment provided a comprehensive inventory of the arsenal of iron acquisition genes in the UMH9 genome. These findings informed the iron acquisition systems that were studied in depth in the following chapters.

Introduction

Bacterial access to iron is crucial because of its many roles in cellular processes such as serving as an enzyme cofactor and its involvement in electron transfer. As such, bacteria encode several types of iron uptake systems, many of which have been described across bacterial species. These systems include hundreds of different siderophores as well as heme uptake systems, but also consist of independent siderophore/iron receptors [22, 118]. Siderophores and heme uptake are the main systems involved in bacterial iron scavenging but machinery that takes up ferrous iron or citrate, a very low affinity iron chelator, are also typical across bacterial genomes [119]. This is the case for uropathogenic *E. coli* which encodes four potential siderophores as well as two heme uptake systems. Additionally, it possesses "orphan" receptors that are not located within siderophore biosynthetic loci that still take up ferri-siderophores, and citrate import genes [19].

The iron acquisition machinery of many human bacterial pathogens has been described; however, research is severely lacking on iron uptake ability and how it relates to pathogenesis for emerging pathogens such as *Serratia marcescens*. Sm, initially thought of as an exclusively

environmental pathogen and nonvirulent in humans, is being seen with increasing prevalence in the clinic causing fatal bloodstream infections [99]. Some of its virulence factors have been described including the production of a hemolysin, ShlA, and a rigid capsule [90, 98]. Nonetheless, how iron acquisition contributes to the pathogenesis of a bacterium that has evolved into a concerning clinical pathogen is yet to be explored.

Two heme uptake systems have been identified previously in nonclinical isolates of Sm [101, 120]; however, the full repertoire of iron uptake genes has not been described in a clinical isolate of Sm, let alone Sm itself. Therefore, in this Chapter, I identified the complete iron-regulated transcriptome of Sm clinical isolate UMH9 using RNA-seq to acquire a comprehensive understanding of all dedicated iron uptake systems, as well as orphan genes related to iron. The results of this study enabled me to identify two siderophore loci within the Sm genome that had not been reported on in clinical isolates of Sm. This global approach provided a big picture snapshot of all the iron uptake machinery encoded by UMH9, providing an appreciation for iron acquisition in a clinical isolate of Sm.

The results presented here guided the direction of this total project with the overarching goal of achieving a complete characterization of iron acquisition in Sm as an opportunistic mammalian pathogen. In the following Chapters, I homed in on the identified major iron uptake systems that were hypothesized to contribute most impactfully to Sm pathogenesis.

Results

Identification of the *S. marcescens* transcriptome during iron limitation

To identify iron-dependent genome-wide changes in transcription, differential gene expression of *S. marcescens* strain UMH9 under iron-rich and iron-limited conditions was quantified using RNA-seq. Three concentrations (125μM, 200μM, 250μM) of dipyridyl, an iron chelator, were added to LB medium to empirically find sub-inhibitory levels of iron-limitation (Figure 2.1). Transcripts isolated at mid-log phase (3 hours) from UMH9 cultured in LB and LB supplemented with 200μM dipyridyl were sequenced and analyzed to identify differentially regulated genes. 114 genes were significantly up-regulated (Appendix A, Table A.1) and 46 genes were significantly down-regulated (Appendix A, Table A.2) during iron-limitation.

Upregulated genes consisted of those involved in iron-transport and siderophore biosynthesis, confirming that iron-limitation was achieved. Genes downregulated in iron poor conditions were involved in iron storage as well as metabolic processes such as glycolysis, nitrate anaerobic respiration, and succinate metabolism consistent with the reduced cellular growth observed under these conditions, suggesting that cells potentially do not achieve a metabolic phase where these genes are necessary.

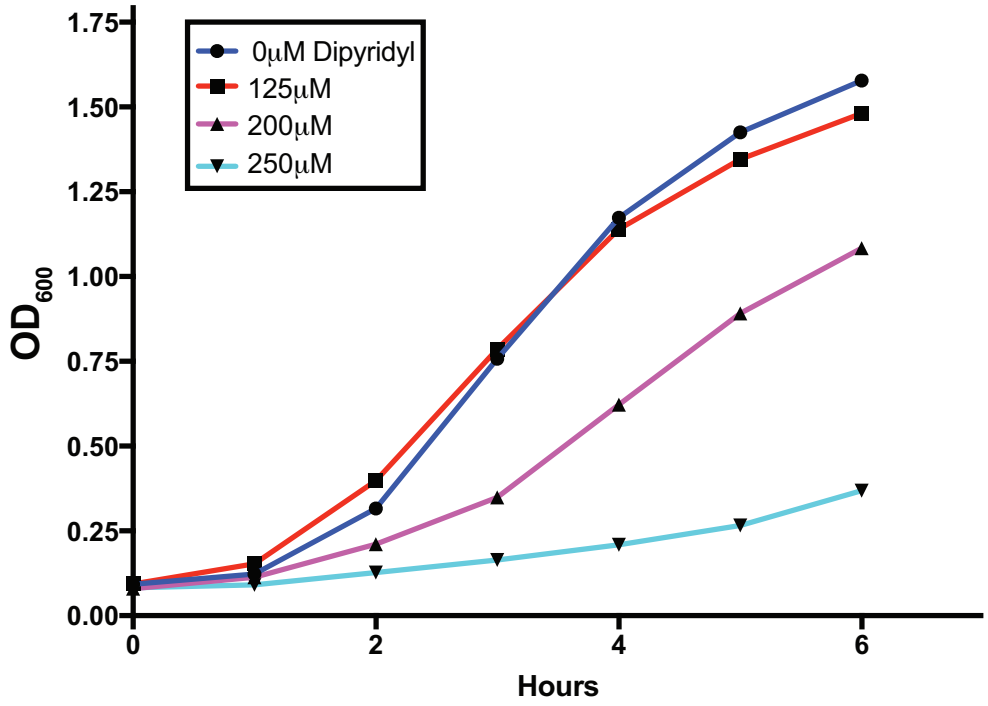

Figure 2.1. *Serratia marcescens* UMH9 growth is abrogated by increasing concentrations of dipyridyl.

Dipyridyl was added 0, 125, 200, and 250μM to *S. marcescens* UMH9 cultured in LB medium. Bacterial growth was measured by monitoring OD_{600} every hour as cultures were incubated with aeration at 37˚C. A concentration of 200μM dipyridyl was used to achieve iron-limiting conditions for RNA-sequencing. Results are representative of three independent experiments.

Up-regulated genes related to iron uptake were grouped into systems. Heme uptake systems, *hem* and *has*, were identified. The *hem* operon is composed of seven genes including an outer membrane heme receptor as well as components for ABC transport through the perisplasm. The *has* system also has seven genes that include genes encoding the hasA hemophore and the corresponding hasR receptor. Genes involved in ferrous iron uptake were upregulated and identified as the *sit* and *efe* systems. The *sit* system is composed of four genes, *sitABCD*, that constitute components for ABC transport through the inner membrane. Three genes were identified in the *efe* ferrous iron uptake system, *efeBOU*, consisting of a peroxidase, periplasmic binding protein, and a permease. A ferric-citrate uptake system, *fecARI*, was upregulated that encoded a receptor and two regulatory elements. The results also identified two putative siderophore operons. The first locus was composed of five genes (BVG96_RS08795-08815), encoding a receptor, exporter, and biosynthetic elements. The second locus had fifteen upregulated genes: eight involved in biosynthesis, three involved in transport, one involved in degradation, and three hypothetical proteins. Seven additional orphan TonB-dependent transporters were up-regulated as well, including a predicted aerobactin receptor, suggesting that UMH9 can import siderophores through multiple transporters or bring in xenosiderophores. Functions were predicted based on gene similarity studies (Table 2.1).

Table 2.1. Up-regulated iron acquisition systems in Serratia marcescens UMH9 during iron-limited RNA-seq.

Function	Locus Tag BVG96_RS…	Gene	Description	Log_2FC[a]
Heme uptake	*01515*	*hasI*	RNA polymerase sigma factor	3.38
	01520	*hasS*	Antisigma factor	3.09
	01525	*hasR*	TonB-dependent receptor	5.25
	01530	*hasA*	Hemophore	6.64
	01535	*hasD*	Type I secretion system permease/ATPase	4.04
	01540	*hasE*	Periplasmic adaptor subunit	3.90
	01545	*tonB/hasB*	Energy transducer	3.03
	07350	*hemV*	Heme ABC transporter ATP-binding protein	5.70
	07355	*hemU*	Hemin ABC transporter permease	6.54
	07360	*hemT*	Periplasmic hemin-binding protein	6.25
	07365	*hemS*	Hemin-degrading factor	6.89
	07370	*hemR*	TonB-dependent receptor	7.77
	07375	*hemP*	Hemin uptake protein	7.48
	07380		Glutathione peroxidase	3.97
Ferrous iron uptake	*07170*	*sitD*	Iron ABC transporter, inner membrane permease	2.18
	07175	*sitC*	Iron ABC transporter, inner membrane permease	Not represented
	07180	*sitB*	Iron ABC transporter, ATP-binding protein	2.87
	07185	*sitA*	Iron ABC transporter, periplasmic-binding protein	3.36
	11025	*efeB*	Iron transport peroxidase	2.75
	11030	*efeO*	Iron transport periplasmic protein	2.79
	11035	*efeU*	Iron transport permease	2.77
Ferric citrate transport	*07970*	*fecA*	TonB dependent receptor	5.45
	07975	*fecR*	Operon regulator	6.02
	07980	*fecI*	RNA polymerase sigma factor	6.16
Putative siderophore biosynthesis and transport	*08795*		Siderophore exporter	3.89
	08800		Non-ribosomal peptide synthetase	6.30
	08805		Chaperone	6.74
	08810		Esterase	6.86
	08815		TonB-dependent receptor	6.28
	21965		Condensation protein	5.12
	21970		Adenylation protein	5.96
	21975		Glutamate racemase	6.05

	21980		TonB-dependent receptor	7.62
	21985		Condensation protein	6.65
	21990		Hypothetical protein	6.47
	21995		TonB-dependent receptor	4.41
	22000		Esterase	5.47
	22005		Chaperone	5.80
	22010		Non-ribosomal peptide synthetase	4.60
	22015		Siderophore exporter	3.61
	22020		Isochorismate synthase	5.32
	22025		DHB adenylate synthase-AMP ligase	5.59
	22030		Isochorismatase	5.62
	22035		Hypothetical protein	5.55
Additional Iron Transporters	*12820*		TonB-dependent siderophore receptor	7.03
	01005	*iutA*	Aerobactin siderophore receptor	4.04
	01485		TonB-dependent siderophore receptor	5.88
	11645		TonB-dependent receptor	4.51
	14005		TonB-dependent siderophore receptor	5.54
	14175		TonB-dependent receptor	5.74
	14360		TonB-dependent siderophore receptor	3.91

[a]FC: fold change

Discussion

This Chapter took a global approach using RNA-seq to identify the iron-regulated transcriptome of a clinical isolate of *Serratia marcescens*. The results revealed all genes involved in iron acquisition and provided a starting point for follow-on studies examining the identified systems.

Results from iron-depleted RNA-sequencing identified iron uptake systems including siderophore biosynthetic loci, heme uptake systems, ferrous iron uptake, and citrate utilization systems. An additional seven Ton-B dependent receptors were also regulated by iron acquisition that were located outside of these loci. While these systems have been reported in other Gram-negatives, this is the first study to comprehensively identify all genes and systems involved in *Serratia marcescens* iron acquisition, a bacterium that has a unique history as an environmental pathogen evolving to become pathogenic in humans.

Because *Serratia* has a wide breadth of hosts, both environmental and mammalian, it is interesting to hypothesize where the identified iron acquisition systems may be most advantageous. For example, ferrous iron is more abundant in soils than in the human host [121]; therefore, the *sit* and *efe* systems may play a larger role in the environment than in mammalian infection. Iron acquisition via citrate uptake may prove to be advantageous in plant or insect pathogenesis where a lower affinity iron chelator is sufficient [122].

Not only does UMH9 encode dedicated systems for siderophore, heme, ferrous iron, and citrate uptake, but the RNA-seq also identified seven “ophan” receptors that contribute to iron acquisition. It is unknown what role these receptors play in iron uptake; however, it is

hypothesized that they are additional receptors for siderophore import or piracy of siderophores produced by surrounding microbes.

Together, these results provide a high-level perspective on all of the iron acquisition systems that well-equip Sm for iron uptake in many environments. Although, we do not know which ones contribute most significantly to human pathogenesis. Based on the RNA-seq results and the role siderophores and heme uptake play in mammalian infection caused by other Gram-negatives, I crafted the studies presented in the proceeding chapters to elucidate how these systems contribute to the virulence of Sm.

The results from this RNA-seq experiment were utilized to achieve the ambitious goal of this dissertation project, which was to fully characterize the major iron acquisition systems in a clinical isolate of *S. marcescens*.

Methods and Materials

Bacterial Culture and Development of Iron-Limited Conditions

S. marcescens strain UMH9 was routinely cultured in LB medium at 37˚C. To achieve iron-depletion, overnight cultures of UMH9 in LB medium were collected by centrifugation the following day. Cultures were washed three times with LB medium containing 200 μM dipyridyl, an iron chelator. Bacteria were then sub-cultured into LB medium containing either 0 μM, 100 μM, 200 μM, or 250 μM dipyridyl to determine an appropriate dipyridyl concentration before proceeding with RNA-seq.

RNA Purification and Sequencing

S. marcescens strain UMH9 was cultured overnight at 37˚C in LB medium. The following day, bacteria were collected by centrifugation and washed three times with LB medium containing 200 μM dipyridyl. Washed bacteria were diluted 1:100 into either LB or LB + 200 μM dipyridyl, and incubated at 30˚C with shaking until an optical density at 600nm (OD_{600}) between 0.4 and 0.5 was reached. RNA was stabilized using RNAprotect (Qiagen). Bacteria were lysed by incubation for 10 minutes at room temperature with 15mg/ml lysozyme (Sigma-Aldrich) and 20mg/ml Proteinase K (Qiagen). The RNAeasy mini kit (Qiagen) was used to purify RNA according to the directions of the manufacturer. Turbo DNase (Thermo Fisher) was used to deplete genomic DNA contamination. RNA was further purified using the RNEasy mini kit (Qiagen). rRNA removal, library preparation, and sequencing were performed by the University of Michigan Sequencing Core using the ScriptSeq Complete Kit (bacteria) library kit (Illumina). cDNA libraries were sequenced using Illumina HiSeq 2500 (single-end, 50bp read length). Detailed methods outlining the RNA-seq analysis can be found in Appendix A.

Chapter III

Elucidating the Role of *cbsF* and *schF0*, Components of the NRPS Machinery, in Iron Transport

Notes. The introduction of this chapter was adapted from the following article:

Weakland DR, Smith SN, Bell B, Tripathi A, Mobley HLT. The *Serratia marcescens* Siderophore Serratiochelin Is Necessary for Full Virulence during Bloodstream Infection. *Infect Immun*. 2020; 88(8): e00117-20. Published 2020 Jul 21. doi:10.1128/IAI.00117-20

Abstract.

S. marcescens possesses broad environmental niches, and was initially dismissed as being a human pathogen. However, over the last several decades, it has caused severe infections with increasing frequency. Because *S. marcescens* has only recently been recognized as a threat to public health, little is known about factors contributing to *S. marcescens* virulence specifically regarding iron acquisition. The initial objective was to define how two siderophore loci, *cbs* and *sch*, found by RNA-sequencing analysis contribute to the pathogenesis of UMH9, a *S. marcecens* bloodstream isolate. Deletions were made mutating the non-ribosomal peptide synthetase (NRPS) machinery in each siderophore operon and then a double mutant deleting both together. Culturing in iron-poor conditions revealed that the double NRPS mutant had defective growth;

however, it still produced siderophore demonstrated by chrome azurol S (CAS) assay and mass spectrometry. The single NRPS mutants behaved similarly to wild type. These results suggest that the two NRPS genes could have redundant roles in siderophore transport, challenging the paradigm that NRPS genes are non-redundant and exclusively functional in biosynthesis.

Introduction

Historically*, Serratia marcescens* has been considered an environmental pathogen due to its ability to infect insects and survive in soil and aquatic reservoirs. However, over the last several decades, *S. marcescens* has emerged as a major opportunistic pathogen in humans causing deadly infections that include bacteremia and endocarditis [99]. Antibiotic-resistant isolates of this Gram-negative pathogen continue to arise [99] and emergent strains have been found to carry multiple virulence factors including a hemolysin, various proteases and nucleases, and a polysaccharide capsule[98, 123]. Despite these observations, it is clear that significant research is still required to advance our understanding of the pathogenesis of *S. marcescens*.

Iron is essential to many cellular processes in bacteria, and therefore critical to pathogenesis [124]. Humans harbor approximately three to four grams of total iron within their bloodstream and tissues [125]; however, most of this iron is not readily available, as it is sequestered by host proteins including transferrin, ferritin, ferroportin, lactoferrin, myoglobin, and hemoglobin [126-128]. As such, free iron concentrations in serum are less than 10^{-24} M at physiological pH, requiring microbes to have developed specific strategies to access iron sequestered within host proteins and enable survival [129]. For example, heme acquisition systems use dedicated cell surface receptors in concert with the TonB complex to bind and

internalize host heme, releasing the iron molecule into the bacterial cytoplasm [37]. In addition, siderophores, small organic molecules with high affinities for iron ($K_d > 10^{-30}$ M) [14], are synthesized by bacteria and exported to the extracellular space to scavenge iron from host proteins, including transferrin, lactoferrin, and ferritin. Outer membrane TonB-dependent receptors then facilitate the import of iron-loaded siderophores into the bacterial cytoplasm [127].

Iron acquisition has been studied extensively in the context of other Gram-negative pathogens, especially *Escherichia coli* [19]. For example, uropathogenic *E. coli* mutants lacking receptors for specific siderophores or heme import show decreased fitness in both the bladder and kidney in a mouse model of ascending urinary tract infection, establishing the importance of iron uptake during infections of the bladder and kidneys [18]. Additionally, hypervirulent strains of *Klebsiella pneumoniae* encode up to four siderophore systems [100]. These systems have been shown to induce host inflammatory cytokines and facilitate bacterial dissemination during pneumonia [101].

Despite the importance of iron acquisition to the pathogenesis of other Gram-negative bacteria, comparatively little is known about the contribution of *S. marcescens* iron uptake systems to its pathogenesis in mammalian hosts. Nevertheless, there has been some work defining the molecular mechanisms of *S. marcescens* iron acquisition with particular focus on heme uptake, characterizing two systems, Hem and Has [130]; however, the only studies defining *S. marcescens* siderophores have been performed in non-mammalian systems. A transposon library constructed in *S. marcescens* Db11, initially described as a *Drosophila melanogaster* pathogen, was used to identify a mutation within a predicted siderophore biosynthetic gene that displayed reduced virulence in a *Caenorhabditis elegans* model of

infection [105]. Previous studies have shown several potential siderophores produced by *Serratia* species. For example, *Serratia liquefaciens* and *Serratia ficaria* produce the siderophore aerobactin, whereas *S. marcescens* does not. Many isolates, however, typically encode an aerobactin receptor [106, 108]. *S. marcescens* W225 synthesizes another siderophore, enterobactin, and can utilize ferric citrate as an iron source as well [108].

A siderophore, designated serratiochelin, is also commonly produced by the *S. marcescens* and *Serratia plymuthica* species. Biochemical studies have been undertaken to analyze serratiochelin synthesis. The results allowed the authors to hypothesize that serratiochelin is a molecular hybrid of enterobactin and vibriobactin, based on gene similarity and mutagenesis experiments [107]. Other studies have shown that *S. marcescens* also produces a low-affinity siderophore, chrysobactin, first identified in *Dickeya chrysanthemi* [120]. Genes associated with the synthesis of either serratiochelin or chrysobactin have been found in sequenced genomes of other *S. marcescens* strains. For example, a clinical isolate of *S. marcescens*, SM6, is predicted to produce serratiochelin and chrysobactin based on genetic identity to the *schF* (nonribosomal peptide synthetase [NRPS] in *S. plymuthica* V4) and *cbsF* (NRPS in *D. dadantii* 3937) genes, respectively [131].

Many siderophores are synthesized through non-ribosomal peptide synthetase (NRPS) dependent pathways. Starting with precursor molecules, such as dihydroxybenzoate, siderophores are built by a series of enzymatic reactions on multidomain protein assembly lines called NRPSs that elongate the intermediate siderophore molecule. NRPSs typically consist of an initiation module, elongation module, and termination module, which, depending on the organism and complexity of the siderophore, can be encoded by many separate genes within the biosynthetic operon or within just a few. These three modules combined synthesize the final

siderophores by incorporating amino acids into the peptide product. Variations in the functional domains of the NRPS result in the production of many bacterial siderophores [16, 132].

In this chapter, two siderophore loci were identified in a bloodstream isolate of *Serratia marcescens* UMH9 and predicted to synthesize chrysobactin (*cbs*) and serratiochelin (*sch*) based on previous literature. Deletions in predicted biosynthesis genes involved in the NRPS machinery from each operon (*ΔcbsF* and *ΔschF0*) individually had no effect on growth in iron-poor medium or iron chelation. However, when NRPS components were deleted together in a double mutant (*ΔcbsF*/*schF0*), the double mutant had defective growth in iron-limited conditions. Despite this inhibited growth, siderophore production was notably increased compared to the WT and single mutants. Mass spectrometry identified serratiochelin to be present in all mutant supernatants, ruling out the production of an ineffectual siderophore caused by the double mutation. These results suggest a yet to be described novel role in siderophore transport of the NRPS machinery in both the *sch* and *cbs* loci of *Serratia marcescens*.

Results

cbsF and *schF0* are non-ribosomal peptide synthetases involved in siderophore biosynthesis.

From the RNAseq results in Chapter II, I identified two potential siderophore operons in UMH9. Based on their similarity to published chrysobactin and serratiochelin loci, I labeled them *cbs* and *sch*, respectively. To examine how each siderophore contributed to bacterial pathogenesis, I began by investigating *cbsF* and *schF0*. *cbsF* and *schF0* encode non-ribosomal peptide synthetases (NRPS) theoretically involved in the biosynthesis of chrysobactin and

serratiochelin, respectively. Further details on the composition of these loci will be covered in Chapter IV.

Serratiochelin and chrysobactin both depend on NRPSs for production. Within the 28 kb locus responsible for serratiochelin biosynthesis, three to four genes, *schF0, schF1, schF2, and schF3*, presumably constitute the full NRPS machinery based on gene similarity to other known NRPSs. *schF0* contains modules characteristic of an NRPS such as condensation, adenylation, thiolation, and thioesterase domains likely involved in elongation and termination processes. Several other genes likely involved in the NRPS machinery are also found in this locus (Figure 3.1A). The chrysobactin locus is much smaller with only five genes, including an exporter, a receptor, a chaperone, and two biosynthesis genes. One large gene, *cbsF*, encodes all NRPS modules, including condensation, adenylation, thiolation, epimerization, and a thioesterase. It also contains repeated condensation, adenylation, and thiolation domains that incorporate additional amino acids into the growing siderophore within the same protein, negating the need for additional NRPS genes. This siderophore locus structure is often seen within fungal organisms; however, there are no reports detailing if chrysobactin has fungal origins (Figure 3.1B) [133, 134].

I confirmed that the *cbs* and *sch* operons, including *cbsF* and *schF0*, were regulated by iron concentration using qRT-PCR from mid-log phase cultures in iron rich and iron-limited conditions (Figure 3.1C).

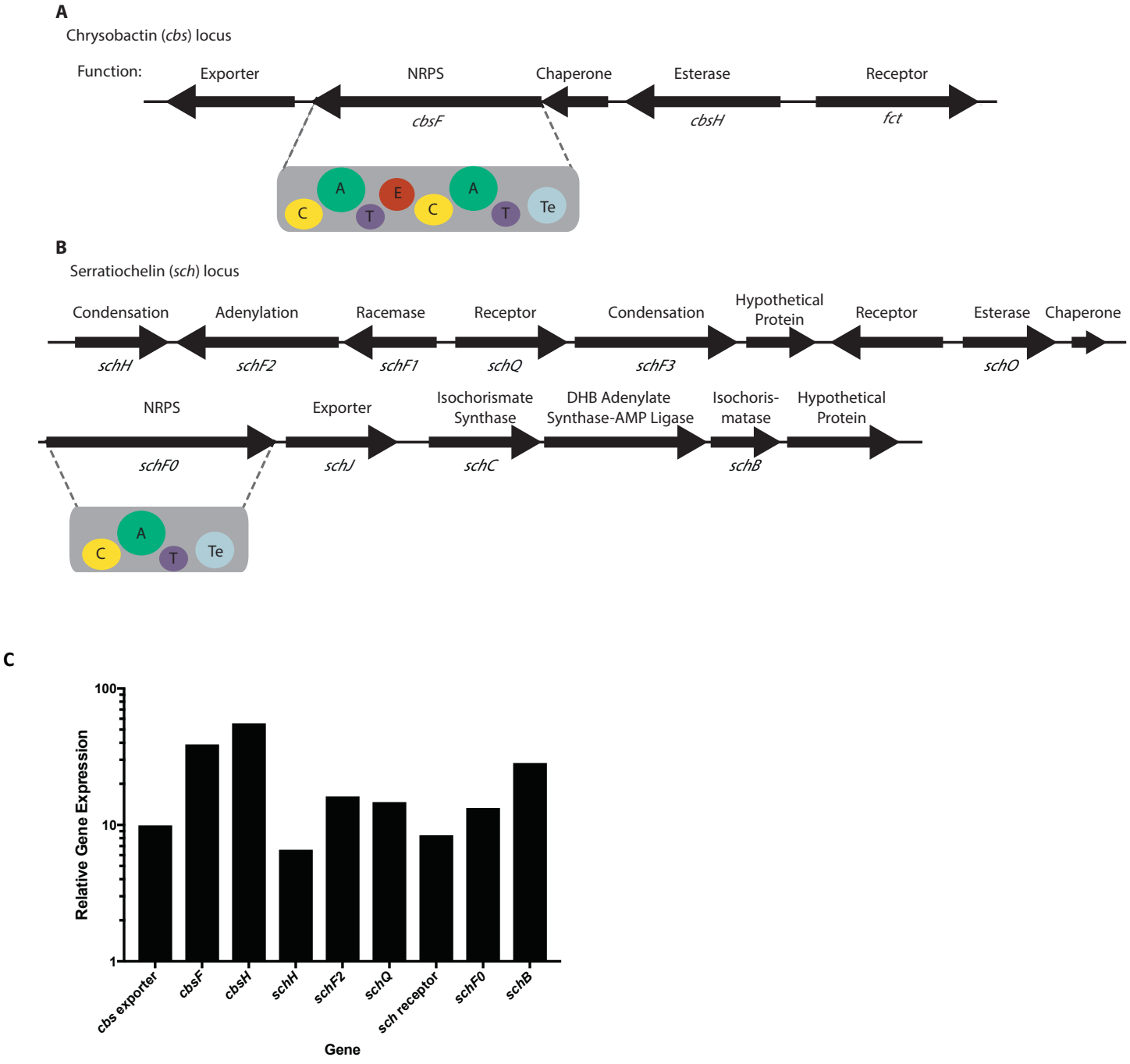

Figure 3.1. Domain structure of *cbsF* and *schF0* reveal important moieties for siderophore synthesis and are up-regulated under iron-limitation.

The structure of the *cbs* (A) and *sch* (B) loci are depicted. Genes are annotated based on similarity to genes found in the chrysobactin and serratiochelin loci of *Dickeya dadantii* and *Serratia plymuthica*, respectively. More information on the *Dickeya dadantii* chrysobactin locus and the *Serratia plymuthica* serratiochelin locus can be found in Chapter IV (Figure 4.1). *cbsF* (A) and *schF0* (B) contain domains pertinent to siderophore production. C = condensation, A = adenylation, T = thiolation, E = epimerization, Te = thioesterase. (C) cDNA from UMH9 WT cultured with and without dipyridyl were used to confirm the expression of *cbsF* and *schF0* under iron limitation. Transcript expression is shown in iron-depleted conditions relative to iron-rich conditions.

The *ΔcbsF/schF0* mutant had defective growth in iron-limited conditions.

I deleted *cbsF* (*ΔcbsF*) and *schF0* (*ΔschF0*) individually and in combination (*ΔcbsF/schF0*) in the UMH9 wild type strain to abolish siderophore synthesis. Because NRPSs are typically essential for siderophore biosynthesis, I measured the ability of each mutant to grow in several conditions with varying iron concentrations. I expected the single mutants to perform similarly to WT as they still produced an intact siderophore, while the double mutant would have inhibited growth in iron-poor conditions since siderophore biosynthesis is presumably abolished.

First, I measured growth in several M9 minimal medium conditions where iron was removed or added back in at 36 μM FeSo4. As expected, in growth medium where iron was replete, all strains grew similarly (Figure 3.2C, D). However, when iron was limited, the double mutant, *ΔcbsF/schF0*, grew worse than the other strains. The *ΔcbsF/schF0* mutant was severely growth restricted under these conditions, and this growth defect was exclusive to iron-limitation as it grew similarly to the other strains when there was sufficient iron in the medium (Figure 3.2A, B). This prompted me to examine at what concentration of iron the double mutant is able to overcome this growth defect. To test this, I titrated FeSO4 into iron-depleted M9 minimal medium at 0 μM, 1 μM, 10 μM, 20 μM, and 30 μM, and measured growth. The WT grew similarly at all tested iron concentrations with a slightly lowered saturation point at 0 μM FeSO4 (Figure 3.3A). The double mutant had defective growth at 0 μM and 1 μM FeSO4, but grew comparably to WT at all other tested concentrations (Figure 3.3B). These results suggest that only a small amount of iron is needed for normal growth, and the double mutant is growth restricted at low iron concentrations where the WT is able to grow adequately.

Finally, I examined growth in LB medium supplemented with dipyridyl (an iron chelator) to see how the double mutant fared when it had to compete for iron from a chelator already

present in the medium. Dipyridyl was titrated into LB medium at 0 μM, 125 μM, and 220 μM. WT and *ΔcbsF/schF0* grew similarly in LB medium alone. While both the WT and double mutant had decreased growth with increasing concentration of dipyridyl, the *ΔcbsF/schF0* mutant showed notable defective growth at both of the tested dipyridyl concentrations. At 125 μM dipryidyl, the WT saw similar growth to 0 μM, but the double mutant did show impaired growth (Figure 3.4A). Then, *ΔcbsF/schF0* was growth restricted compared to the WT at 220 μM dipyridyl. The IC_{50} for dipyridyl was determined to be 152 μM for the double mutant, compared to 210 μM for the WT (Figure 3.4B).

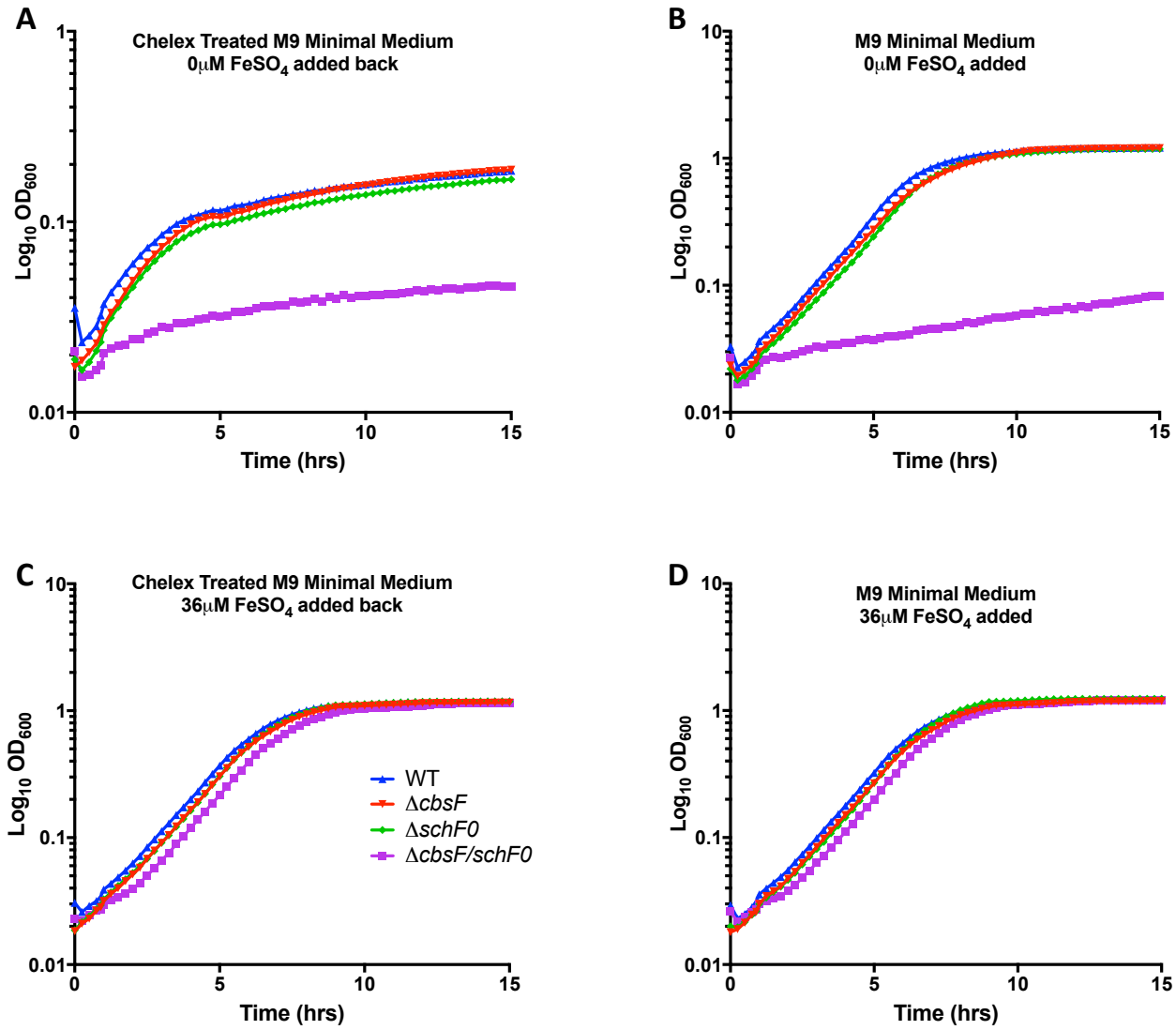

Figure 3.2. The *ΔcbsF/schF0* mutant displays defective growth in iron-poor media.

The indicated strains were grown in either chelex treated (iron removed) (A, C) or normal M9 minimal medium (B, D). 36μM $FeSO_4$ was added to the cultures where indicated (C, D). Cultures were incubated with aeration at 37˚C and OD_{600} readings were taken every 15 minutes to measure bacterial growth. Results are representative of three biological replicates.

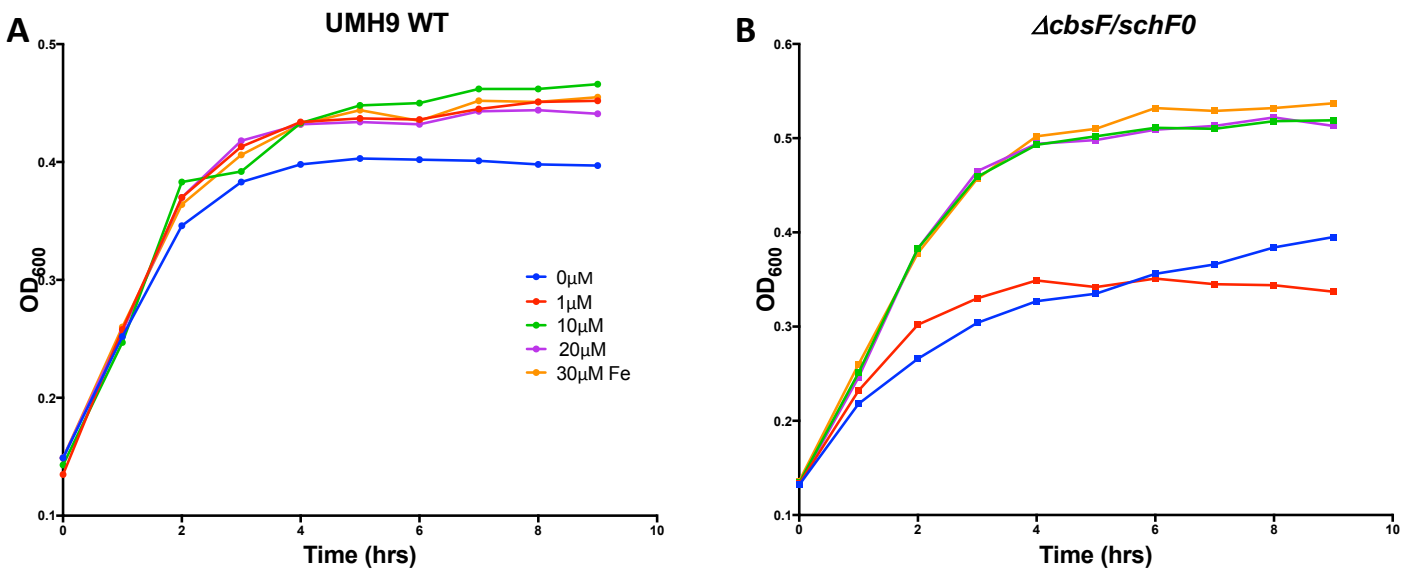

Figure 3.3. *ΔcbsF/schF0* struggles to overcome its growth defect at low iron concentrations. The WT (A) and *ΔcbsF/schF0* (B) strains were grown in chelex treated M9 minimal medium with 0 μM, 1 μM, 10 μM, 20 μM, or 30 μM $FeSO_4$ supplemented into the culture. Cultures were incubated at 37 ˚C with OD_{600} readings were taken every hour for 9 hours. Results are representative of three biological replicates.

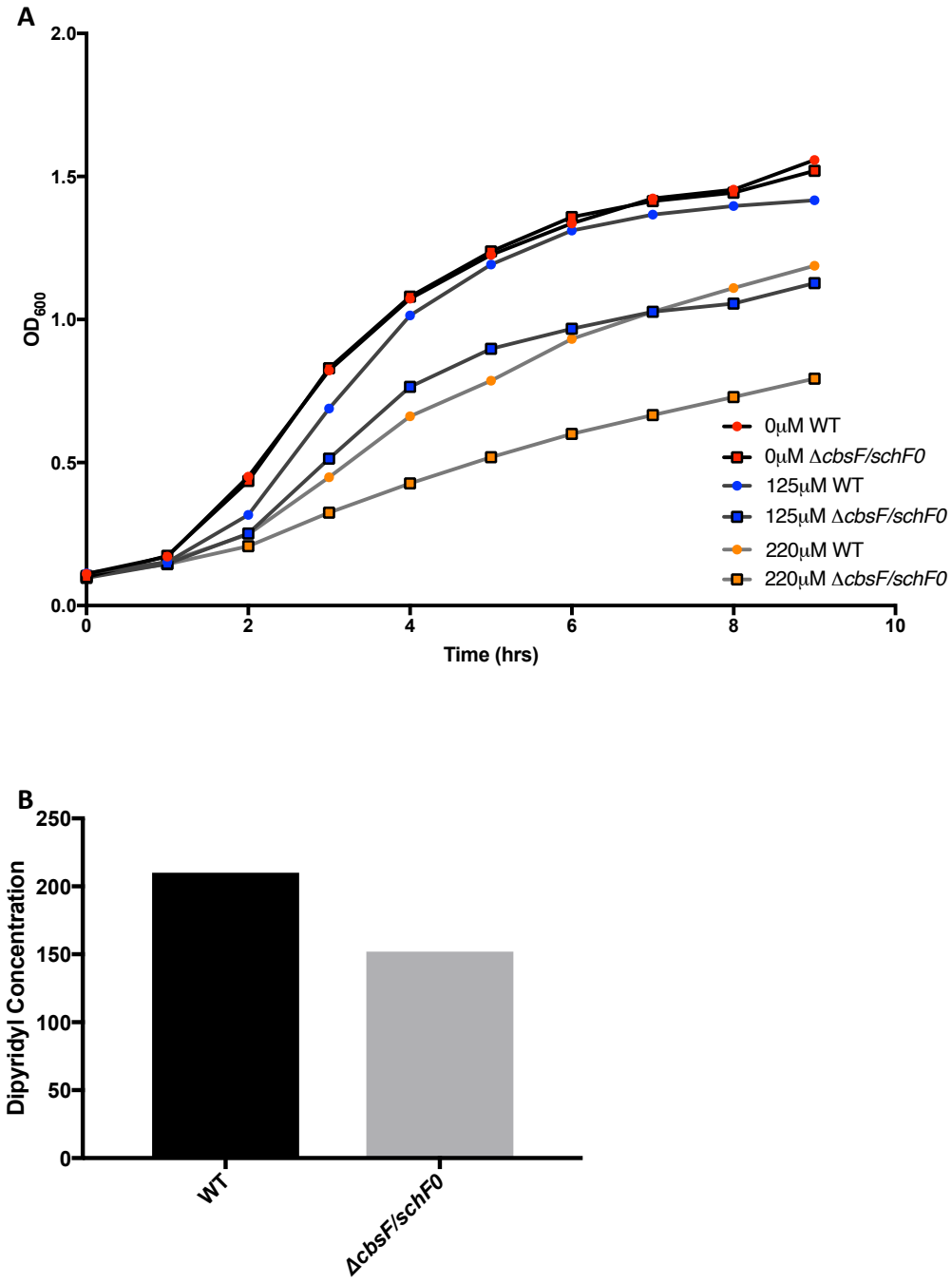

Figure 3.4. *ΔcbsF/schF0* is inhibited by lower dipyridyl concentrations compared to WT. (A) The wild type and *ΔcbsF/schF0* strains were grown in LB with 0μM, 125μM, or 220μM dipyridyl and growth was measured every hour for 9 hours. (B) The half maximal inhibitory

concentration (IC_{50}) of dipyridyl was calculated for the WT and *ΔcbsF/schF0* strains based on the tested dipyridyl concentrations.

Loss of both *cbsF* and *schF0* together resulted in increased iron chelation.

As expected, the double mutant severely struggled to grow in iron-limited conditions most likely due to insufficient iron uptake from the loss of siderophore function. In a chrome azurol S (CAS) assay measuring siderophore production, I hypothesized individual NRPS mutants would have minimal to no reduction in iron chelation since the other siderophore was still intact, while the double mutant would have significant reduction in siderophore production. To test the amount of siderophore production by each strain, I measured iron chelation using CAS agar. Strains were grown overnight in iron-depleted M9 minimal medium. These cultures were inoculated onto CAS agar the following day. After 48 hours of incubation at 37 °C, the WT, *ΔcbsF*, *ΔschF0* mutants showed comparable iron chelation as they all had yellow circles of similar diameter surrounding the point of inoculation. Surprisingly, the double mutant, *ΔcbsF/schF0*, demonstrated notably more iron chelation than any other strain even though it had defective growth in iron-limited conditions. This suggests that a siderophore is still being produced but the bound iron is not able to be used when both *cbsF* and *schF0* are deleted. Interestingly, the single mutants had phenotypes similar to the WT suggesting a redundant function of the *cbsF* and *schF0* genes in UMH9 iron uptake (Figure 3.5A, B).

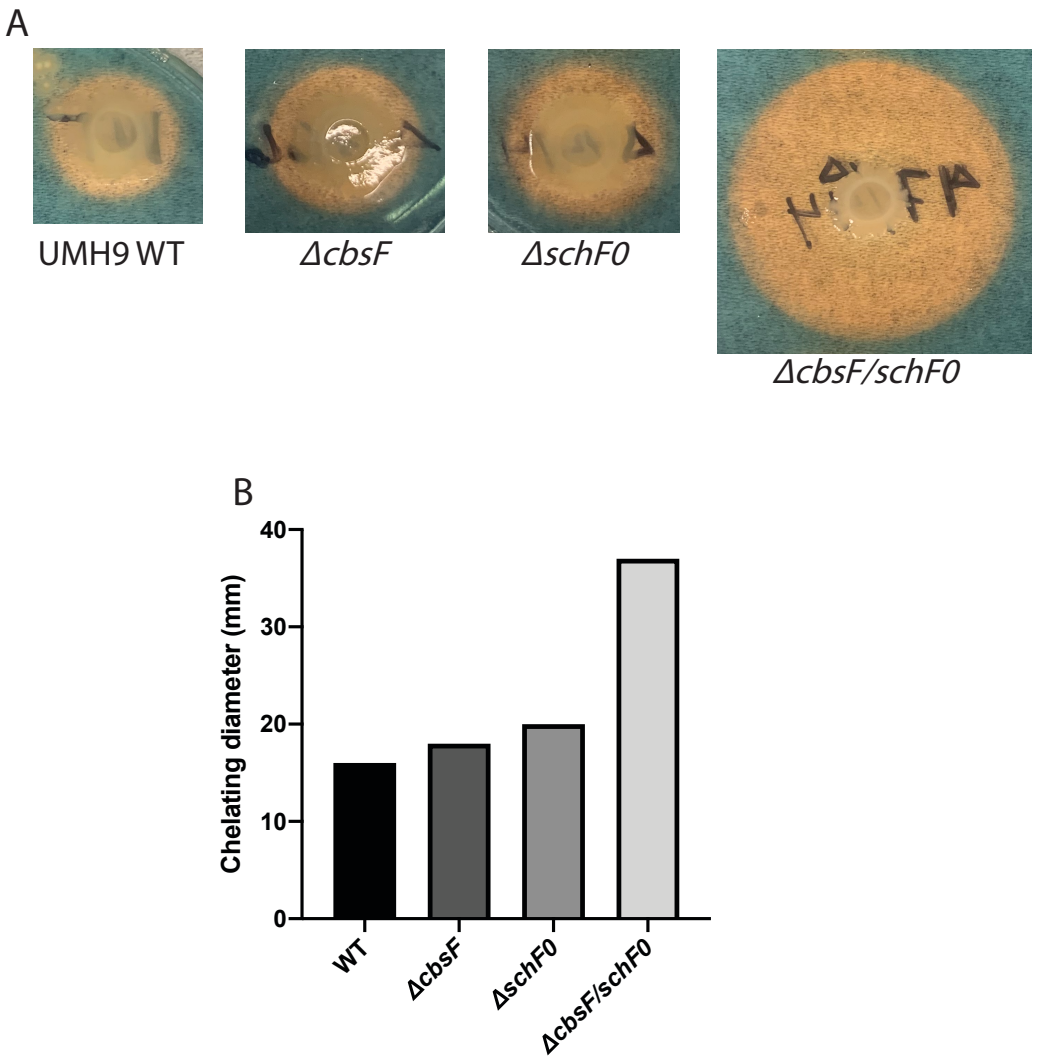

Figure 3.5. The *ΔcbsF/schF0* mutant showed increased siderophore production.

Iron chelation was measured using CAS agar plates. UMH9 WT and the mutant strains were cultured overnight in M9 minimal medium and spotted onto CAS agar the following day. A larger yellow circle surrounding the point of inoculation correlates to increased siderophore production. Images of the CAS plate for each strain after two days of incubation are shown (A). (B) The diameter of the yellow circle surrounding each bacterial strain was measured.

Serratiochelin was detected *in ΔcbsF/schF0* supernatants by mass spectrometry.

Interestingly, *ΔcbsF/schF0* had increased siderophore production observed on CAS agar despite the defective growth seen in iron-limited conditions. This suggests an alteration to the produced chelator caused by the double mutation that is affecting cellular use of the siderophore. Thus, I sought to identify siderophore precursor molecules of chrysobactin and serratiochelin that could be contributing to the increased chelation, but are potentially less able to provide sufficient iron to the bacterial cell.

Mass spectrometry (MS) was performed on bacterial supernatants after WT, *ΔcbsF*, *ΔschF0*, and *ΔcbsF/schF0* were cultured overnight in iron-depleted M9 minimal medium as well as in minimal medium supplemented with 36 μM $FeSO_4$. Based on previous literature and the similarity of the putative *sch* locus to serratiochelin-producing operons, we used fragmentation patterns matching that of serratiochelin as a reference. MS/MS spectra obtained from bacterial extracts of the wild type and mutants were first analyzed using a global natural product search (GNPS)-based DEREPLICATOR+ algorithm for probing the presence of serratiochelin [135, 136]. The algorithm compared our data set to all spectra in the GNPS database enabling high throughput identification of known natural products present in the bacterial extract.

To analyze our samples using DEREPLICATOR+, we opted for a stringent score threshold of 0% false discovery rate (FDR) and removed the metabolites present in blank samples that consisted of M9 growth medium only. The analysis clearly showed the presence of an $[M+H]^+$ ion at 430.1723 *m/z* and an $[M+Na]^+$ ion at 452.1470 *m/z* (Appendix A, Figure A.1) with the molecular formula of $C_{21}H_{23}N_3O_7$, identifying the presence of serratiochelin A in all supernatants, including *ΔcbsF/schF0*, when iron was depleted. Serratiochelin was not found in culture supernatants supplemented with iron as expected (Figure 3.6). Taking these results with

the iron-depleted growth phenotypes, I hypothesize that the single NRPS mutants play a redundant role in iron uptake that is abolished when both genes are deleted in the double mutant.

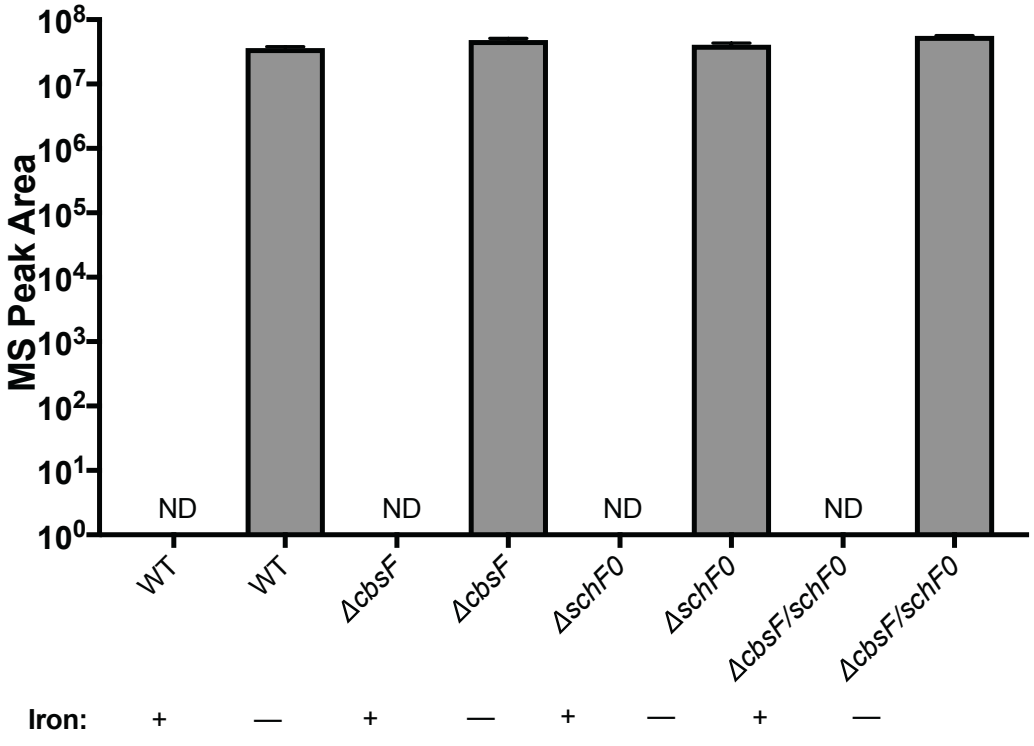

Figure 3.6. Serratiochelin is detected in all bacterial mutants by mass spectrometry.

WT and the *ΔcbsF*, *ΔschF0*, and *ΔcbsF/schF0* were cultured overnight in M9 minimal medium with or without iron. Mass spectrometry was performed on bacterial supernatants and identified serratiochelin in all supernatants that were taken from iron-depleted bacterial cultures.

The *ΔcbsF/schF0* mutant is less fit and attenuated in the murine bacteremia model compared to WT.

Next, I hypothesized that the inability to use serratiochelin in the double mutant may translate into a colonization or competitive disadvantage in the mouse bacteremia model [137], and since UMH9 was isolated from a bacteremic patient; I wanted to determine if its *cbsF* and *schF0* contributed to its pathogenesis *in vivo*. I examined fitness of *ΔcbsF/schF0* compared to WT by injecting an inoculum containing a 1:1 mixture of the double mutant and WT culture into the mouse tail vein to model bacteremia. Each mouse received 5 x 10^7 CFU of inoculum. The competitive index was calculated for the spleen and liver 24 hours after infection. The *ΔcbsF/schF0* had a slight competitive disadvantage in both the spleen and liver (log CI, <0) (Figure 3.7A).

Mice were also mono-challenged with WT and the double mutant to determine how the mutant persisted in the bloodstream independently. Bacterial burdens were calculated after 24 hours in the liver and spleen. *ΔcbsF/schF0* had significantly less recovered bacteria compared to wildtype in both the spleen and liver (Figure 3.7B, C). These results suggest that the effects of the double mutation *ΔcbsF/schF0* result in a loss of fitness during bacteremia.

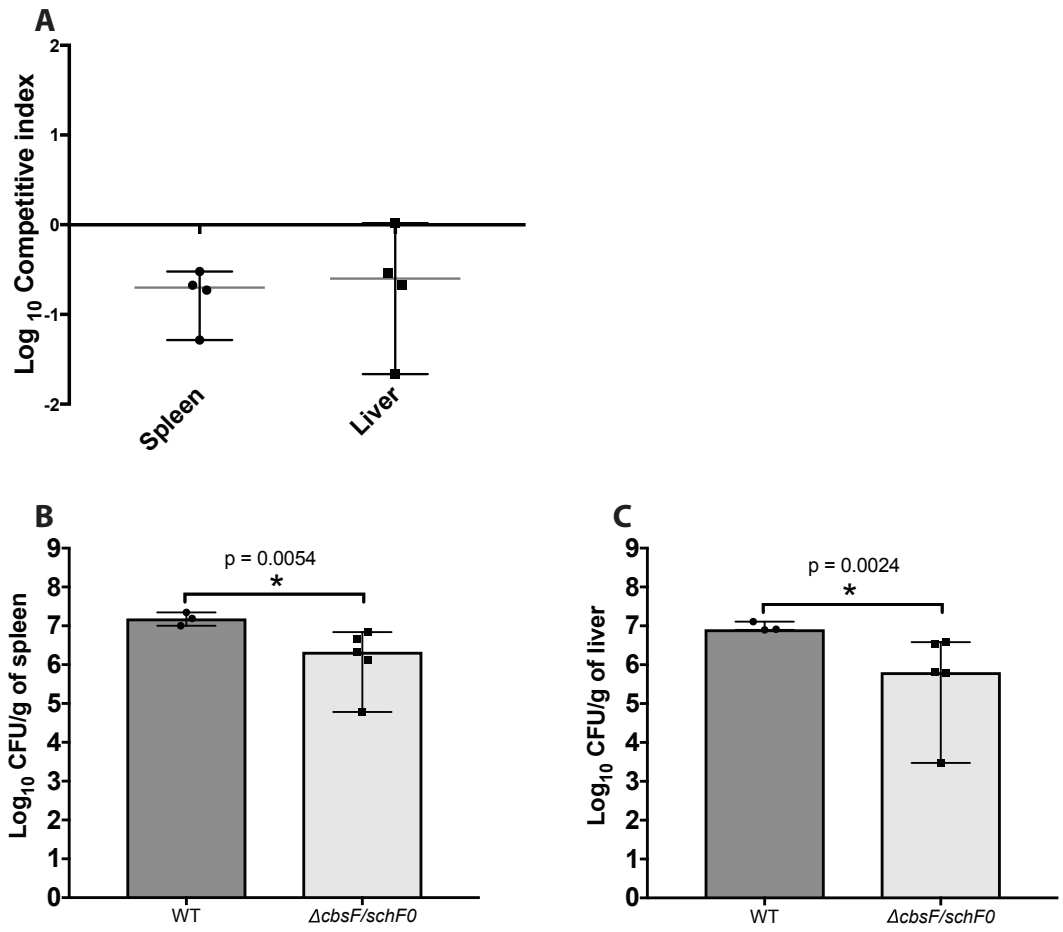

Figure 3.7. The *ΔcbsF/schF0* mutant was slightly attenuated in the murine bloodstream. (A) CBA/J mice were infected with 5×10^7 CFU/mouse in a 1:1 mixture of the wild type and the *ΔcbsF/schF0* double mutant via the tail vein. Mice were euthanized at 24 h and the spleen and liver were collected from each mouse. Organs were homogenized. Homogenates were diluted and selectively plated. The relative fitness for the mutant was compared to that of the wild type and calculated as a competitive index (CI). The solid black line represents a CI of 1.0, meaning that the two strains competed equally. Solid grey lines represent median CI. Statistics were calculated using the Wilcoxon signed-rank test with a theoretical median of 0. (B,C) Mice were independently inoculated with either WT or *ΔcbsF/schF0* mutant via the tail vein. Mice were

euthanized 24 h post inoculation. Spleens (B), and livers (C) were collected and homogenized. Homogenates were diluted and plated. The dotted line indicates the limit of detection. Significance, determined by the Mann-Whitney test, is indicated with asterisks.

Discussion

Here I demonstrate that UMH9 has two siderophore gene clusters found by RNA-sequencing analysis (Figure 3.1), and upon mutation of the NRPS machinery in both loci, growth was inhibited under iron-limited conditions (Figure 3.2). However, despite this defective growth, the double NRPS mutant still excreted intact serratiochelin to wild type levels (Figure 3.6). Additionally, I show that this mutation may affect UMH9 fitness and its ability to infect the murine bloodstream. This is the first description of a potential novel role for the NRPS machinery in the context of gram-negative infections. Prior to these results, NRPSs were not thought to have a significant role outside of small molecule synthesis; however, the findings within this chapter suggest otherwise.

The double *ΔcbsF/schF0* had interesting phenotypes that prompt several hypotheses. Both single mutants show phenotypes similar to that of WT in all experiments which is not surprising given that when knocking out one siderophore locus or the other, there is potential redundancy and compensation from the other gene cluster. However, in this case, the double mutant still produces intact serratiochelin yet struggles to grow in iron limitation. This suggests novel complementary roles of the CbsF and SchF0 proteins that when deleted together, can no longer be performed. Taking the CAS and iron-limited growth results alone, I hypothesized that the double mutant was excreting siderophore precursor molecules that bind up the extracellular iron, but are less able to be used by the bacterium. This would account for the increased iron chelation seen and the defective growth in iron-poor medium. However, upon analysis of bacterial supernatants by mass spectrometry, it became clear that precursor molecules were not responsible for these phenotypes as intact serratiochelin was being produced in the double

mutant. This raises questions regarding the produced serratiochelin; is it defective in some way that the bound iron can't be used? Or, is there a siderophore transport issue in the double mutant either bringing in too much iron or not enough? Both would result in poor growth. This suggests that *cbsF* and *schF0* have a yet to be determined role in transport. Furthermore, these findings suggest that serratiochelin is continually being produced, resulting in increased CAS activity, because internal iron levels are too low to cause Fur repression of iron uptake gene expression.

NRPSs have been long appreciated for their essential role in siderophore synthesis. The NRPS biochemical pathway used in siderophore elongation by amino acid transfer and attachment has been extensively studied in the context of many siderophores including enterobactin, vibriobactin, yersiniabactin, etc. While *schF0* is not the only NRPS component in the serratiochelin locus; *sch* is unique in that the *schF0* NRPS component is completely skipped in the biosynthesis of serratiochelin as shown by my mass spectrometry results and also reported by Seyedsayamdost. The *schF0* element contains a termination domain with similarity to *entF* found in the enterobactin biosynthesis pathway responsible for incorporating an L-Serine into the enterobactin structure. Interestingly, the results from Seyedsayamdost *et al.* show evolutionary mixing and matching of the enterobactin and vibriobactin loci to form the serratiochelin locus. The enterobactin related genes seem to mainly be involved in the formation of earlier molecules in the pathway while the vibriobactin cluster mostly makes up the NRPS machinery involved later in the pathway [108]. This prompts the question of what role *schF0* plays, if any.

Previous studies looking at enterobactin production and transport have shown EntF and other NRPS components to be associated with the bacterial membrane despite being cytoplasmic proteins. These studies found EntF in membrane preparations and in the periplasmic space, potentially suggesting that these NRPS elements play a role in siderophore excretion and

transport. The authors also postulated that EntF along with other NRPS proteins might associate with cytoplasmic membrane pumps [16, 138]. These studies support my hypothesis that CbsF and SchF0, EntF homologs, could be involved in serratiochelin transport across either the outer membrane, periplasm, or cytoplasmic membrane.

More work is required to confirm this hypothesis starting by determining the location of CbsF and SchF0 with membrane fractionation. This would then inform what proteins CbsF and SchF0 are potentially interacting with in the transport pathway, requiring protein-protein interaction studies. If they're found in the outer membrane, CbsF and SchF0 could be chaperoning transport through the receptor itself. The periplasm and cytoplasmic membranes would suggest potential interaction with the TonB complex or the ATP powered complexes such as the *S. marcescens* FepBCGD/FhuABCD homologs that carry molecules across the inner membrane. It should also be determined if serratiochelin is reentering the bacterium at all after excretion, and at what step in transport it is blocked. Complementation studies should also be performed to confirm that the phenotype is rescued when both *cbsF* and *schF0* are complemented individually into the double mutant background. This would confirm a redundancy hypothesis.

An alternative hypothesis is the possible role in regulation of *cbsF* and *schF0*. These genes may feedback to the ferric uptake regulator (Fur), signaling to turn off siderophore production once iron requirements are met. Without this signal, there is constant siderophore production leading to too much iron, generating toxic superoxide radicals, and thus defective growth. Another hypothesis is that the ferri-siderophore is being transported, but the iron is unable to be accessed once inside the bacterium.

To conclude, while this chapter had the initial intention of determining how *S. marcescens* UMH9 siderophores contribute to pathogenesis, it uncovered something unexpected: a potential redundancy of two NRPS genes and a novel role in iron acquisition outside of biosynthesis. Even though much more work is left to fully understand the underlying mechanism behind the results presented here, these findings challenge our typical understanding of how NRPSs function and the role they play in bacterial pathogenesis.

Methods and Materials

Bacterial Strains and Culture Conditions

All *Serratia marcescens* strains used in this study are described in Table 3.1. Luria broth (10 g/L tryptone, 5 g/L yeast extract, 0.5 g/L NaCl) was used for routine culture of bacteria. Antibiotics were added to cultures at the following concentrations when appropriate: kanamycin (25 µg/ml), chloramphenicol (30 µg/ml), spectinomycin (100 µg/ml). 2,2'-dipyridyl (Sigma-Aldrich), an iron chelator, was added to LB cultures at the indicated concentrations to achieve iron limitation. M9 defined medium (0.1 mM $CaCl_2$, 1mM $MgSO_4$, 0.4% glucose) was used to culture bacteria for mass spectrometry. M9 was treated with Chelex-100 to remove iron, creating iron-limited conditions. $FeSO_4$ (36 µM) was added back to M9 cultures where indicated.

Table 3.1. *S. marcescens* strains and plasmids

Name	Relevant genotype	Description	Reference or source
S. marcescens			
UMH9	Wild type	Bloodstream infection isolate	[98]
ΔcbsF	*cbsF::kan*	Deletion of gene *08800, cbsF,* replaced with kanamycin cassette from pKD4.	This study
ΔschF0	*schF0::cam*	Deletion of gene *22010*, *schF0*, replaced with chloramphenicol cassette from pKD3.	This study
ΔcbsF/schF0	*cbsF::kan, schF0::cam*	Double mutant with both gene, *cbsF* and *schF0*, deletions replaced with the indicated antibiotic cassette.	This study
Plasmids			
pKD4		Source of kanamycin resistance gene	[139]
pKD3		Source of chloramphenicol resistance gene	[139]
pSIM19		Recombineering plasmid	[140]

Mutant Construction

The lambda red recombinase system was used to make mutations in the *cbsF* and *schF0* loci. Using pKD4 and pKD3, the kanamycin and chloramphenicol resistance cassettes, respectively, were PCR amplified using primers with ~50 bp homology to the 5' end of the gene locus and ~20 bp of homology to the pKD3/4 3' end of the primer. Primers used are listed in Table 3.2. PCR products were digested with DpnI and electroporated into UMH9 cells harboring pSIM19 after heat treatment for 20 minutes at 42C. pSIM19 was removed from the mutants cells.

Table 3.2. Primers for mutant construction[a]

Gene	Forward Primer	Reverse Primer
cbsF	acatcgatacattccgtttgaggaaaaggacagacaccatgtcagaaacggtgtaggctggagctgcttc	gcccggttgcgttataccaacccgtattgctgcgtcagcaacgaatgcaaatgggaattagccatggtcc
schF0	catctgggtcgccgatcaaatctccccgcatcgcaatgcctacgcggtggtgtaggctggagctgcttc	agatggcgaaatcaataatgataataaaactcattgatattcaactgtgatgggaattagccatggtcc

[a]Primer sequences are listed 5' to 3'. Underlined sequences in mutant construction primers are identical to regions at the 5' to 3' ends of the locus to be disrupted.

Preparation of Samples for Mass Spectrometry

Bacterial samples were cultured overnight in LB medium with the appropriate antibiotics. Samples were harvested and washed in M9 minimal medium the following day, then inoculated into overnight cultures consisting of M9 minimal medium that had been treated with Chelex 100 to remove iron or M9 defined medium that had 36 μM of FeSO4 added. Supernatants were collected by centrifugation the next day. Extraction and mass spectrometry was performed by the University of Michigan Natural Products Discovery Core as described in Appendix A.

Measuring siderophore production on CAS agar.

UMH9 and the mutant strains were cultured overnight in LB medium and collected by centrifugation the following day. Bacteria were washed in M9 minimal medium, then inoculated 1:100 into M9 minimal medium overnight cultures with the iron removed. The next day, cultures were OD matched and 5uL were spotted onto chrome azurol S (CAS) agar prepared as previously described [141]. Plates were incubated for two days at 37C. A color change from blue to yellow was observed on the plates in a circle around the point of inoculation. The diameter of the circle was measured to quantify siderophore production.

Growth in Iron-Depleted Medium

Bacterial growth was evaluated in several iron-limited conditions in both defined and undefined media. First, bacterial growth was measured in M9 minimal medium after treatment with Chelex 100 to remove iron. After initial overnight growth in LB medium, bacterial cultures were centrifuged and pellets were washed twice, then resuspended in M9 defined medium. 3uL was used to inoculate each well of a Bioscreen growth plate to an OD600 of 0.01. The medium

consisted of M9 medium after Chelex treatment, Chelex treated M9 medium but FeSO4 added back at the indicated concentration, M9 medium without Chelex treatment, and M9 medium without Chelex treatment but FeSO4 added back at the indicated concentration. Plates were incubated at 37°C with continuous shaking, and the OD_{600} was measured every 15 min for 21 h using a BioScreenC plate reader.

Iron-limited conditions were also created in LB undefined medium by adding 2,2 dipyridyl, an iron chelor. Samples were prepared as above, but inoculated 1:100 into 3mL of LB with the indicated concentration of dipyridyl. OD600 measurements were taken every hour using a spectrometer (BioTek). IC50 concentrations were determined using a nonlinear regression calculation.

RNA Purification and Quantification of Gene Expression by qRT-PCR

UMH9 WT was grown overnight in LB medium, harvested the following day, and washed in LB supplemented with 2,2 dipyridyl at 200 μM. Washed bacteria were subcultured 1:10 into LB medium with and without 200 μM dipryidyl. Cultures were incubated at 30C. When an OD600 between 0.4-0.5 was reached, 2 volumes of RNA Protect was added to the cultures and incubated at room temperature for five minutes. Samples were centrifuged for 10 minutes (5,000 xg) at 4C. Supernatants were decanted and excess RNA Protect was removed. Bacteria were lysed using lysozyme and proteinase K. The RNAeasy minikit was used to purify RNA by the manufacturer's instruction. Samples were DNase treated to remove DNA from the RNA samples. RNA was repurified following the RNAeasy minikit protocol.

cDNA was synthesized by mixing 1μg of RNA, 1 U random hexamers, and 10mM dNTPs, and incubating at 65C for five minutes then cooled on ice to room temperature. Reverse

transcription was performed by adding 200 U Superscript III reverse transcriptase and 1 u RNaseOUT. Remaining RNA template was removed using 1μL of RNAseH added to samples and incubated at 37C for 30 minutes. cDNA was purified using the Epoch PCR Clean up Kit.

qPCR was performed to compare iron gene expression in culture conditions with and without dipyridyl. 1ng of template cDNA was aliquoted per reaction and expression of each gene was measured in triplicate. Primers were constructed to amplify a ~100-bp internal region of the target gene. gyrB was used as the internal control and a no template control was included as the negative control. Brilliant III Ultra-Fast SYBR green (Agilent) was used to detect product amplification on a QuantStudio3 qPCR system. Relative gene expression was calculated using the delta, delta CT method.

Bacteremia Mouse Model

Overnight cultures of WT and the *ΔcbsF/schF0* mutant were harvested by centrifugation (3,500 × *g* for 30 min at 4°C) and resuspended in phosphate-buffered saline (PBS) to a density of 5×10^8 CFU/ml. Two groups of 10 female CBA/J mice (Jackson 000656) aged 6 to 8 weeks were independently inoculated with either UMH9 WT or Δ*cbsF/schF0*. An inoculum (100 μL) of 5×10^8 CFU/ml was injected into the tail vein. Infection was allowed to progress for 24 h [137]. Mice were euthanized by anesthetic overdose. Spleen and liver were collected and homogenized in PBS. Homogenates were diluted and plated onto LB agar or LB agar containing the appropriate antibiotics using an Autoplate 4000 spiral plater (Spiral Biotech) and incubated overnight at 37°C. Bacterial colonies were counted the following day using a QCount (Chemopharm). For cochallenge experiments, the following modifications were made. The Δ*cbsF/schF0* mutant strain was combined in a 1:1 mixture with the UMH9 WT strain at

5×10^8CFU/ml. Competitive indices were calculated using the following equation: $\log_{10}$ [(CFU of mutant/CFU of wild type) output/(CFU of mutant/CFU of wild type) input]. All animal experiments were conducted using protocols approved by the Institutional Animal Care and Use Committee.

Chapter IV

The *Serratia marcescens* Siderophore, Serratiochelin, is Necessary for Full Virulence during Bloodstream Infection

Notes. The material presented in this chapter was adapted from the following article:

Weakland DR, Smith SN, Bell B, Tripathi A, Mobley HLT. The *Serratia marcescens* Siderophore Serratiochelin Is Necessary for Full Virulence during Bloodstream Infection. *Infect Immun*. 2020; 88(8): e00117-20. Published 2020 Jul 21. doi:10.1128/IAI.00117-20

The introduction and figure numbers have been updated to conform to the dissertation. Otherwise, the text remains as published with minor editorial changes.

Abstract.

Serratia marcescens is a bacterium frequently found in the environment, but over the last several decades has evolved into a concerning clinical pathogen, causing fatal bacteremia. To establish these infections, pathogens require specific nutrients—one very limited but essential nutrient is iron. After characterizing the iron acquisition systems in *S. marcescens* isolate UMH9, which was recovered from a clinical bloodstream infection using RNA-sequencing (RNA-seq) in Chapter II, we honed in on two predicted siderophore gene clusters (*cbs* and *sch*) that were

regulated by iron. Mutants were constructed to delete each iron acquisition locus individually and in conjunction, generating both single and double mutants for the putative siderophore systems. Mutants lacking the *sch* gene cluster lost their iron-chelating ability as quantified by chrome azurol S (CAS) assay, whereas the *cbs* mutant retained wild type activity. Mass spectrometry-based analysis identified the chelating siderophore to be serratiochelin, a siderophore previously identified in *Serratia plymuthica*. Serratiochelin-producing mutants also displayed a decreased growth rate in iron-limited conditions created by dipyridyl added to LB medium. Additionally, mutants lacking serratiochelin were significantly outcompeted during co-challenge with wild type UMH9 in the kidneys and spleen after inoculation via the tail vein. This result was further confirmed by an independent challenge in a bacteremia mouse model, suggesting that serratiochelin is required for full *S. marcescens* pathogenesis in the bloodstream. Nine other clinical isolates have at least 90% protein identity to the UMH9 serratiochelin system; therefore, our results are broadly applicable to emerging clinical isolates of *S. marcescens* causing bacteremia.

Introduction

Iron is intrinsically important for nearly all cellular life as it serves as a cofactor for processes involved in DNA replication, ATP generation, and electron transfer. As such, acquiring iron is necessary for bacterial pathogen survival and virulence; however, mammals tightly regulate free iron levels by binding up iron in circulating proteins such as ferritin, transferrin, and heme [126, 127]. Bacteria overcome these low levels of available iron by synthesizing and secreting small molecules called siderophores. Siderophores scavenge ferric iron found in the extracellular space by stripping host proteins of their bound iron [111, 127]. Bacteria encode specific transporters to import the siderophore-bound iron across the membrane and into the cytoplasm where iron is released by dedicated proteins.

Siderophores have been characterized as virulence factors in many bacterial species including *E. coli*, and *Klebsiella pneumoniae* [18, 19, 100]. However, for many emerging pathogens, siderophores and their contribution to infection have not been characterized. One such pathogen is *Serratia marcescens*. Once in the blood, *S. marcescens* quickly disseminates resulting in multi-organ failure and high rates of mortality [142]. To establish these clinically important infections, *S. marcescens* requires an adequate supply of iron; however, the systems that contribute to iron acquisition have not been thoroughly studied.

In the previous chapter, the initial goal was to elucidate how Sm siderophores contributed to pathogenesis in the bloodstream. Two potential siderophore loci (*cbs* and *sch*) were identified by RNAseq (Chapter II) and deletion mutants in components of the NRPS machinery were constructed. A *cbsF* mutant was made in the cbs locus, the *schF0* gene was deleted in the sch locus, and then a double mutant deleting both *cbsF* and *schF0* together. Growth of these mutants

was tested in iron-limited conditions. Both the cbsF and *schF0* mutants grew comparably to the WT strain; however, *cbsF*/*schF0* had severely defective growth in these conditions, suggesting redundant roles of the individual siderophores resulting in a phenotype that was only evident when both NRPS components were deleted most likely due to insufficient iron uptake. However, when cultured on CAS agar to measure iron chelation, the double mutant had notably more siderophore production than the *cbsF* mutant, *schF0* mutant, and WT. The *cbsF* and *schF0* mutants showed siderophore production comparable to the WT. Then, mass spectrometry confirmed usable serratiochelin was present in all mutant supernatants. These results suggest that even though serratiochelin is being produced in the double mutant, it cannot be utilized by the bacterium. Since the single mutants perform comparably to the WT, this suggests that *cbsF* and *schF0* have redundant roles in serratiochelin transport potentially modifying the siderophore upon reuptake, challenging canonical ideas of NRPS function.

Given the results of the preceding chapter, *Serratia* iron acquisition is more complicated than initially appreciated and more work is required to understand the possibility of NRPS redundancy and function in siderophore transport. However, in this chapter, to answer the original question of how Sm siderophores affect its pathogenesis, full *cbs* and *sch* operon knockouts were constructed to ensure disruption of siderophore synthesis. Mutants lacking the full *sch* locus lost iron-chelating ability quantified by the CAS assay, compared to iron chelation observed in the wild type and full *cbs* locus mutant. Similar to Chapter II results, mass spectrometry analysis identified the chelating siderophore to be serratiochelin. Mutants lacking serratiochelin were significantly outcompeted during co-challenge by wild type UMH9 in the kidneys and spleen. This result was further confirmed by independent challenge in a bacteremia

mouse model, demonstrating that serratiochelin is required for full *S. marcescens* pathogenesis in the bloodstream.

Results

Characterization of two putative siderophore operons.

The two identified siderophore gene loci are organized in potential operons and appear distinct as they contain unique gene compositions relative to one another and are located in different regions of the chromosome. The first putative operon (referred to as *cbs*) is 13,859 base pairs and has fewer genes than what is typical of a pathogen-associated siderophore locus [110]. *cbs* encodes a TonB-dependent receptor (gene tag: BVG96_RS08815) as well as an exporter (BVG96_RS08795) presumably for the molecule it produces. The majority of this operon is comprised of a single predicted non-ribosomal peptide synthetase (NRPS) (BVG96_RS08800)-encoding gene (Figure 4.1A). Genes within the *cbs* operon have similarity (four corresponding genes have >60% amino acid identity) to the chrysobactin locus of *Dickeya dadantii 3937* and previous studies have reported that certain *S. marcescens* strains produce chrysobactin (Figure 4.1B) [107]. However, this operon lacks several essential genes in the chrysobactin biosynthesis pathway such as an isochorismate synthase, a 2,3-dihydroxybenzoate-AMP ligase, an isochorismatase, and a 2/3-dihydro-2,3-dihydroxybenzoate dehydrogenase. These genes are encoded elsewhere in the UMH9 genome, several of which are found in the second identified operon [110].

The second putative operon (referred to as *sch*) is much larger than the first (27,686 base pairs) and appears to contain all genes predicted for the complete biosynthetic pathway of a

NRPS-dependent siderophore including genes required to encode enzymes that could synthesize siderophore precursor molecules, and the obligate NRPS [16]. Additionally, *sch* encodes two TonB-dependent receptors as well as an exporter. The composition of the *sch* genetic region is more typical of a pathogen-associated siderophore and displays similarity to components of the serratiochelin biosynthetic operon of *S. plymuthica* (10 genes have over 65% identity) (Figure 4.1C). Serratiochelin, a *Serratia*-specific siderophore, was first identified in *S. marcescens* TW [107]. The biosynthesis pathway has been described in *Serratia spp.* V4 by predicting evolutionary mixing of the vibriobactin and enterobactin biosynthetic operons to produce serratiochelin [108]. While the UMH9 *sch* operon is not identical to the operon in *Serratia spp.* V4, we nevertheless predict that UMH9 uses this similar biosynthetic pathway to produce serratiochelin. Interestingly, some of the biosynthetic genes missing from *cbs* are present in *sch* suggesting that the ability of *cbs* to encode synthesis of a siderophore may be dependent on *sch* (Figure 4.2). Due to the similarity of these genetic regions to reported chrysobactin and serratiochelin loci, the putative siderophore operons are heretofore referred to as *cbs* and *sch*, respectively.

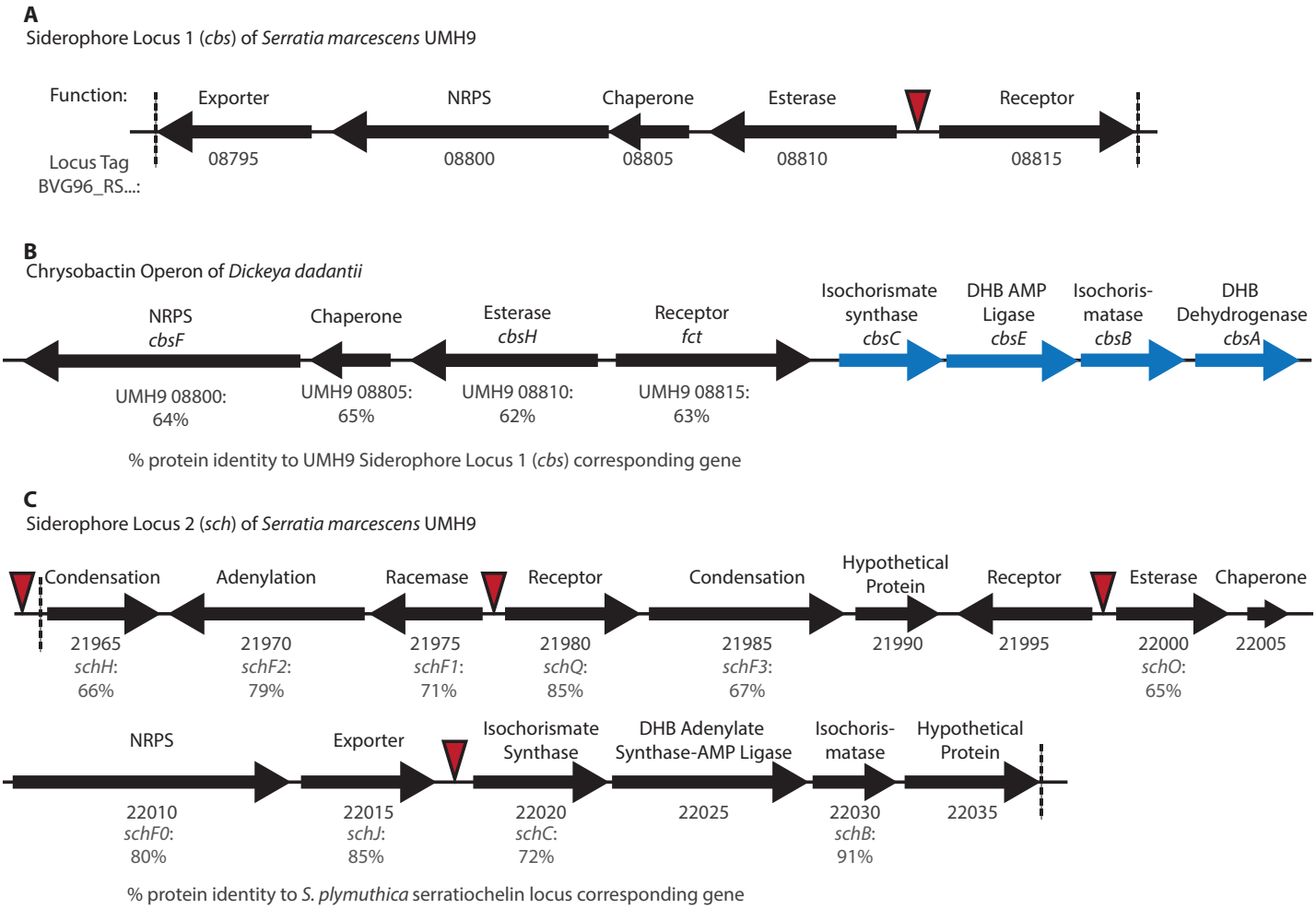

Figure 4.1. Siderophore locus 1 (*cbs*) is similar to the chrysobactin operon in *Dickeya dadantii* while Siderophore locus 2 (*sch*) shows similarity to *Serratia plymuthica* serratiochelin genes.

A) The UMH9 *cbs* locus has an organization similar to the chrysobactin operon found in *Dickeya dadantii* (B). Four genes (in blue) are missing from the UMH9 *cbs* locus that are present in the *D. dadantii* chrysobactin operon. However, these genes, involved in the production of chrysobactin precursor molecules, are found elsewhere in the UMH9 genome. The percentages reported underneath the genes in panel B are the protein percent identity to the UMH9 Siderophore Locus 1 corresponding gene in panel A. C) The UMH9 *sch* locus contains genes

predicted to be necessary for siderophore biosynthesis and transport. The percentages reported under the genes in panel C are the amino acid percent identity to the *S. plymuthica* serratiochelin locus corresponding gene. The gene function is noted above each arrow. The UMH9 locus tag number (BVG96_RS…) is referenced below each arrow for panels A and C. Red triangles indicate the location of putative ferric uptake regulator (Fur) binding sequences in the UMH9 genome. The genes located between the vertical hashed lines in panels A and C were deleted in the *cbs::kan* and *sch::kan* mutants, respectively as well as in the *cbs::cam sch::kan* mutant together.

Loss of *sch* abrogates iron-chelation in *S. marcescens*.

Each siderophore locus was disrupted individually (*cbs::kan* [*Δcbs*], *sch::kan* [*Δsch*]) and in combination (*cbs::cam sch::kan* [*Δcbs/sch*]) in the parent strain UMH9 (WT). In each case, the entire siderophore-encoding locus was deleted and replaced with a kanamycin or chloramphenicol resistance cassette. To determine how each locus contributes to siderophore production, the wild type strain and each construct were cultured overnight in iron-depleted M9 minimal medium or M9 medium supplemented with 36μM $FeSO_4$. Culture supernatants were used in a soluble CAS assay the following day to quantify siderophore synthesis. As expected, the WT strain and deletion constructs showed no siderophore production under iron-replete conditions (Figure 4.2). Conversely, WT showed the greatest amount of CAS activity under iron-limitation. CAS activity comparable to WT was observed for the *Δcbs* mutant. However, significant loss of iron chelation activity was observed in the *Δsch* and *Δcbs/sch* mutants. These results suggested that under iron-limitation, UMH9 produces a siderophore that can chelate iron from the ferri-CAS complex, and the *sch* locus is necessary for the production of the chelating activity.

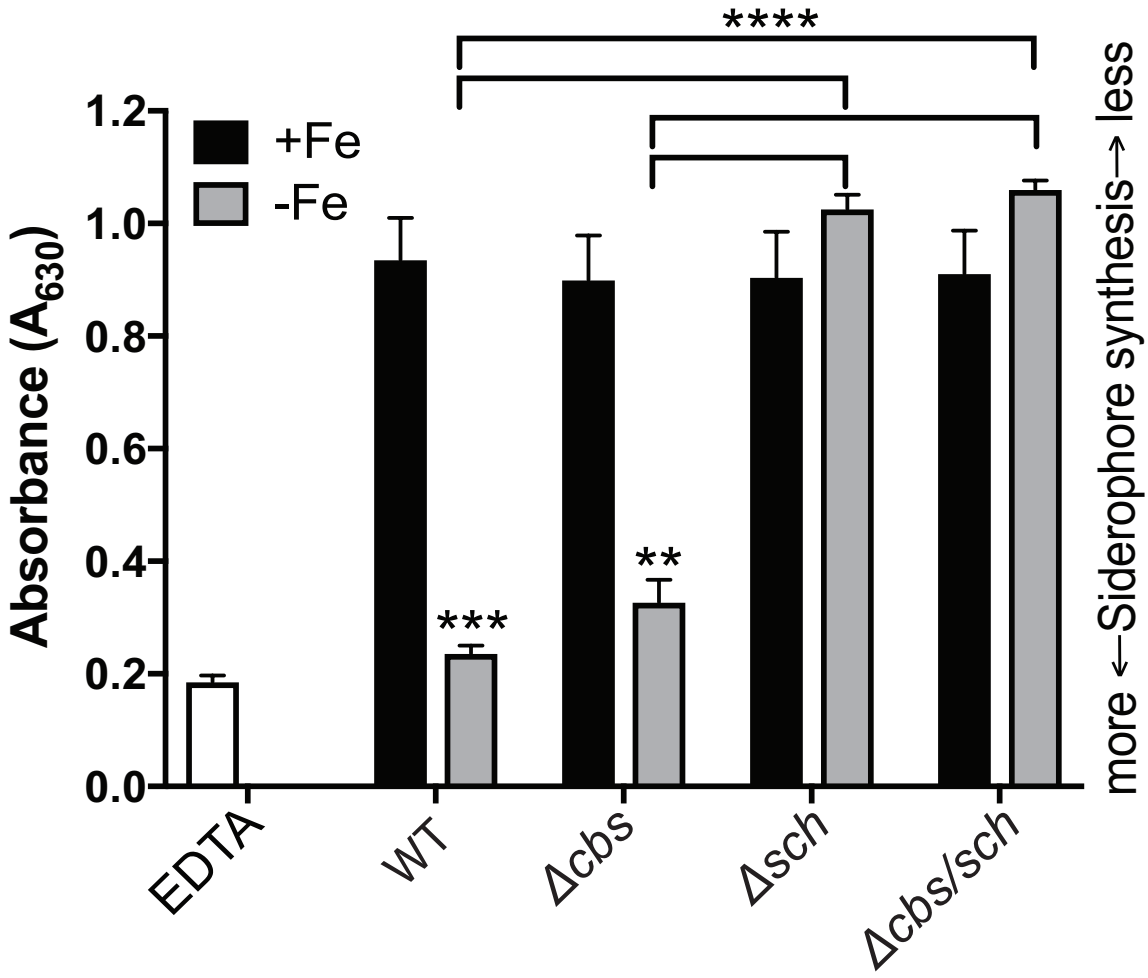

Figure 4.2. The *sch* locus is responsible for detectable siderophore production.

Siderophore production was quantified by liquid chrome azurol S (CAS) assay on bacterial supernatants. Bacteria were cultured overnight in M9 minimal medium with (black bars) or without (grey bars) 36μM $FeSO_4$. 10μM EDTA serves as the positive control for iron-limitation. Low absorbance (A_{630}) values indicate more siderophore production. Shown is the mean of three independent replicates and error bars represent standard error of the mean. Significant differences (**, $p<0.01$; ***, $p<0.001$; ****, $p<0.0001$) were determined using a two-tailed unpaired *t*-test.

Mass spectrometry reveals that the *sch* operon produces serratiochelin A.

Because the siderophore produced by the *sch* locus is responsible for detectable CAS activity, we wanted to definitively identify the siderophore being produced by the *sch* locus using mass spectrometry (MS). Wild type UMH9 and the three siderophore mutants, *Δcbs*, *Δsch*, and *Δcbs/sch,* were cultured overnight in both iron-depleted M9 minimal medium and M9 medium supplemented with 36μM $FeSO_4$. MS was performed on bacterial supernatants as described in Chapter III. Fragmentation patterns matching serratiochelin A were identified in samples WT –Fe, and *Δcbs* –Fe and absent in samples *Δsch* +Fe, *Δsch* –Fe, *Δcbs/sch* +Fe, and *Δcbs/sch* –Fe (Figure 4.3).

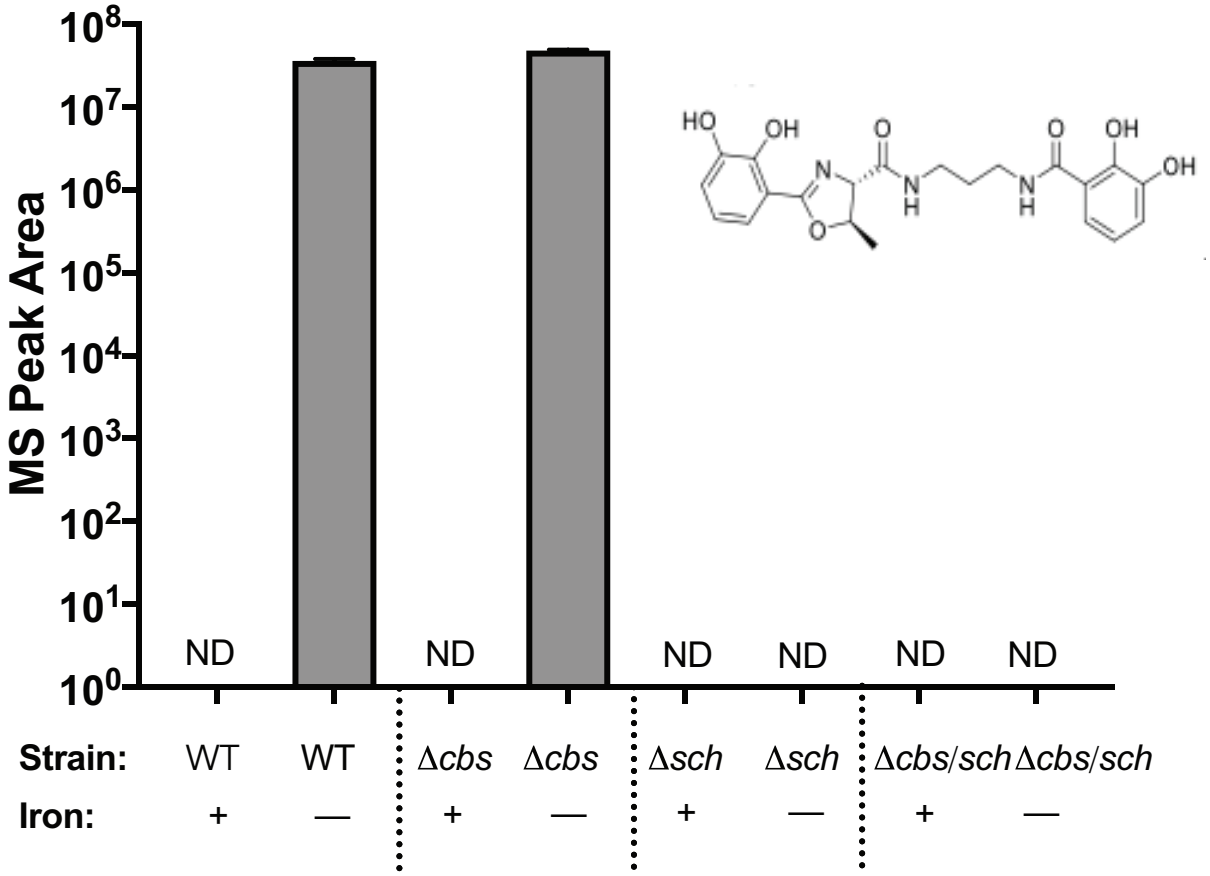

Figure 4.3. Serratiochelin A production is lost in a *sch* mutant.

An intensity plot of serratiochelin A was generated using mass spectrometry performed on the supernatants of the indicated strains after overnight culture in M9 minimal medium with and without iron (where indicated). A directed approach identified serratiochelin A with a retention time of 4.84 minutes to be associated with the *sch* operon. The molecular structure of serratiochelin A is shown. ND = Not detected.

Serratiochelin A is necessary for growth under iron-limitation *in vitro.*

Mass spectrometry results indicated that the *sch* locus encodes enzymes required to synthesize serratiochelin A and serratiochelin is most likely responsible for iron chelation as indicated by the CAS assay. A very low concentration of chrysobactin was present in wild type supernatants by mass spectrometry associated with the *cbs* locus (data not shown). Unlike the *sch* locus, chrysobactin did not demonstrate any notable iron chelation by CAS assay, likely due to its low concentration. Based on these results, we hypothesized that *in vitro* growth under iron-limiting conditions would be contingent on the presence of the *sch* locus that encodes enzymes required for serratiochelin A production.

To test this, increasingly iron-limited conditions were established by titrating dipyridyl into LB. UMH9 WT, *Δcbs* mutant, *Δsch* mutant, and the *Δcbs/sch* double mutant all grew similarly in LB medium without dipyridyl (Figure 4.4A). As dipyridyl concentrations increased, all strains exhibited less growth, as expected (Figure 4.4). WT and the *Δcbs* mutant had comparable growth in 200μM dipyridyl, while the *Δsch* and *Δcbs/sch* mutants displayed noticeably inhibited growth (Figure 4.4B). At 250μM (Appendix A, Figure A.2A) and 300μM (Figure 4.4C) dipyridyl concentrations, the *Δsch* and *Δcbs/sch* mutants showed notably decreased growth compared to the WT and *Δcbs* mutant. The *Δcbs* mutant had the most robust growth under these conditions while WT had mildly decreased growth compared to the *Δcbs* mutant. The *Δsch* and *Δcbs/sch* mutants failed to grow at dipyridyl concentrations of 350μM (Appendix A, Figure A.2B) and 400μM (Figure 4.4D). The *Δcbs* mutant continued to display the best growth under these concentrations. The WT had abrogated growth at 350μM dipyridyl and minimal growth at 400μM dipyridyl. Because the mutants lacking the *sch* locus struggled to grow under these conditions, the half maximal inhibitory concentration (IC_{50}) of dipyridyl for the

Δsch and *Δcbs/sch* mutants was notably lower than the IC_{50} for the WT and *Δcbs* mutant (Figure 4.4E).

These results suggested that the *sch* locus is essential for growth under these iron-limited conditions. Without *sch*, UMH9 is much more inhibited by dipyridyl iron-limitation than the WT strain. Interestingly, the absence of *cbs* appears to provide a growth advantage in UMH9. Additionally, because the *Δcbs/sch* mutant shows severely inhibited growth comparable to that seen in the *Δsch* mutant, the inhibited growth related to the loss of *sch* cannot be overcome by the growth advantage related to losing the *cbs* locus under iron-limitation.

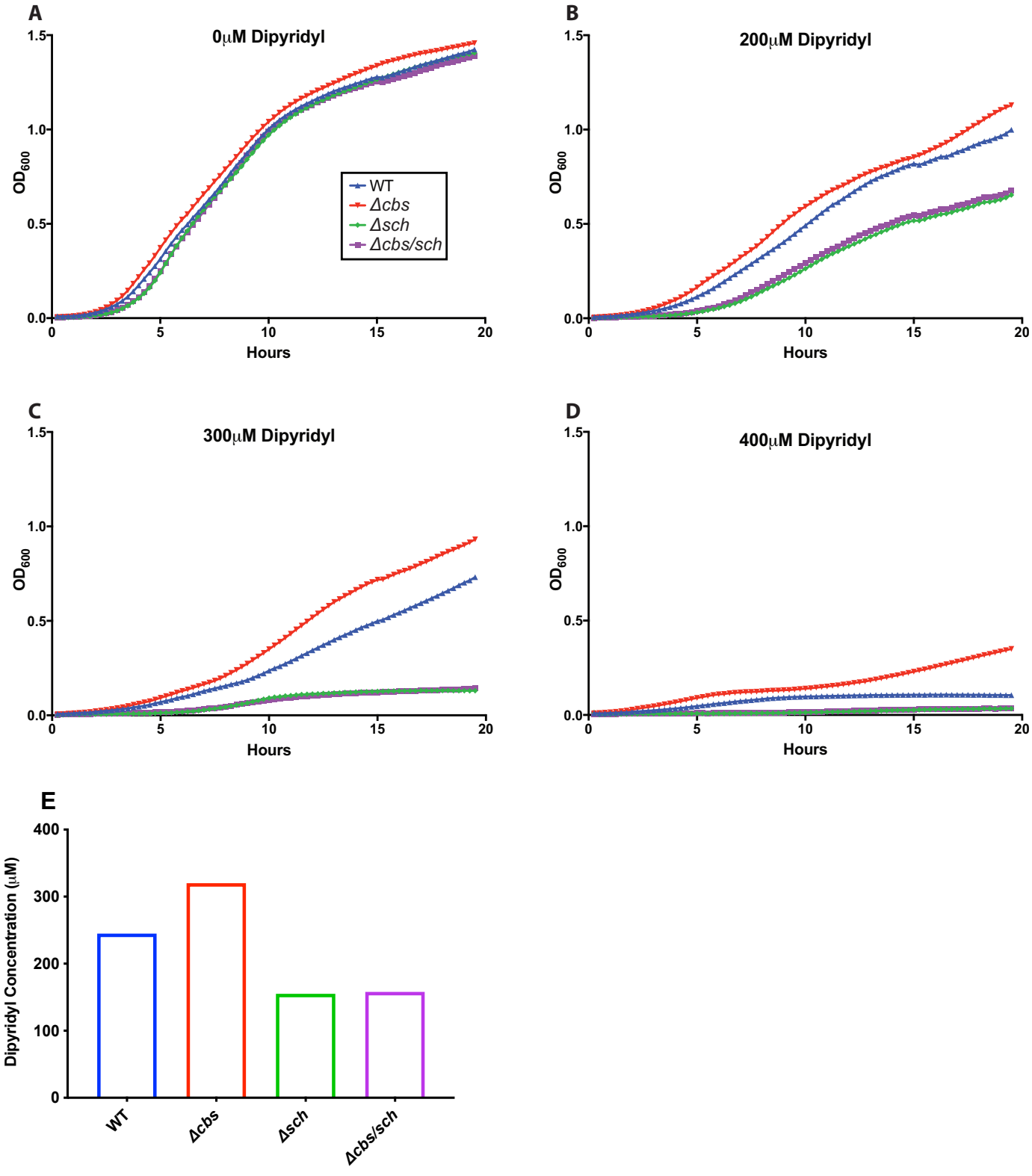

Figure 4.4. UMH9 growth under iron-limitation is dependent upon presence of the *sch* locus.

S. marcescens UMH9 wild type, the *cbs* locus mutant (*Δcbs*), the *sch* locus mutant (*Δsch*), and the *cbs/sch* double loci mutant (*Δcbs/sch*) were inoculated into LB medium containing 0μM (A), 200μM (B), 300μM (C), or 400μM (D) dipyridyl after culture overnight in LB with 250μM dipyridyl. Cultures were incubated with aeration at 37˚C and OD_{600} readings were taken every 15 minutes to measure bacterial growth. The mean of three independent replicates is shown. (E) The half maximal inhibitory concentration (IC_{50}) of dipyridyl was calculated for each mutant based on the tested dipyridyl concentrations.

Serratiochelin is required for growth in human serum.

Although both *cbs* and *sch* affect growth in LB culture with dipyridyl, the importance of these genes *in vivo* remained to be determined. To explore their role in a physiologically relevant iron-limited condition, we first assessed the wild type and mutant growth in 100% heat-inactivated human serum (Figure 4.5). Iron bound to transferrin is the principal iron carrier in the blood and the main source of iron in human serum [143]; therefore, we hypothesized that the ability to produce a siderophore would be advantageous to growth in this medium.

The WT strain and the three mutants displayed an initial decrease in optical density likely due to bacterial aggregation during the lag phase (Figure 4.5A). Eventually, the bacterial aggregates dispersed and logarithmic growth was observed. WT began to grow after nearly eight hours while *Δcbs*, *Δsch*, and *Δcbs/sch* mutants showed growth at ten hours. After initial growth at ten hours, *Δsch* and *Δcbs/sch* mutants reached the stationary phase at approximately 16 hours, whereas the WT and *Δcbs* strains grew beyond 20 hours. The final OD_{600} was significantly higher in WT and *Δcbs* compared to the final OD_{600} of *Δsch* and *Δcbs/sch* mutants (Figure 4.5B).

These results suggest that the *sch* locus contributes to the growth of *S. marcescens* in human serum. Taking growth in serum with the growth in dipyridyl conditions together, the *cbs* operon appears dispensable for growth under iron-limitation and does not contribute significantly to growth even in physiologically relevant iron-limited conditions.

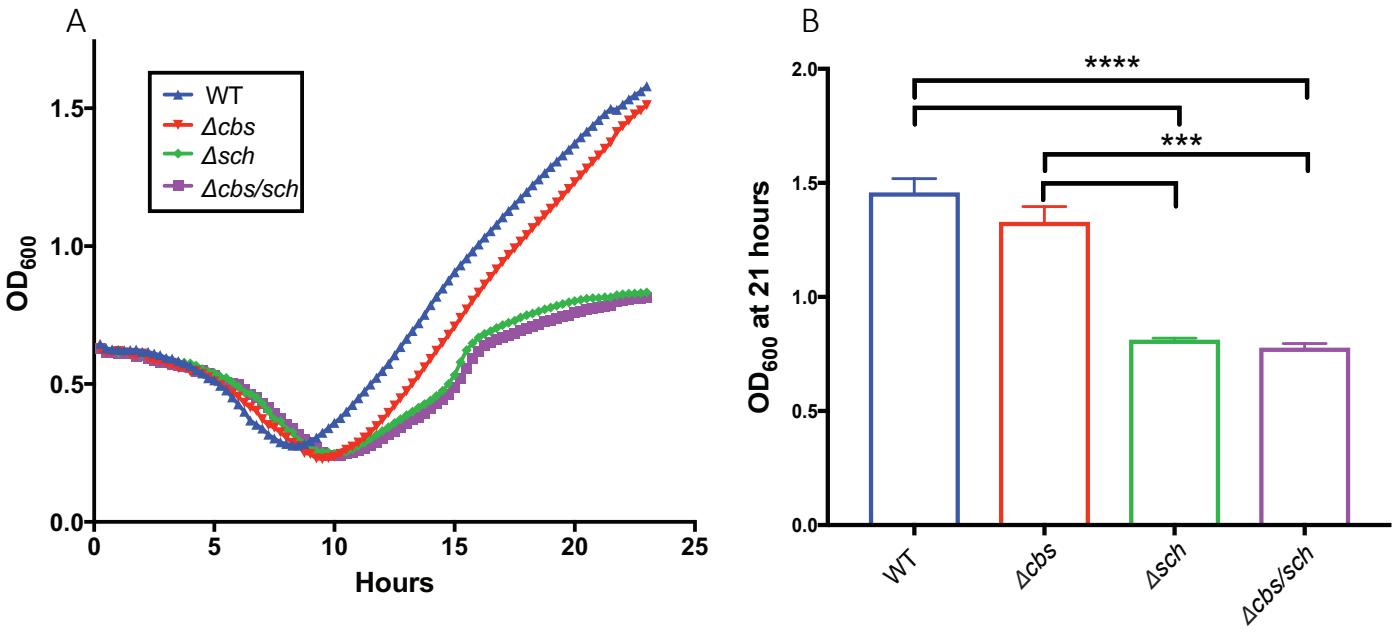

Figure 4.5. Serratiochelin mutants grow poorly in human serum.

(A) *S. marcescens* UMH9 wild type, *Δcbs*, *Δsch*, and *Δcbs/sch* mutants were cultured in 100% heat-inactivated human serum at 37°C with aeration. OD_{600} readings were taken every 15 minutes to measure bacterial growth. Data represent the means from three independent replicates. (B) Serratiochelin mutants have significantly lower final stationary phase OD_{600} measurements compared to wild type in human serum. *S. marcescens* UMH9 wild type, *Δcbs*, *Δsch*, and *Δcbs/sch* mutants were cultured in 100% heat-inactivated human serum at 37°C with aeration. Final stationary phase OD_{600} of the above strains at 21 hours was compared. Shown is the mean of three-independent replicates and error bars represent standard error of the mean. Significant differences (***, $p<0.001$; ****, $p<0.0001$) were determined using a two-tailed unpaired *t*-test.

Mutants lacking *sch* are attenuated during bacteremia.

Siderophores have been found to contribute significantly to virulence in murine models of infection [19], and since I had different *in vitro* results with the full operon knockouts as compared to the single gene deletions in Chapter III, I decided to revisit the mouse model. Since serratiochelin was essential for growth in the low iron medium *in vitro*, we hypothesized that it would contribute to its pathogenesis in the bloodstream. Using a murine model of bacteremia adapted from use with *E. coli* [137], we evaluated the fitness of the siderophore mutants in the bloodstream using competition experiments. We prepared a 1:1 mixture of each siderophore mutant with UMH9 WT, and then co-inoculated mice with 5 x 10^7 CFU of this suspension via the tail vein. Competitive indices (CI) of mutant and wild type bacteria were calculated in the kidneys, spleen, and liver 24 hours post-infection (hpi). The *Δsch* and *Δcbs/sch* mutants displayed a significant competitive disadvantage (log CI, < 0) in the kidney (Figure 4.6A) and spleen (Figure 4.6B) with a modest disadvantage observed in the liver (Figure 4.6C). The *Δcbs* mutant competed equally with wild type in the spleen and liver (log CI, = 0) (Figure 4.7B, 4.6C), but a competitive advantage was observed in the kidney (log CI, > 0), suggesting that loss of the *cbs* locus was advantageous to kidney colonization (Figure 4.6A). These results echo my earlier *in vitro* findings and suggest that serratiochelin is necessary for complete fitness in the bloodstream.

Although the entire *sch* gene cluster, including the serratiochelin receptor gene, was deleted, we hypothesized that serratiochelin produced by the wild type strain may have partially cross-complemented the mutant strains since the mutants retained genes that were annotated as encoding putative orphan siderophore receptors. Therefore, we performed independent infections with each strain, enumerating bacterial burden in the kidneys, spleen, and liver, 24 hpi. Mutants

lacking *sch* (*Δsch* and *Δcbs/sch*) had significantly fewer CFUs recovered from the kidney compared to the wild type and the *Δcbs* mutant ($p<0.0007$), suggesting that mutants unable to produce serratiochelin are attenuated in the kidney (Figure 4.7A). The *Δcbs/sch* mutant colonized the spleen significantly less well than WT (Figure 4.7B). The presence or absence of serratiochelin did not appear to affect colonization in the liver (Figure 4.7C). Since *sch* mutants were attenuated in both co-challenge and independent challenge experiments, this rules out that the wild type strain contributed to any significant cross-feeding of the *sch* mutant during co-challenge. Together, these data indicate that serratiochelin is required for full pathogenicity in the bloodstream.

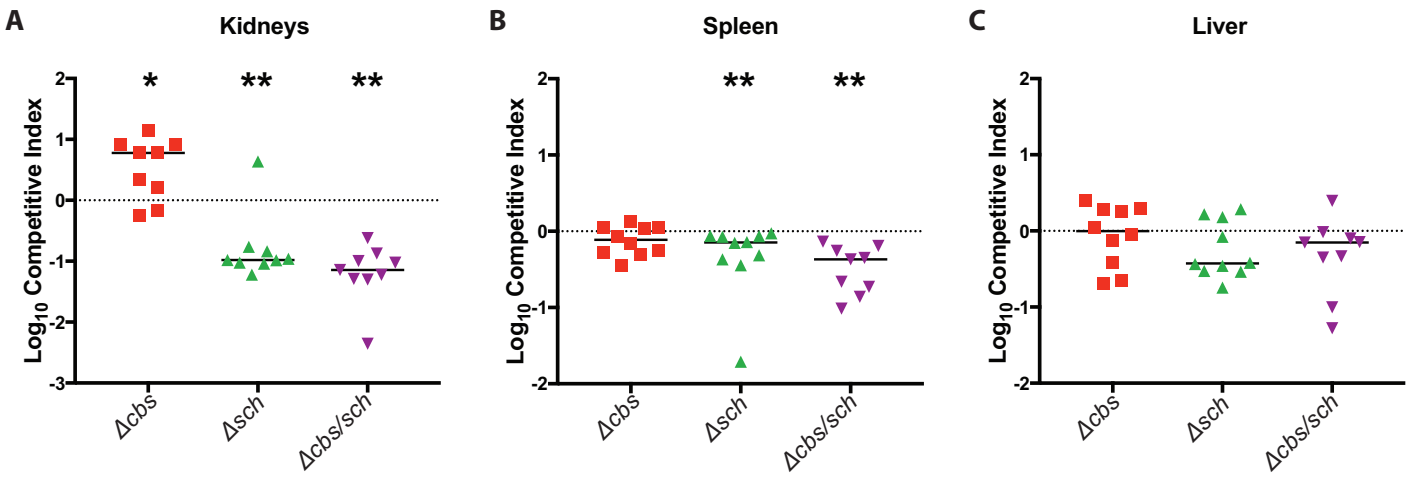

Figure 4.6. Fitness of UMH9 siderophore mutants in a murine model of bacteremia.

CBA/J mice were infected with 5 x 10^7 CFU/mouse in a 1:1 mixture of wild type and the indicated mutant strain via the tail vein. Mice were euthanized at 24 hours and kidney (A), spleen (B), and liver (C) were collected from each mouse. Organs were homogenized. Homogenates were diluted and selectively plated. The relative fitness for each mutant compared to the wild type was calculated as a competitive index (CI). The dotted line represents a CI of 1.0, meaning the two strains compete equally. Solid lines represent median CI. Statistics were calculated using the Wilcoxon Signed Rank Test with a theoretical median of 0 (*, $p<0.05$; **, $p<0.01$).

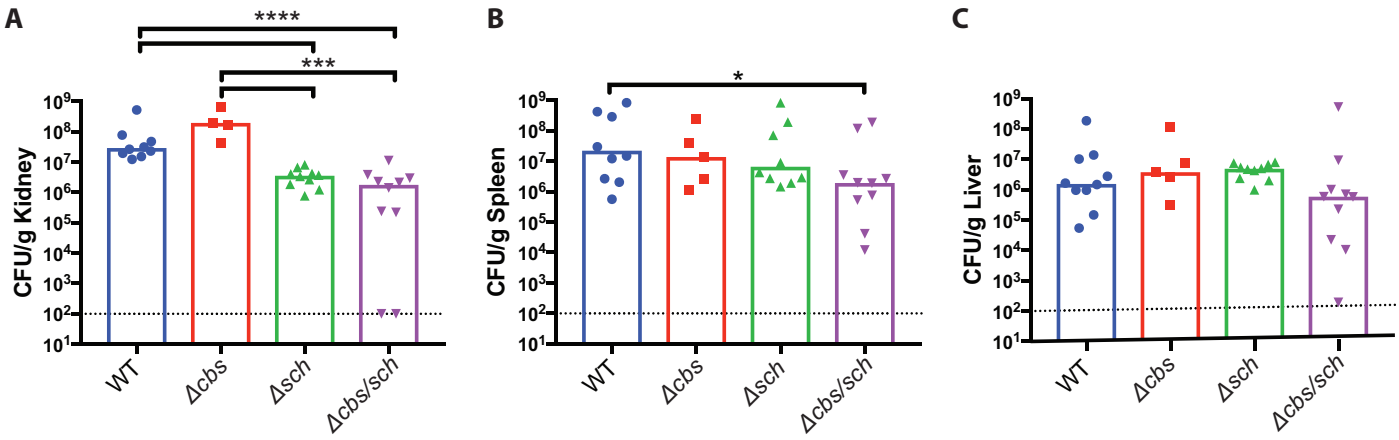

Figure 4.7. Independent infections of UMH9 siderophore mutants in a murine model of bacteremia.

CBA/J mice were independently inoculated with the indicated strain via the tail vein. Mice were euthanized 24 hours post-inoculation. Kidneys (A), spleens (B), and livers (C) were collected and homogenized. Homogenates were diluted and plated. The dotted line indicates the limit of detection. Significance determined by the Mann-Whitney test is indicated with an asterisk (*, $p<0.05$; ***, $p<0.001$; ****, $p<0.0001$).

The characterized siderophore operons are conserved across clinical isolates of *S. marcescens.*

S. marcescens is a diverse species with a core genome of 3,372 genes and an accessory pangenome consisting of 10,215 genes [144]. To determine whether the two putative siderophore loci are conserved among *S. marcescens* strains, we used PATRIC to compare predicted protein sequence similarity of nine clinical bloodstream isolates of *S. marcescens* to UMH9 [145]. We found that genes within the *cbs* and *sch* loci are conserved and individual predicted proteins typically have more than 90% amino acid sequence identity to UMH9 proteins (Figure 4.8).

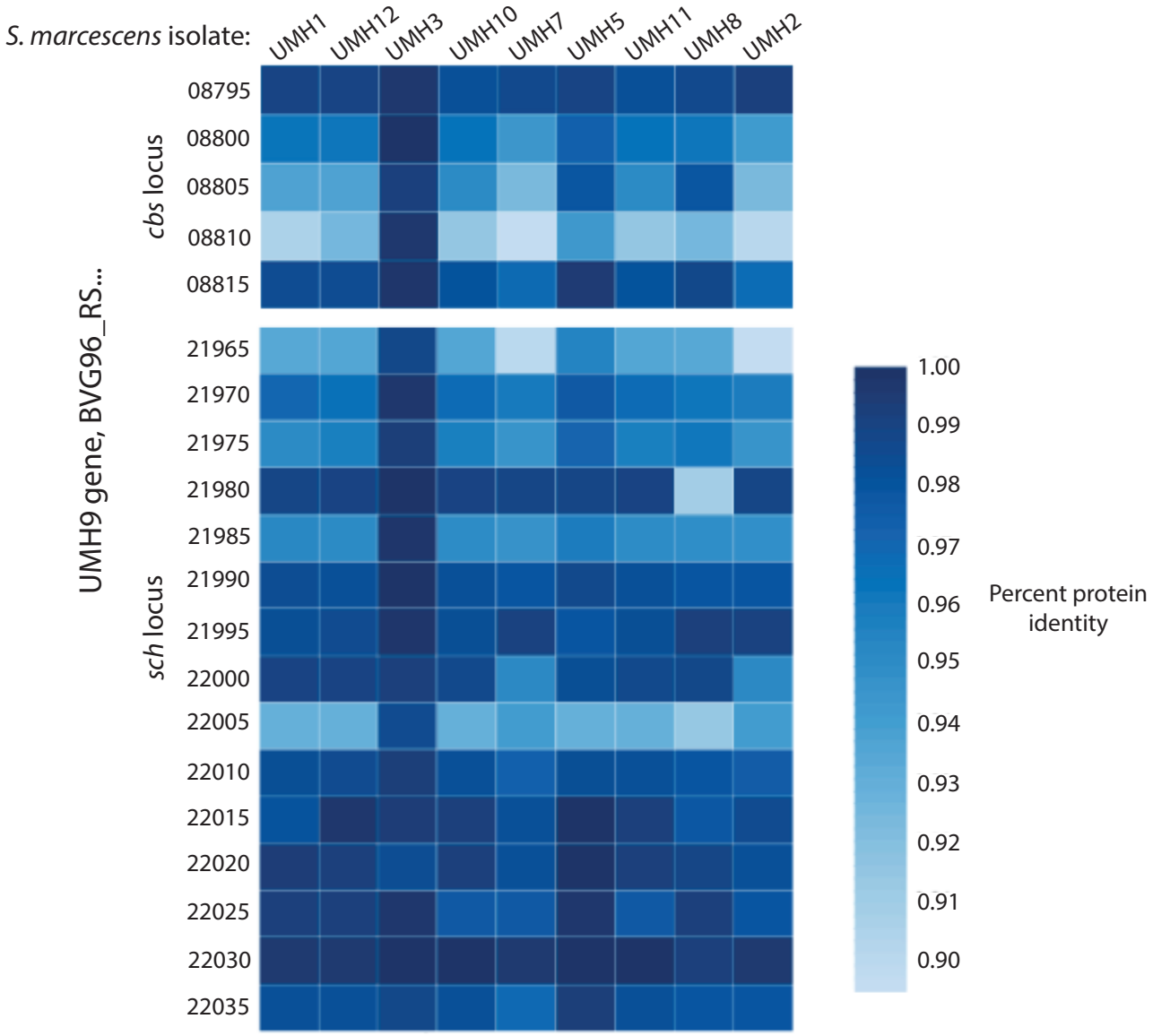

Figure 4.8. The *cbs* and *sch* genetic regions are conserved among clinical isolates of *Serratia marcescens*.

The amino acid sequences of the UMH9 siderophore loci were compared to the siderophore loci of nine other bacteremic isolates of *Serratia marcescens.* Using PATRIC's online protein identity platform, we determined the conservation of these loci among other *S. marcescens* clinical strains.

Discussion

The contribution of siderophores to infection has been well established for a large number of bacterial pathogens [22, 111, 124, 146]. However, because *S. marcescens* was thought to largely reside in environmental reservoirs, we aimed to determine the importance of *Serratia* siderophores to infection within the mammalian host. Prior to this work, *S. marcescens* siderophore systems had not been described in bacteremia infection models relevant to human disease. Two identified siderophore operons had been reported previously; however, this is the first study detailing their up-regulation under iron-limited conditions (Chapter II) as well as their contribution to *S. marcescens* pathogenesis. We demonstrate that serratiochelin A is produced by the *sch* locus and *sch* is necessary for *S. marcescens* UMH9 to grow under iron-limiting conditions both *in vitro* (Fig. 4.4, Fig. 4.5) and *in vivo* (Fig. 4.6, Fig. 4.7). The *cbs* locus is dispensable for infection and does not significantly contribute to growth under iron limitation. Indeed, under some conditions, the expression of *cbs* seems to limit UMH9 growth. However, despite the different contributions to fitness between the two siderophore loci in the conditions tested here, both are highly conserved among other sequenced clinical isolates.

S. marcescens occupy broad environmental niches beyond the mammalian host as it also infects insects and survives in aquatic environments [99]. Because the *cbs* locus is dispensable in the mammalian model of infection, we speculate that *cbs* might be important for *S. marcescens* survival in the environment rather than within the host. The UMH9 *cbs* locus encodes proteins that share close amino acid similarity to those encoded by the chrysobactin operon in the plant pathogen, *Erwinia chrysanthemi (Dickeya dadantii)*. Chrysobactin, a virulence factor for *E. chrysanthemi*, is responsible for pathogen dissemination throughout the host plant [109].

Therefore, *cbs* may contribute to pathogenesis in environmental niches and chrysobactin production may be dependent on an unknown environmental cue; however, it does not significantly contribute to pathogenesis within the mammalian host.

Additionally, despite the increased expression of genes in the *cbs* locus under iron limitation, there is little detectable chrysobactin. And in fact, the *cbs* mutant conferred a growth advantage under some conditions compared to wild type growth. We do not believe this growth advantage is related to increased serratiochelin production when the *cbs* locus is deleted because the mass spectrometry results showed comparable serratiochelin levels in wild type and *cbs* mutant supernatants in M9 minimal medium. We expect this is likely the case in LB medium with dipyridyl as well although it has not been tested. We hypothesize that synthesis of the enzymes encoded by *cbs* could be energetically costly to produce resulting in increased growth of the *cbs* mutant during iron-limitation. Interestingly, chrysobactin synthesis may be biosynthetically dependent on several genes within the *sch* locus. *sch* genes BVG96_RS22020, 22025, and 22030 have similarity to chrysobactin biosynthetic genes *cbsC*, *cbsE*, and *cbsB*, respectively. These genes can be found in the *D. dadantii* chrysobactin operon, but are absent in the *S. marcescens* UMH9 *cbs* locus. These genes are involved in both serratiochelin and chrysobactin precursor production according to previously published biosynthetic pathways of these molecules [108, 110]. In strain UMH9, once these precursor molecules are produced, they are most likely used to produce serratiochelin. These products can also be used for chrysobactin synthesis, but given the small amount of chrysobactin identified in WT UMH9 supernatants, this most likely occurs to a lower extent. Additionally, there are possibly hurdles in efficiently coordinating small molecule biosynthesis across differentially regulated operons. The low level

of chrysobactin production could be explained by this inefficiency. However, further research is needed to explore possible interactions between the *sch* and *cbs* loci.

Gram-negative pathogens can utilize siderophores made by other bacteria, a strategy often used in polymicrobial settings [32]. *S. marcescens* possesses a receptor for aerobactin, IutA, but does not produce aerobactin itself. It also has a receptor with similarity to FepA, an enterobactin transporter. Additionally, UMH9 has several orphan hypothetical siderophore receptors outside of the *sch* and *cbs* siderophore gene clusters suggesting its ability to import other potential siderophores that it does not itself produce. Therefore, considering these observations along with *S. marcescens* being a known opportunist, it is likely that *S. marcescens* depends on xenosiderophores in polymicrobial infections especially since it possesses only one siderophore that contributes to pathogenesis whereas other Gram-negative pathogens typically have two or more [18, 19]. Interestingly, it is unknown whether other Gram-negative pathogens can utilize serratiochelin or chrysobactin.

S. marcescens also acquires iron from heme using two well-known systems, Hem and Has. Given the high concentration of heme in the bloodstream, we hypothesize that these systems also play a role in iron acquisition during bacteremia, which will be discussed further in Chapter V. Previous literature has highlighted the redundancies between the major iron acquisition systems in other pathogens, which may explain why we see little to no decrease in colonization in the mouse spleen and liver when *sch* is deleted [19]. In these environments, iron acquired from heme may be the dominant iron source, whereas, in the kidney, siderophores play a larger role. *S. marcescens* also possesses a ferric citrate transport system that was up-regulated during iron-limited RNA-seq experiments. Citrate is capable of binding and importing iron; however, its affinity for iron is weak compared to that of siderophores [22]. Nonetheless, citrate

has been shown to act as a siderophore and may play a redundant role in iron acquisition along with serratiochelin, chrysobactin, and heme uptake [119, 147]. To fully understand iron import during bacteremia, future studies evaluating the contribution of the heme uptake systems and ferric citrate import should be performed. Additionally, it is possible that heme uptake can compensate for siderophores, and vice versa; therefore, a mutant in which all siderophore systems, as well as heme systems, are deleted would be an interesting tool to evaluate the contribution of iron acquisition irrespective of specific systems.

We recognize that this study examines one clinical isolate of *Serratia marcescens* and that additional isolates could possess additional iron acquisition systems. Our lab has sequenced the genomes of nine clinical *S. marcescens* strains isolated from humans with bacteremia. Genome comparison studies show that other *S. marcescens* isolates also possess the *cbs* and *sch* loci and have a high amino acid sequence identity to the operons found in UMH9. Therefore, our results may be considered broadly applicable to the virulence of bacteremic strains of *S. marcescens*.

In summary, we have defined the iron-regulated transcriptome of *S. marcescens* UMH9 to identify the full repertoire of iron-acquisition systems and components within this important opportunistic pathogen. We characterized the expression of two well-conserved putative siderophore systems (*sch* and *cbs*), identified the molecular products synthesized, and implicated the *sch* locus product, serratiochelin A, as contributing to the pathogenesis in the murine bloodstream. However, the *cbs* locus has a yet undetermined role in pathogenesis and does not appear to contribute to *S. marcescens* UMH9 virulence in mice. These findings clearly show that the *sch* product, serratiochelin, is a *bona fide* virulence factor during bacteremia.

Materials and Methods

Bacterial Strains and Culture Conditions

S. marcescens strains and plasmids used in this study are listed in Table 4.1. Bacteria were routinely cultured in luria broth medium (LB) (10 g/liter tryptone, 5 g/liter yeast extract, 0.5 g/liter NaCl). Antibiotics were added to cultures at the following concentrations when appropriate: kanamycin (25 μg/ml), chloramphenicol (30 μg/ml), spectinomycin (100 μg/ml). 2,2'-dipyridyl (Sigma-Aldrich), an iron chelator, was added to LB cultures at the indicated concentrations to achieve iron limitation. M9 defined medium (0.1 mM $CaCl_2$, 1mM $MgSO_4$, 0.4% glucose) was used to culture bacteria for mass spectrometry and chrome azurol S (CAS) experiments [131]. M9 was treated with Chelex-100 to remove iron, creating iron-limited conditions. $FeSO_4$ (36 μM) was added back to M9 cultures where indicated.

Table 4.1. *S. marcescens* strains and plasmids

Name	Relevant genotype	Description	Reference or source
S. marcescens			
UMH9	Wild type	Bloodstream infection isolate	[98]
Siderophore 1 (*cbs*)	*cbs::kan* (*Δcbs)*	Full operon deletion from gene *08795* to *08815*, replaced with kanamycin cassette from pKD4.	This study
Siderophore 2 (*sch*)	*sch::kan (Δsch)*	Full operon deletion from gene *21965* to *22035*, replaced with kanamycin cassette from pKD4.	This study
Siderophore 1 and Siderophore 2 (*cbs/sch*)	*cbs::cam, sch::kan (Δcbs/sch)*	Double mutant with both full operon deletions replaced with the indicated antibiotic cassette.	This study
Plasmids			
pKD4		Source of kanamycin resistance gene	[139]
pKD3		Source of chloramphenicol resistance gene	[139]
pSIM19		Recombineering plasmid	[140]

Construction of UMH9 Mutants

Single and double mutations of the *cbs* and *sch* loci were constructed using the lambda red recombinase system [148]. PCR amplification of the kanamycin- or chloramphenicol-resistance cassettes from pKD4 and pKD3, respectively, was performed using primers with ~50-bp of homology at the 5' end to the siderophore locus and ~20-bp homology to pKD3/4 at the 3' end of each primer. Primers for mutant construction are listed in Table 4.2. PCR products were digested with DpnI (New England Biolabs), then transformed into UMH9 cells expressing lambda red recombinase from pSIM19 after heat treatment for 20 minutes at 42˚C. pSIM19 was removed from the mutant strains as described previously [148]. Mutants were confirmed by PCR and Sanger sequencing (Table 4.2).

Table 4.2. Primers for mutant construction[a]

Operon	Forward Primer	Reverse Primer
Siderophore 1 (*cbs*)	cgccgctgaggttgccggcgcgggctcatc gtgctcgaccaaggcgttcggtgtaggctgg agctgcttc	tgaccgaagcgatgatgctgcggccgctgcc gtagaaacaggcgtactcgatgggaattagcc atggtcc
Siderophore 2 (*sch*)	cgctttggcctctgaatggttgccgctggcgc cagcgcagcttgatttctgtgtaggctggagct gcttc	gcggatcacgtcgtccggcgcggtggcttcttt ctcgcggctggaagcctatgggaattagccat ggtcc

[a]Primer sequences are listed 5' to 3'. Underlined sequences in mutant construction primers are identical to regions at the 5' to 3' ends of the locus to be disrupted.

Growth of *S. marcescens* Strains

Bacterial strains were cultured with aeration overnight in LB medium at 37˚C. The following day, bacteria were collected by centrifugation and washed twice with LB medium containing 250 μM dipyridyl. Bacteria were suspended in LB + 250 μM dipyridyl and 30 μL were used to inoculate 3 mL of LB + 250 μM dipyridyl for overnight cultures. A sample of culture (3 μL) was used to inoculate each well of a 100-well growth plate containing 300 μL of LB with the indicated dipyridyl concentration to an OD_{600} of 0.01. Growth was also measured in 100% heat-inactivated human serum. Bacteria were cultured and loaded into the serum-containing growth plate as described above. Growth curves were performed in biological and technical triplicates. Plates were incubated at 37˚C with continuous shaking and OD_{600} was measured every 15 minutes for 21 hours using a BioScreenC plate reader. Due to technical reasons, blank serum measurements were not subtracted from growth measurements, accounting for the higher starting OD_{600}.

Murine Model of Bacteremia

Overnight cultures of WT and mutant constructs were harvested by centrifugation (3500*x g* for 30 minutes at 4˚C) and resuspended in phosphate-buffered saline (PBS) to a density of 5 x 10^8 CFU/ml. Four groups of ten female CBA/J mice (Jackson 000656) aged 6-8 weeks were independently inoculated with either UMH9 WT, *Δcbs*, *Δsch*, or *Δcbs/sch* constructs. An inoculum (100 μL) of 5 x 10^8 CFU/ml was injected into the tail vein. Infection was allowed to progress for 24 hours, or until mice appeared moribund. Mice were euthanized by anesthetic overdose. Spleen, kidney, and liver were collected and homogenized in PBS. Homogenates were diluted and plated onto LB agar or LB agar containing the appropriate antibiotics using an

Autoplate 4000 spiral plater (Spiral Biotech) and incubated overnight at 37˚C. Bacterial colonies were counted the following day using a QCount (Chemopharm). For co-challenge experiments, the following modifications were made. Each mutant strain was combined in a 1:1 mixture with the UMH9 WT strain at 5 x 10^8 CFU/ml. Competitive indices were calculated using the following equation: $\log_{10}$ [(CFU mutant/CFU wild-type) output / (CFU mutant/ CFU wild-type) input]. All animal experiments were conducted using protocols approved by the Institutional Animal Care and Use Committee.

Extraction and Sample Preparation for Mass Spectrometry

S. marcescens UMH9 WT and mutant constructs were cultured overnight in LB with the appropriate antibiotics. The following day, cultures were centrifuged and pellets were washed twice in M9 minimal medium. Cultures were diluted 1:100 into M9 minimal medium with and without supplemented $FeSO_4$ (36 μM) and then cultured overnight. Bacterial pellets and supernatants were collected by centrifugation (5,000*x g*, 7 minutes, 4°C) the next day, then delivered to the University of Michigan Natural Products Discovery Core. Detailed methods outlining the mass spectrometry protocol and analysis can be found in Appendix A.

Detection of Siderophore Production

Bacteria were cultured overnight in LB medium with aeration at 37˚C, and harvested by centrifugation the next day. Bacterial pellets were washed twice with M9 minimal medium and then diluted 1:100 into M9 minimal medium for overnight cultures with and without 36 μM $FeSO_4$. The following day, cultures were adjusted to OD_{600} = 1.5 and then centrifuged (5,000*x g*, 7 minutes, 4°C). Supernatants were removed. 100 μL of chrome azurol S (CAS) shuttle solution

was added to 100 µL of siderophore-containing supernatant [141]. 10 µM EDTA was used as a positive control. The CAS-supernatant mixture was allowed to develop for 20 minutes at room temperature. A visible color change from blue to red indicates siderophore production. This color change was measured using a MicroQuant spectrophotometer (Bio-Tek) at an absorbance of 630 nm. Samples were measured in biological and technical triplicates. Final absorbance was calculated by dividing the average absorbance of triplicate samples by the absorbance of the M9 solution alone. Error bars were calculated as the standard error of the mean. Statistical significance was determined using an unpaired *t*-test in Prism v.14.

Data Availability

All RNA-seq data in this publication have been deposited in NCBI's Gene Expression Omnibus repository under accession no. GSE145587.

Chapter V

Characterizing the *Serratia marcescens* Heme Acquisition Systems in the Context of Heme Toxicity and Pathogenesis

Notes. Special thank you to the Snitkin Lab, especially Stephanie Thiede, who assisted with genome assembly and sequence variance analysis performed in this chapter.

Heme and hemin are used interchangeably throughout this chapter.

Abstract.

In addition to siderophore systems scavenging iron, Gram-negative bacteria acquire iron from host heme using dedicated heme uptake systems. Typically, bacteria either encode a dedicated outer membrane transporter to uptake heme or a hemophore, a siderophore like molecule that is secreted from the bacterium and binds heme extracellularly, along with its own dedicated transporter. Interestingly, *S. marcescens* encodes both an independent receptor, and a hemophore system, called *hem* and *has*, respectively, to optimize its ability to uptake iron from heme. These systems have been described previously; however, they have not been examined in the context of mammalian infection. I began this study by mutating each heme system individually and then in conjunction in a double mutant in UMH9 to investigate heme acquisition as a fitness factor for Sm in the mammalian host. When these mutants were grown in culture conditions supplemented

with heme, the *hem* single mutant and *hem/has* double mutant exhibited normal growth, while the WT and *has* mutant exhibited an abnormally long lag phase before all strains reached a similar saturation. These end point cultures were reinoculated into new hemin conditions and the WT and *Δhas* mutant lag was resolved, but was recapitulated after routine culturing. Sequencing revealed mutations in a heme biosynthesis gene as well as in an iron storage locus in the WT and *Δhas* mutant, potentially explaining these *in vitro* growth phenotypes. To investigate how the *hem* and *has* systems contribute to *in vivo* pathogenesis, independent and mixed infections were performed in the bacteremia mouse model with the *Δhem/has* double mutant and WT. However, the *Δhem/has* double mutant did not display significant attenuation or fitness defect during infection, suggesting that heme uptake may not significantly contribute to Sm virulence in mammalian bloodstream infection.

Introduction

Access to iron is a growth limiting step for almost all bacterial pathogens and because of the crucial importance of iron, bacteria have capitalized on obtaining it from nearly all sources found in the human host. In previous chapters, I focused on iron acquisition from host proteins such as ferritin, transferrin, and lactoferrin via siderophores, small iron chelating molecules synthesized by the bacterium with a greater affinity for iron than these host proteins. This chapter focuses on obtaining iron bound to heme molecules within hemoglobin or hemopexin proteins that are abundant within the mammalian host [4].

To acquire iron from heme, bacteria have evolved systems to strip the heme-bound iron found in hemoglobin, hemopexin, and myoglobin. These proteins contain up to four heme

molecules and constitute a major source of iron for pathogens. Typically, Gram-negative pathogens utilize either a hemophore or a dedicated heme receptor, and often employ hemolysins to acquire heme from red blood cells. These hemolysins disrupt the RBC membrane, liberating massive amounts of hemoglobin, which then initiates heme acquisition. The extensive machinery bacteria have developed to acquire iron from heme highlights the importance of these systems despite the presence of other iron acquisition systems, such as siderophores. Additionally, over 30 heme receptors have been described in Gram-negative microbes, and some bacteria, such as *Haemophilus* sp., require exogenous heme to grow at all, further hinting at the importance of heme as an iron source [149-151].

Similar to toxic iron levels, uncontrolled heme import and inefficient heme degradation once inside the cell can result in detrimental toxicity to the bacterium [152]. "Free" heme interacts with membranes potentiating toxicity; therefore, organisms must have strategies to resist these toxic effects. Gram-negatives tend to be inherently resistant to heme toxicity because of their double membrane. In *E. coli*, a protein called HemS alleviates heme toxicity, and in *Yersinia enterocolitica*, HemS is essential for heme to be used as an iron source [38, 153].

Two heme uptake systems have been described in isolates of *S. marcescens*, called *hem* and *has*. The *hem* system consists of an outer-membrane, TonB-dependent receptor that is able to directly transport heme [101]. A previous study examined the mechanism of heme import by the *has* system by reconstituting the *has* locus into an *E. coli* mutant devoid of heme biosynthesis. They found that the *has* system encodes a secreted hemophore, HasA, that scavenges iron bound to heme. HasA then interacts with HasR, a membrane receptor, to handoff the scavenged heme and import it into the bacterium [103, 154, 155]. The *has* system is versatile in that it can acquire heme from a variety of heme sources, including hemopexin [156, 157]. The same is not true for

hem, making it more restricted in that it only takes up heme itself. Interestingly, the *hem* and *has* systems are differentially regulated depending on the external heme concentration. The *hem* system is preferred at heme concentrations above 10^{-6} M while the *has* system functions at concentrations of 10^{-8} M. Because *hem* and *has* do not function redundantly, *S. marcescens* theoretically is more plastic compared to other Gram-negatives in its heme uptake and has a larger pool of what iron it has access to. *S. marcescens* also utilizes a hemolysin, ShlA, to aid in iron-heme uptake by lysing red blood cells. Similar to *E. coli* and *Y. enetocolitica*, HemS is also found in the *S. marcescens hem* operon, but its function in heme degradation or utilization has not been determined.

Currently, the role of heme acquisition during *Serratia marcescens* infection is unknown. My previous studies of *S. marcescens* iron acquisition via siderophores suggests that heme is the preferred iron acquisition system in specific organ sites (Chapter IV). Deletion of the serratiochelin locus reduced pathogenesis in the murine kidney and spleen but not the liver, whereas the *cbs* locus was dispensable in all organ sites examined. Moreover, a *cbs*/*sch* double knockout was less fit than the WT UMH9, but was still able to colonize the murine kidney, spleen, and liver [17]. This indicates that bacteria can persist without replication or that iron acquisition during infection is still possible through a non-siderophore system, such as heme. The importance of heme acquisition during pathogenesis has been established for some pathogens. For example, in *E. coli*, a deletion mutant knocking out both *hma* and *chuA* heme uptake systems had a fitness defect when competed against other iron acquisition uptake mutants in a mouse model of UTI [19]. I hypothesize that heme uptake is a preferred iron acquisition system and accounts for bacterial growth even when siderophores are absent.

In this chapter, the *hem* and *has* heme uptake systems of *S. marcescens* UMH9 are examined. Mutants were constructed that deleted the full *hem* and *has* loci individually (*Δhem* and *Δhas)* and together in a double mutant (*Δhem/has)*. When grown in hemin conditions, the WT and *Δhas* mutant experienced a notably longer lag phase than the *Δhem* and *Δhem*/has mutants that was resolved upon direct re-exposure to heme. However, when strains were re-cultured without heme, then exposed to heme again, the WT and *Δhas* mutant lag was recapitulated. Sequencing revealed potential mutations in heme biosynthesis and iron storage that may contribute to heme detoxification. Further, upon inoculation of the *Δhem/has* double mutant into the mouse bacteremia model, no defect in fitness or virulence was observed. These results together suggest a new understanding of the heme uptake systems in the context of heme toxicity and question their role in pathogenesis.

Results

The *Δhas* mutant and WT displayed lagging growth in hemin culture conditions.

In order to determine how the heme acquisition systems contribute to the ability of Sm to import iron from heme, I individually deleted the *hem* and *has* systems in the UMH9 background as well as created a double mutant abrogating the function of both systems. I grew wild type UMH9 and the mutants in iron-deplete M9 minimal medium supplemented with varying concentrations of hemin (0 μM, 10 μM, 30 μM, 50 μM, and 75 μM). At all tested hemin concentrations, the *Δhem* mutant and *Δhem/has* double mutant had a short lag phase, followed by exponential growth until saturation was reached at an OD_{600} of ~0.8 after 10 to 15 hours. Interestingly, the

WT strain and *Δhas* mutant consistently had a notably longer lag phase, wherein exponential growth began after 10 to 15 hours (Figure 5.1A-D). These mutants reached a similar saturation point as the *Δhem* and *Δhem/has* mutants; however, saturation was not reached until almost 20 hours. This lag was reproducible at many hemin concentrations including nanomolar concentrations as low as 500 nM (Figure 5.2) and was exclusive to hemin conditions. When mutants were grown without hemin, all mutants grew comparably (Figure 5.1E). A similar trend was seen when iron was removed from the medium using Chelex-100 and added back at 36 μM $FeSO_4$ (Figure 5.1F). Therefore, this phenotype is dependent on bacterial exposure to hemin.

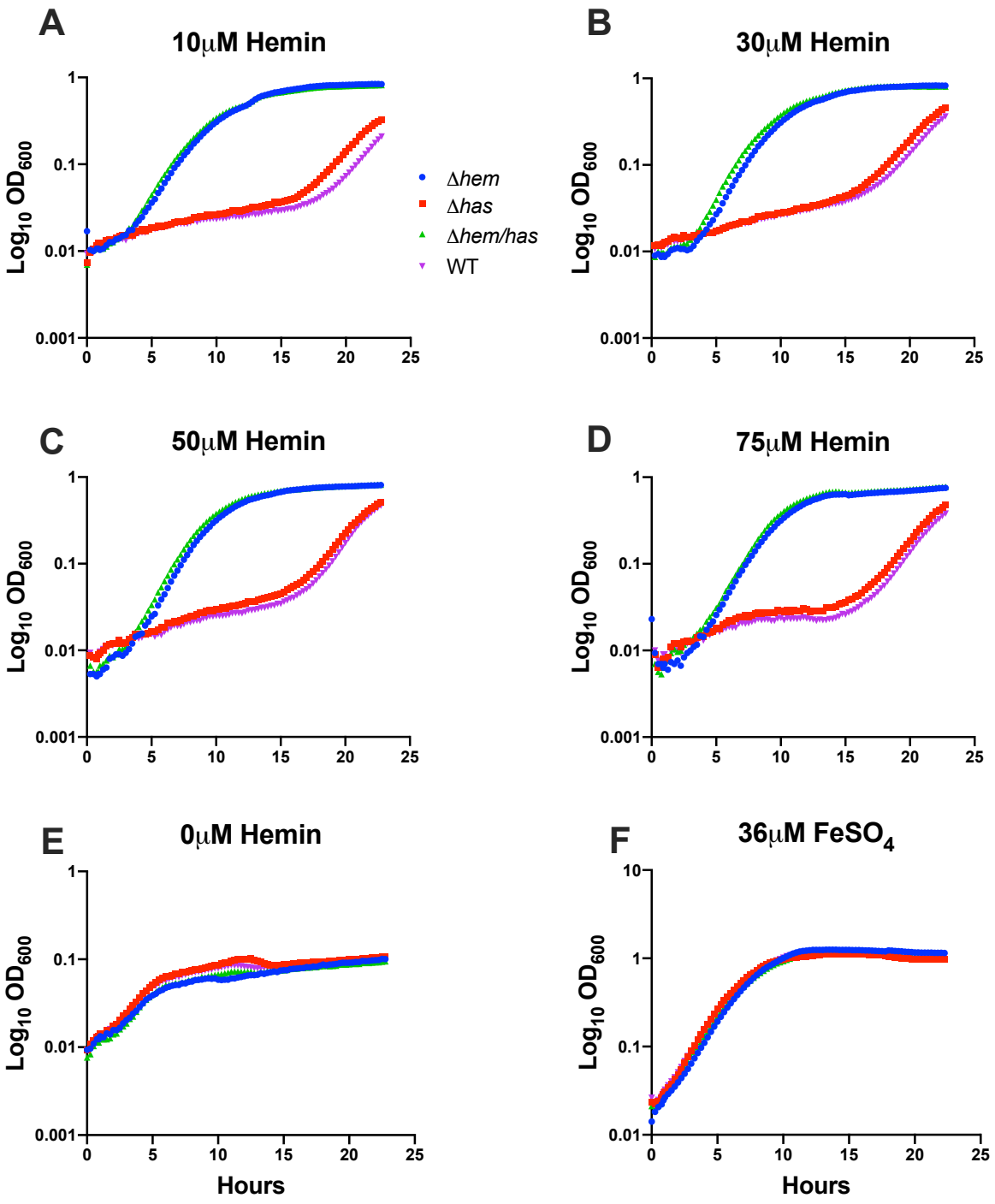

Figure 5.1. The WT and *Δhas* mutant exhibited a notably longer lag phase compared to the *Δhem* and *Δhem/has* mutants when grown in hemin.

S. marcescens UMH9 wild type, the *Δhem* locus mutant, the *Δhas* locus mutant, and the *Δhem/has* double loci mutant were inoculated into chelexed M9 minimal medium containing 10 μM (A), 30 μM (B), 50 μM (C), 75 μM (D), 0 μM (E) hemin and 36 μM $FeSO_4$ (F) after overnight culture in M9 minimal medium. Cultures were incubated with aeration at 37 °C and OD_{600} measurements were taken every 15 minutes.

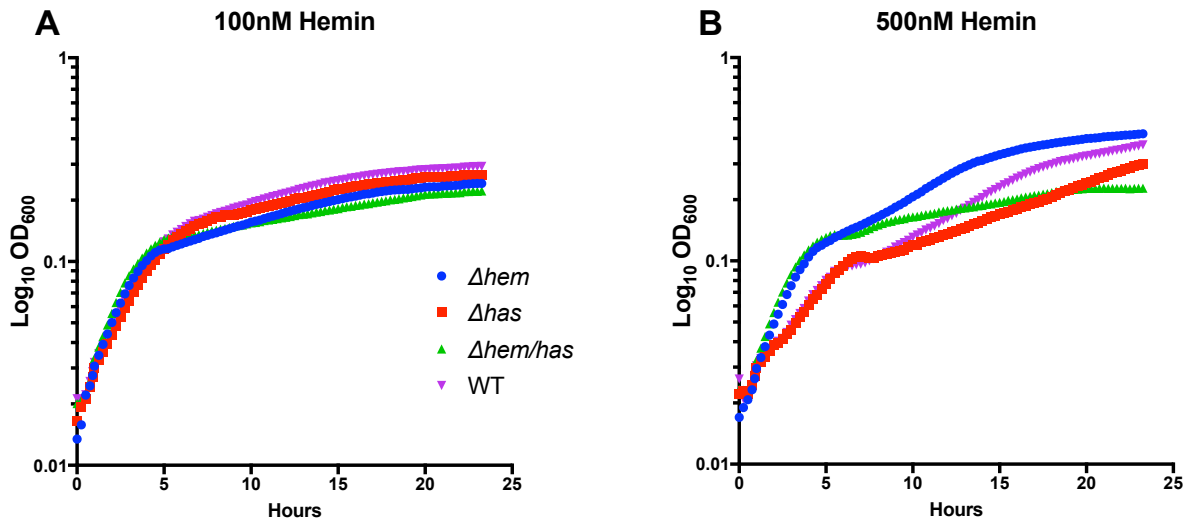

Figure 5.2. The WT and *Δhas* mutant have slower growth even at nanomolar hemin concentrations.

S. marcescens UMH9 wild type, the *Δhem* locus mutant, the *Δhas* locus mutant, and the *Δhem/has* double loci mutant were inoculated into chelexed M9 minimal medium containing 100 nM (A) or 500 nM (B) hemin after overnight culture in M9 minimal medium. Cultures were incubated with aeration at 37 °C and OD_{600} measurements were taken every 15 minutes.

The *Δhas* mutant and WT lag was lost when end-point cultures from hemin conditions were re-inoculated.

The *Δhas* mutant and WT had an extended lag phase when grown in hemin conditions; however, they did eventually reach a comparable stationary phase to what was observed with the *Δhem* and *Δhem/has* mutants, suggesting that a potential suppressor mutation occurred during growth. To further explore this possibility, the heme system mutants and wild type were grown in differing hemin concentration as above. Then, end point primary cultures were re-inoculated into fresh iron-depleted media containing matching hemin conditions to determine if the extended lag phase was still observed. After the end-point cultures were re-inoculated into hemin conditions, the *Δhas* mutant and wild type no longer displayed a delayed lag phase and had exponential growth comparable to what was seen with the *Δhem* and *Δhem/has* mutants (Figure 5.3). Because the extended lag resolved after initial incubation in hemin conditions, this suggested the presence of a potential suppressor mutation that allowed the *Δhas* mutant and WT to have normal growth.

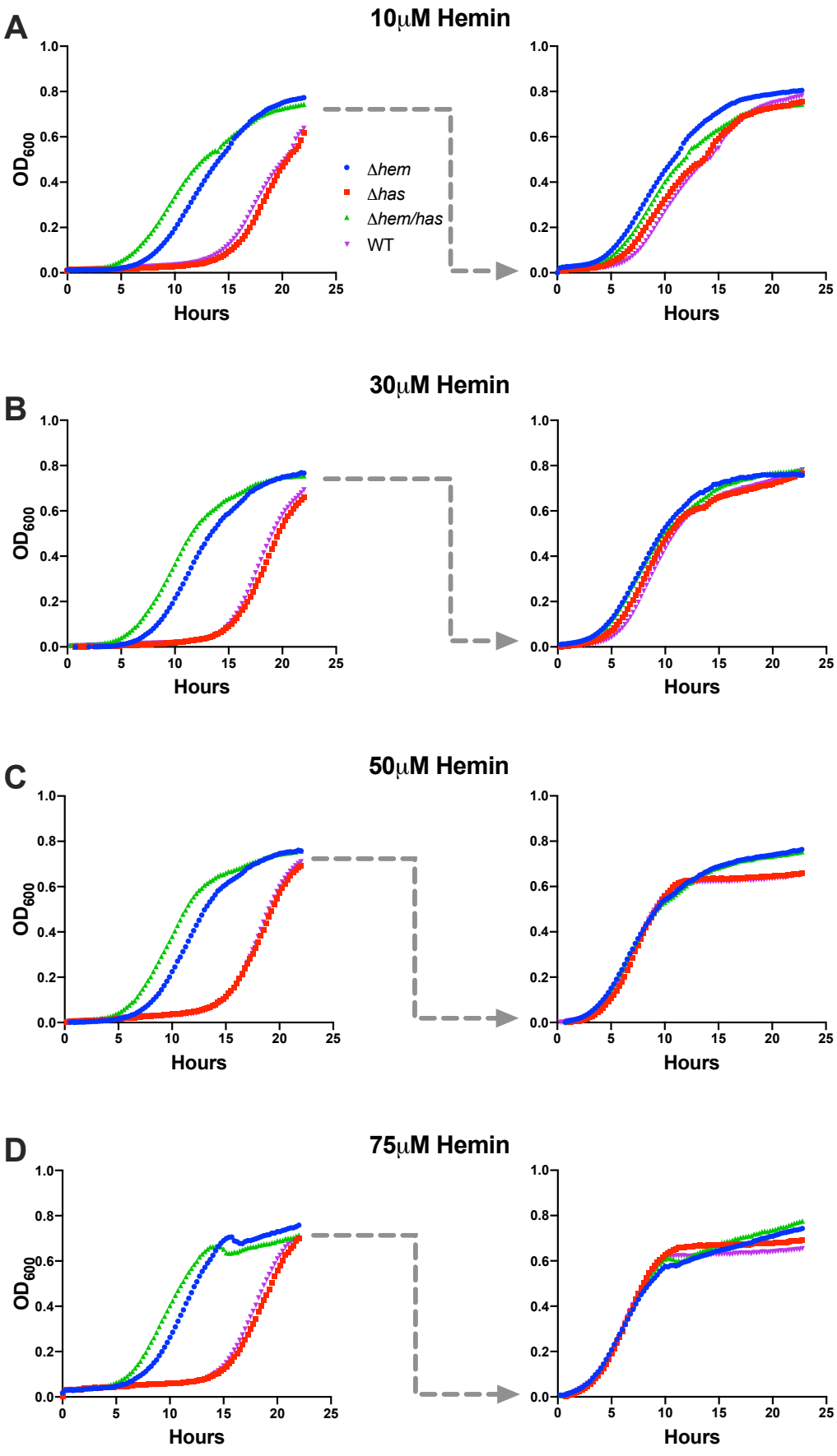
A
10μM Hemin
B
30μM Hemin
C
50μM Hemin
D
75μM Hemin
OD600
Hours
Δhem
Δhas
Δhem/has
WT

Figure 5.3. The WT and *Δhas* mutant lag were resolved after cultures exposed to hemin overnight were directly reinoculated into hemin conditions.

All bacterial strains were grown overnight in either 10 μM (A), 30 μM (B), 50 μM (C), or 75 μM (D) hemin. The following day, these cultures were reinoculated into a new growth plate with matching hemin conditions. Bacterial growth was measured every 15 minutes at an optical density of 600 nm for both the initial hemin incubation (first column) and the endpoint reinoculation (second column). Grey arrows indicate the end-point cultures that were used as the starting culture to inoculate the second hemin growth plate.

When end-point cultures were passaged and re-cultured, the *Δhas* mutant and WT lag was recapitulated.

Upon direct re-inoculation of end-point cultures into a new growth plate, the extended lag seen in the has mutant and wild type growth was resolved. To confirm that this result was due to a suppressor mutation, I took end-point cultures after a lag was seen but when cultures reached stationary phase levels comparable to the hem and hem/has mutants, and struck them onto LB plates. Colonies were picked and grown in LB the following day. These cultures were then cultured in M9 minimal medium as they were when inoculated into the initial growth plate. I hypothesized that if the observed lag was due to a suppressor mutation, passaging and re-culturing of the strains should not affect disappearance of the extended lag phase. However, when the *Δhas* mutant and WT were once again exposed to hemin, the prolonged lag phase was seen again, suggesting that a suppressor mutation did not occur (Figure 5.4). Rather, because the lag resolved when strains were directly transferred into hemin, but was seen again after re-culturing, this potentially suggests phase variation from an invertible element, or the result of polynucleotide tracts, which are transient genetic variations usually in promoter regions that cause downstream genes to be affected.

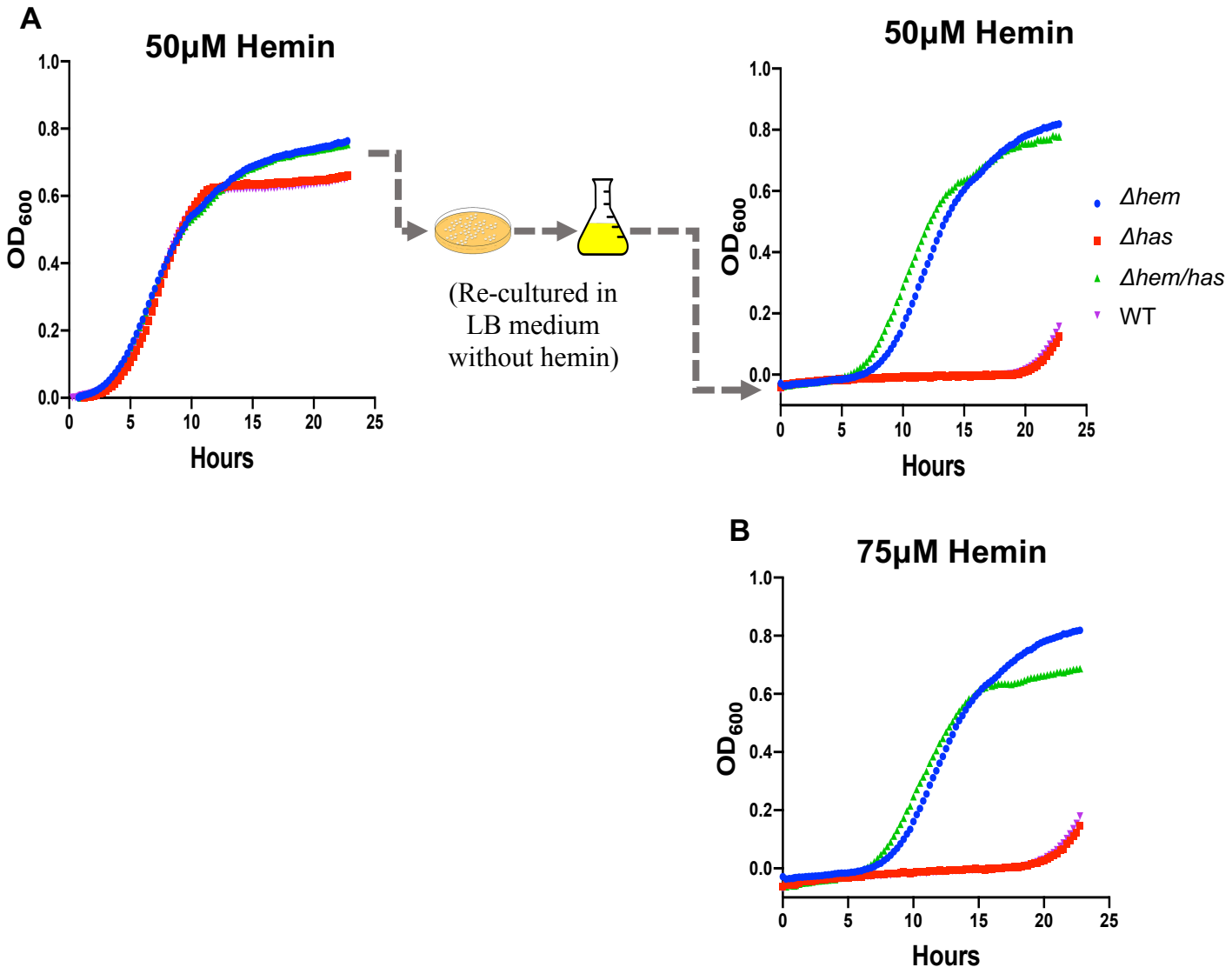

Figure 5.4. The WT and *Δhas* mutant lag is recapitulated after hemin end-point cultures are passaged before secondary hemin exposure.

The WT, *Δhem* mutant, *Δhas* mutant, and *Δhem/has* mutant were initially exposed to heme and then end-point cultures were directly reinoculated into heme-matched conditions. These end-point cultures were streaked onto plates, and re-cultured overnight in M9 minimal medium without hemin. The following day, cultures were inoculated into a new growth plate containing

the indicated heme concentrations [50 μM (A) or 75 μM (B)], and OD_{600} measurements were taken every 15 minutes to examine bacterial growth.

Mutations in heme biosynthesis and iron storage may account for the observed WT and *Δhas* mutant growth phenotypes

To test the possibility that an invertible element or polynucleotide tract is responsible for these growth phenotypes, DNA sequencing was performed. The *Δhem*, *Δhas*, *Δhem*/*has*, and WT were exposed to heme in a bacterial growth plate. Once all strains reached similar saturation but after *Δhas* and WT lag was observed, DNA from these endpoint cultures was extracted, as a genetic element potentially resolving the lag would still be present in the genome. These cultures were also streaked onto LB and re-cultured without hemin so that the *Δhas* and WT lag would once again be observed if exposed to hemin, like previously shown after passaging (Figure 5.4). Because the lag is recapitulated after re-culturing (Figure 5.4) but not when directly re-exposed to heme (Figure 5.3), the potential genetic element that is present after heme exposure is no longer there. Therefore, DNA was extracted from these samples before second exposure to heme to compare to the early samples after initial heme exposure.

Whole genome sequencing was completed and variation analysis between sequences from samples after initial and before second heme exposure was performed. Analysis revealed a potential intergenic modifier upstream of *hemG* as well as an insertion upstream of a bacterioferritin-associated ferredoxin gene in the WT and *Δhas* mutant after initial exposure to heme that may account for the observed phenotypes (Table 5.3).

Table 5.1. Genomic variants found in WT and the *Δhas* mutant after initial heme exposure and after re-culturing without heme[a]

Strain:	Affected Gene/Gene Function:	Reference: After Re-culturing	Variant: After initial heme exposure	Impact:
Wild type	*hemG*; Protoporphyrinogen IX oxidase	GAA	GAG	Intergenic modifier
Δhas	*hemG*; Protoporphyrinogen IX oxidase	TTC	CTC	Intergenic modifier
Wild type	Bacterioferritin-associated ferredoxin	GTAACCCTG	GCCAGGCGACAACGT GAACATGGTT**GTAAC CCTG**	Frameshift insertion
Δhas	Bacterioferritin-associated ferredoxin	GGTTA	**GGTTA**CAACCATGTTC ACGTTGTCGC	In-frame insertion

[a]After initial heme exposure = DNA was extracted immediately after overnight culture with heme. After re-culturing = DNA was extracted from strains that were exposed to heme overnight, and re-cultured without heme.

Heme uptake does not appear to contribute significantly to *in vivo* pathogenesis

Next, I wanted to determine if these *in vitro* phenotypes translated to the mouse bacteremia model. Although the *Δhem/has* double mutant performs better in excess heme than the WT does *in vitro*, I hypothesized that losing both heme systems *in vivo* would be detrimental. Mice were co-challenged with a 1-to-1 inoculum of WT and the *Δhem/has* mutant. After 24 hours, spleen and liver were collected, and competitive indices were calculated. The *Δhem/has* mutant had a slight fitness defect although it was not statistically significant (Figure 5.5A).

The WT and *Δhem/has* mutant were also challenged independently in the mouse model for 24 hours, and bacterial burden was determined in the spleen and liver. Interestingly, there was only a small decrease in recovered bacteria from mice infected with the *Δhem/has* mutant when compared to WT bacteria that were recovered, suggesting that the heme uptake systems may not be crucial to bacteremic infection in the murine host (Figure 5.5B, C).

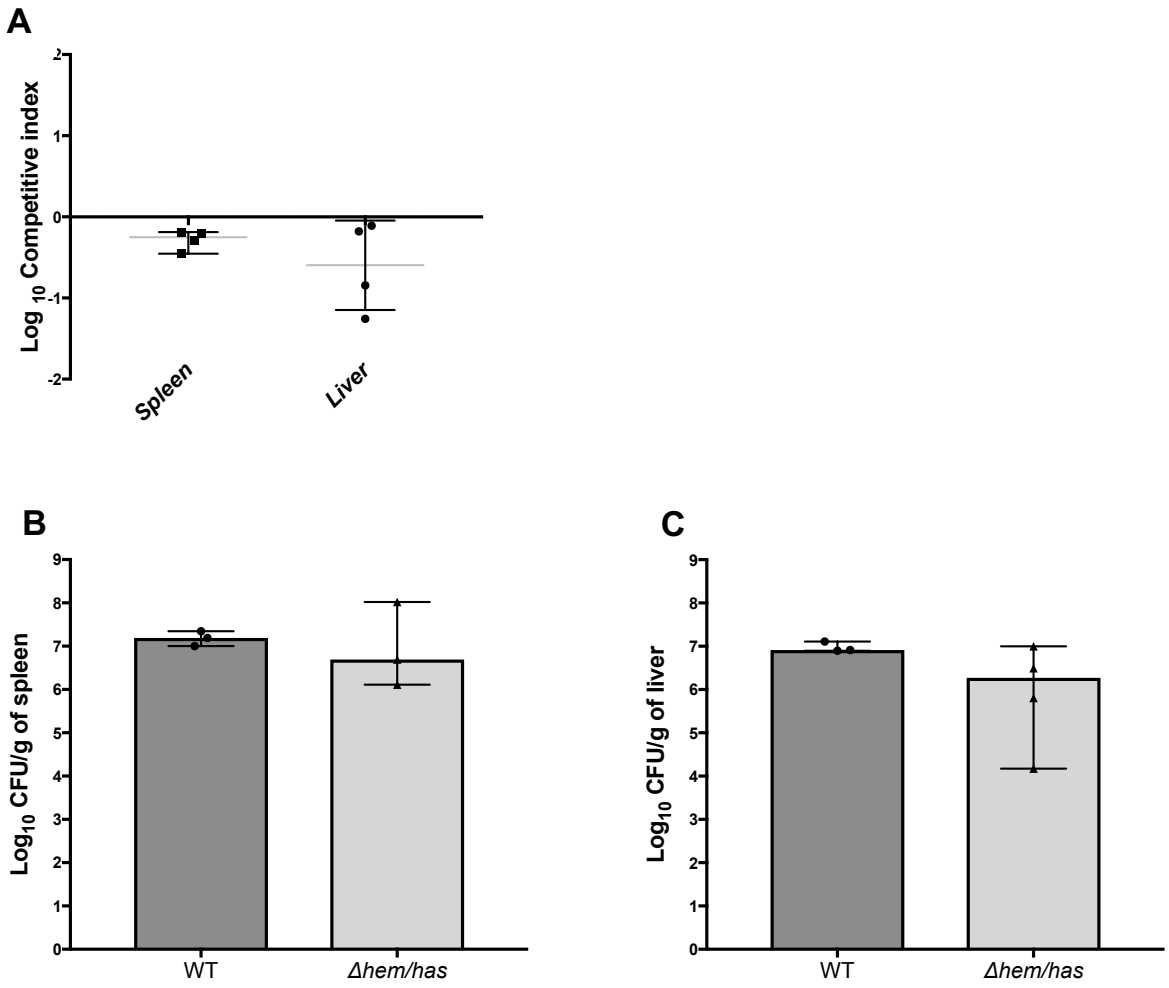

Figure 5.5. The *Δhem/has* double mutant is not attenuated and does not have a fitness defect *in vivo*.

(A) CBA/J mice were infected with 5×10^7 CFU/mouse in a 1:1 mixture of the wild type and the *Δhem/has* double mutant via the tail vein. Mice were euthanized at 24 hours and the spleen and liver were collected from each mouse. Organs were homogenized. Homogenates were diluted and selectively plated. The relative fitness for the mutant was compared to that of the wild type and calculated as a competitive index (CI). The solid black line represents a CI of 1.0, meaning that the two strains competed equally. Solid grey lines represent median CI. Statistics were calculated using the Wilcoxon signed-rank test with a theoretical median of 0. (B,C) Mice were

independently inoculated with either WT or *Δhem/has* mutant via the tail vein. Mice were euthanized 24 h post inoculation. Spleens (B), and livers (C) were collected and homogenized. Homogenates were diluted and plated. The dotted line indicates the limit of detection. Significance, determined by the Mann-Whitney test.

Discussion

Experiments presented in this chapter examined the heme acquisition systems, *hem* and *has*, of S. marcescens UMH9, and revealed new insights into potential heme detoxification mechanisms by which heme is tolerated. Unlike other studies in Gram-negative bacteria, the results presented here suggest that heme uptake systems may not be critical to Sm bloodstream infection but do raise new questions around the utilization of heme in UMH9.

Interestingly, the WT and *Δhas* mutant strains showed severely longer lag phases than the *Δhem* and *Δhem*/*has* mutants when exposed to heme *in vitro*. Heme toxicity may account for this longer lag that is associated with the *hem* system since this phenotype was only seen in strains that had an intact *hem* locus. The mutants lacking the *hem* locus, *Δhem* and *Δhem*/*has*, grew normally. However, all strains reached a similar saturation point by 24 hours which suggested a suppressor mutation in the WT and *Δhas* mutant that allowed them to begin exponential growth.

Sequencing revealed two variances in the WT and *Δhas* mutant that may explain the observed growth phenotypes. The first was a mutation in *hemG*, a protoporphyrinogen IX oxidase involved in bacterial heme biosynthesis. Sm encodes all the required genes to synthesize heme intracellularly so if the WT and *Δhas* mutant are experiencing heme toxicity, a mutation stopping endogenous heme production could alleviate intracellular heme levels [158]. The second mutation was in bacterioferritin-associated ferredoxin, a gene hypothesized to encode a protein (ferredoxin) that liberates iron from an iron storage protein (bacterioferritin). Bacterioferritins possess four intrinsic heme groups that are deeply buried within the protein. Freeing of the iron bound to this heme requires the electron transferring capabilities of ferredoxin [159-161]. Therefore, a mutation in bacterioferritin-associated ferredoxin would inhibit iron liberation from heme molecules bound within bacterioferritin and limit intracellular levels of

iron. This would be particularly beneficial during heme detoxification and may be another explanation of the growth-phenotypes seen in the WT and *Δhas* mutant.

These mutations may enable the WT and *Δhas* mutant to reach a similar saturation point as the *Δhem* and *Δhem.has*; however, it is still unknown why this growth phenotype is only observed in the WT and *Δhas* mutant, strains with intact *hem*. The sequencing analysis did not reveal an association between the *hem* locus and the growth lag. To speculate, the *hem* system is more active when extracellular heme concentrations are higher, above 10^{-6}M, similar to the *in vitro* conditions tested here. The WT and *Δhas* mutant with functional *hem* systems are potentially experiencing such a high influx of heme through the *hem* system that it manages toxicity by transient mutation of heme biosynthesis and iron storage.

Additionally, it is possible that differential regulation is contributing to the growth phenotypes. Because the long lag is recapitulated after re-culturing without heme, this could suggest recalibration of regulatory networks or time needed to synthesize metabolic precursors. RNA-sequencing would address this hypothesis examining gene expression of the WT and *Δhas* mutant as compared to the *Δhem* and *Δhem/has* mutants during the exponential growth phase.

The *in vitro* growth conditions tested here are in the micro-molar range which is a large amount of heme. With these high heme conditions, it may not be surprising that potential heme toxicity is occurring, although it is interesting that this toxicity is occurring only in mutants with an intact *hem* locus. This leads to an important question around physiological concentrations of heme and if Sm would ever encounter such high levels. This is also particularly interesting since the WT experienced the hypothesized toxicity. Free heme concentrations within erythrocytes have been reported to be as high as 21 ± 2 μM [162]; therefore, these *in vitro* heme conditions could be encountered *in vivo* when RBCs are lysed.

Even with previous studies in other bacterial pathogens suggesting the importance of heme uptake *in vivo*, the double *Δhem/has* mutant did not show attenuation or a fitness defect in the mouse bacteremia model. This is perplexing since results in Chapter IV suggest that siderophores are not the sole source of iron uptake in the bloodstream, and heme uptake most likely was playing a role. The mutation found in *hemG*, a heme biosynthesis gene. This suggests that heme biosynthesis is utilized by Sm, suggesting that Sm prefers heme biosynthesis versus uptake, which would explain why there was no phenotype of the double heme mutant *in vivo*. Future research to evaluate this possibility is necessary.

In summary, this chapter proposed interesting insights into heme toxicity related to the *hem* uptake system in UMH9 and hypothesized mechanisms of how this toxicity is overcome based on genomic analysis. While many questions remain regarding the physiological relevance of these findings, it prompts questions around how Sm persists *in vivo* if faced with high heme concentrations. Additionally, even though mouse studies did not reveal a crucial need for heme uptake via the *hem* and *has* systems, this may suggest alternative heme acquisition and metabolism strategies used by *S. marcescens*.

Methods and Materials

Bacterial Strains and Culture Conditions

All *Serratia marcescens* strains used in this study are described in Table 5.1. Luria broth (10 g/L tryptone, 5 g/L yeast extract, 0.5 g/L NaCl) was used for routine culture of bacteria. Antibiotics were added to cultures at the following concentrations when appropriate: kanamycin (25 μg/ml), chloramphenicol (30 μg/ml), spectinomycin (100 μg/ml). M9 defined medium (0.1 mM $CaCl_2$,

1mM $MgSO_4$, 0.4% glucose) was also used to culture bacteria. Where specified, M9 was treated with Chelex-100 to remove iron, creating iron-limited conditions. Hemin (Sigma-Aldrich) was added to M9 cultures at the stated concentrations. $FeSO_4$ (36 μM) was added back to M9 cultures where indicated.

Table 5.2. *S. marcescens* strains and plasmids.

Name	Relevant genotype	Description	Reference or source
S. marcescens			
UMH9	Wild type	Bloodstream infection isolate	[98]
Δhem	*hem::kan*	Deletion of genes *07350 to 07380, hem,* replaced with kanamycin cassette from pKD4.	This study
Δhas	*has::cam*	Deletion of genes *01515 to 01540*, *has*, replaced with chloramphenicol cassette from pKD3.	This study
Δhem/has	*hem::kan, has::cam*	Double mutant with both gene, *hem* and *has*, deletions replaced with the indicated antibiotic cassette.	This study
Plasmids			
pKD4		Source of kanamycin resistance gene	[139]
pKD3		Source of chloramphenicol resistance gene	[139]
pSIM19		Recombineering plasmid	[140]

Construction of UMH9 Heme Mutants

The lambda red recombinase system was used to make single and double mutations in the *hem* and *has* operons [139]. Using pKD4 and pKD3, the kanamycin and chloramphenicol resistance cassettes, respectively, were PCR amplified using primers with `50 bp homology to the 5' end of the gene locus and ~20 bp of homology to the pKD3/4 3' end of the primer. Primers used are listed in Table 5.2. PCR products were digested with DpnI and electroporated into UMH9 cells harboring pSIM19 after heat treatment for 20 minutes at 42 °C. pSIM19 was removed from the mutant cells. Mutants were validated using PCR and whole genome sequencing.

Table 5.3. Primers for mutant construction[a]

Gene	Forward Primer	Reverse Primer
hem	ttcactctctgttatccatcccctgcgtcacgctgcagggcgagcaaaaagtgtaggctggagctgcttc	ggtagacctgcggcagcgacacttcgggatgatgcaccacgccgagatcgatgggaattagccatggtcc
has	tccgagttgcaggcgttgtttctgcgccatatgcggccgctgcaagcctagtgtaggctggagctgcttc	aggcgatcggtcagcggtttgaacaggtagttcatcatcgaacgctcgccatgggaattagccatggtcc

[a]Primer sequences are listed 5' to 3'. Underlined sequences in mutant construction primers are identical to regions at the 5' to 3' ends of the locus to be disrupted.

Growth of *S. marcescens* Strains

Bacterial strains were cultured with aeration overnight in LB medium at 37 ˚C. The following day, bacteria were collected by centrifugation and washed twice with M9 minimal medium. Bacteria were suspended in M9 minimal medium and 30 μL were used to inoculate 3mL of chelexed M9 minimal medium for overnight cultures. A sample of culture (3 μL) was used to inoculate each well of a 100-well growth plate containing 300 μL of chelexed M9 with the indicated hemin concentration to an OD_{600} of 0.01. Control conditions were also included measuring growth in iron depleted M9 minimal medium and M9 minimal medium with 36 μM $FeSO_4$ added back. After initial growth in hemin, endpoint cultures were taken and re-inoculated into a new growth plate with identical hemin conditions. These cultures were also struck onto antibiotic LB plates, recultured overnight in LB, washed with M9 minimal medium, recultured overnight in M9 minimal medium, then inoculated into another hemin growth plate. Growth curves were performed to observe extended lag phase for particular mutants, resolution of this lag upon direct endpoint reinoculation into heme, and then recapitulated lag after reculturing. Growth curves were performed in biological and technical triplicates. Plates were incubated at 37˚C with continuous shaking and OD_{600} was measured every 15 minutes for 21 hours using a BioScreenC plate reader.

DNA Purification and Sequencing

DNA was extracted from *Δhem*, *Δhas*, *Δhem/has*, and WT cultures after initial growth in hemin conditions, and then after re-culturing in LB and M9 minimal medium but before second exposure to hemin. DNA purification was performed using the Gram-negative extraction protocol of the Qiagen Blood and Tissue Kit. Cellular lysis was performed using Proteinase K

and DNA was eluted in Qiagen EB buffer. DNA samples were library-prepped and sequenced by the University of Michigan Advanced Genomics Core. A NovaSeq (S4) 300 cycle was used for sample sequencing, providing an expected 10 million reads per sample with more than 100 X sequence coverage.

Genome Assembly and Variance Analysis

After sequencing, PATRIC's online assembly and variance analysis platforms were used to assemble genomes and identify mutations and genetic variation between particular samples. Parameters for variance analysis consisted of alignment using Bowtie2 and SNP caller, FreeBayes. Variance between samples after initial heme exposure and before second heme exposure after re-culturing without heme were compared. Variances that were found in all mutants were filtered out. Unique mutations found in both the WT and *Δhas* mutant analysis were identified.

Murine Model of Bacteremia

Overnight cultures of WT and *Δhem/has* were harvested by centrifugation (3500*x g* for 30 minutes at 4 ˚C) and resuspended in phosphate-buffered saline (PBS) to a density of 5 x 10^8 CFU/ml. Two groups of five female CBA/J mice (Jackson 000656) aged 6-8 weeks were independently inoculated with either UMH9 WT or the *Δhem/has* double mutant. An inoculum (100 µL) of 5 x 10^8 CFU/ml was injected into the tail vein. Infection was allowed to progress for 24 hours. Spleen, and liver were collected and homogenized in PBS. Homogenates were diluted and plated onto LB agar or LB agar containing the appropriate antibiotics using an Autoplate 4000 spiral plater (Spiral Biotech) and incubated overnight at 37˚C. Bacterial colonies were

counted the following day using a QCount (Chemopharm). For co-challenge experiments, the following modifications were made. The *Δhem/has* mutant strain was combined in a 1:1 mixture with the UMH9 WT strain at 5 x 10^8 CFU/ml. Competitive indices were calculated using the following equation: $\log_{10}$ [(CFU mutant/CFU wild-type) output / (CFU mutant/ CFU wild-type) input].

Chapter VI

Conclusion and Final Thoughts

Summary of Findings

With the emergence of Sm as a pathogen of significant clinical relevance, there is an express need to understand the underpinnings of Sm pathogenesis. Correspondingly, there has been an increase in research to understand Sm infection. While studies have identified relevant virulence factors and provided foundational work to understanding Sm, they have not truly defined Sm pathogenesis in the context of mammalian infection. This work is critically important to ultimately controlling these infections. The work presented in this dissertation aimed to address this gap specifically pertaining to Sm virulence factors involved in iron acquisition. In the pursuit to ascertain this knowledge, I discovered that iron acquisition in Sm is much more intricate than what was originally hypothesized and unexpected, yet interesting insights ultimately emerged, providing a deeper appreciation for a previously underestimated pathogen.

In Chapter II, RNA-sequencing identified all genes involved in iron acquisition in the clinical bloodstream isolate UMH9. This included siderophore biosynthetic loci, heme uptake systems, ferrous iron, and citrate uptake, as well as orphan iron receptors regulated by iron concentration. The results of this Chapter guided the selection of iron acquisition systems to be studied further in the proceeding Chapters.

In Chapter III, the siderophore biosynthetic gene clusters that were identified by RNA-seq in Chapter II were explored. These gene clusters were called *cbs* and *sch*, respectively due to similarities of the UMH9 clusters to previously identified chrysobactin and serratiochelin loci. The absence of two NRPS genes, one from each locus, in a double mutant which deleted presumed essential siderophore biosynthetic machinery, resulted in severely defective growth in iron-limited conditions. Interestingly, this mutant had notably increased siderophore production quantified by the CAS assay, and the presence of serratiochelin in mutant supernatants was confirmed by mass spectrometry. This suggested that despite the ability to produce a siderophore, the double NRPS mutant could not take up the bound iron, resulting in defective growth under iron-limitation. Intriguingly, when the NRPS genes were deleted individually in single mutants, they performed comparably to wild type UMH9 in all assays. The single mutants grew to WT levels in iron-depletion, and showed similar iron chelation levels.

These results are surprising because they suggest that NRPS genes, typically exclusively involved in siderophore biosynthesis, are potentially involved in siderophore transport, and they also suggest that these NRPSs have redundant functions in transport since the single mutants performed to WT levels, and the double mutant displayed the phenotype. This supports the possibility that the siderophore loci in Sm have the ability to crosstalk and support each other via redundancy. How these two NRPSs contribute to transport and iron uptake is currently unknown. Previous work has shown NRPSs to associate with bacterial membranes; therefore, they may interact with receptors or permeases during siderophore transport to facilitate necessary conformational changes that occur during ferri-siderophore uptake. These results challenge the traditional understanding of NRPSs and the role they play in iron acquisition.

In Chapter IV, to definitively determine the contribution of the siderophore loci, *cbs* and *sch*, to mammalian bloodstream infection, full siderophore locus mutants were constructed, in both single and double mutant combinations. Only mutants lacking the *sch* operon (*sch* and *cbs/sch*), and thus lacking serratiochelin, showed defective iron chelation, displayed inhibited growth in iron-poor conditions, and were attenuated in the mouse bacteremia model. All of these results taken together suggested that serratiochelin was necessary for full virulence during bloodstream infection; however, the *cbs* locus was dispensable and played little to no role during *in vitro* iron chelation or *in vivo* infection.

In other Gram-negative bacteria, such as *E. coli* and *K. pneumoniae*, siderophores have redundant, and sometimes hierarchical, roles, but it's uncommon to observe a siderophore with no contribution to infection such as what was seen with chrysobactin in Chapter IV. Because Sm is an environmental pathogen, chrysobactin may contribute to plant or insect pathogenesis or even scavenging iron from soil, but it may not have the iron affinity to effectively compete with host proteins in the context of human infection.

Chapters III and IV demonstrate that siderophore biosynthesis and transport is significantly more complicated than what was initially expected and does not follow the canonical understanding of iron acquisition in Gram-negative bacteria. While serratiochelin plays a significant role in bacteremia, the role of chrysobactin is currently unknown. However, given the results of Chapter III, it is possible that chrysobactin itself does not significantly contribute, but the NRPS, *cbsF*, within its locus may play a role in transport, and thus, is why the *cbs* gene cluster is conserved. It is also worth considering the amount of selective pressure on the *cbs* locus for Sm as a mammalian pathogen versus in its other niches. Additionally, the *schF0* NRPS gene in the serratiochelin locus is completely bypassed in the biosynthesis of

serratiochelin; therefore, much like *cbsF*, it could be conserved due to a potential role in transport.

Chapter V aimed to elucidate the role of heme uptake during bacteremic infection. While the *Δhem/has* mutant did not show virulence attenuation or a fitness defect in the mouse bacteremia model, some interesting hypotheses on heme detoxification mechanisms were proposed based on results from *in vitro* growth in hemin. Upon mutant exposure to heme, a lagging growth phenotype was observed in mutants that had functional *hem* systems, WT and *Δhas.* Sequencing revealed potential mutations in heme biosynthesis and iron storage that would lower the intracellular heme levels, suggesting novel mechanisms by which heme is tolerated. The relevance of these findings to in vivo pathogenesis is still to be determined; however, the results of this chapter provide new insights into the functionality of the *hem* and *has* heme uptake systems

This work provides insight into the complexity of Sm iron uptake and identified potential non-canonical functions of both siderophore and heme acquisition systems. Collectively, these studies contribute to the growing body of work aimed at understanding not just the virulence of *Serratia marcescens* but also other pathogens that are emerging from seemingly harmless origins. Because Sm has unique nuances to its pathogenesis, it's likely that other pathogens do as well. This may ultimately require a new perspective on how these infections are treated and novel approaches to drug development.

Future Directions

The work presented here leads to several open questions, both in the context of my results and more broadly in the field of Gram-negative pathogenesis. More research is required to fully

understand Sm iron acquisition. Future directions stemming from my work include: elucidating Sm siderophore transport, continuing to explore the role of heme acquisition in mammalian infection and the physiological relevance of heme toxicity, and coordination between all iron uptake systems. In a broader context, translatable studies examining iron acquisition systems as druggable targets should be explored.

Next Steps for Siderophores in Pathogenesis Research

Siderophore transport is generally understood from mechanistic studies in *E. coli*, which have been translated to iron uptake via siderophores in other Gram-negative bacteria [163, 164]. My work suggests that this model is not necessarily true for siderophore import in Sm. The implication of the results in Chapter III that particular NRPSs are involved in siderophore transport is novel, thus additional studies should be conducted to confirm this role. It is possible that the NRPSs have a role in siderophore degradation once inside the bacterium to release the iron instead of a direct impact on transport itself. Both hypotheses suggest a unique mechanism of NRPS functionality, and elicit follow up questions around this being a Sm specific feature or a more ubiquitous mechanism among environmental pathogens. Further, my results imply a redundancy in function between the NRPS genes potentially involved in siderophore uptake, that individually each can effectively perform. This may suggest regulatory crosstalk or indicates that baseline levels of the NRPS may be sufficient to compensate for the other. This could also elucidate the role of the *cbs* locus during infection since the actual chrysobactin molecule does not significantly contribute to pathogenesis. Whatever the role of the NRPS in siderophore uptake or iron utilization, it is clear that further exploration will yield interesting findings.

Additionally, Sm requires the siderophore serratiochelin to achieve full virulence during a mouse model of bacteremia [17]. Serratiochelin is an interesting molecule as its biosynthesis is an evolutionary combination of the enterobactin and vibriobactin synthesis pathways [108]. The mixing and matching of these siderophore loci to create serratiochelin suggests that Sm is an important intermediary for genetic transfer between different Enterobacterales. Horizontal genetic transfer drives the evolutionary dynamic of creating diverse genomes and has been documented extensively in the literature. For example, a study examining the repertoire of polysaccharides between 45 Enterobacteriaceae genera found high rates of genetic transfer of both whole loci and individual genes from multiple bacterial species to create high evolutionary diversity within polysaccharide loci [165]. Analogous genetic transfer is seen in the Sm serratiochelin locus; therefore, finding similar biosynthetic pathways among siderophore loci could provide fascinating insights into the evolution of small molecule biosynthesis.

Next Steps for Heme Acquistion Research

Despite previous advances describing the mechanistic function of Sm heme uptake [37, 40, 102, 130, 156], the heme acquisition systems of Sm have a yet to be determined role in pathogenesis, and in the broader context of iron acquisition itself. Even though my results suggested a minor role of heme uptake in bacteremia pathogenesis, a larger contribution of these systems could be found in other infection models such as urinary tract infections or wound infections. While the heme systems are complex on their own and should be understood individually, studying them alongside siderophores will add to our understanding of what iron uptake systems are necessary to colonize certain organs or are temporally required as infection progresses. Since both iron and heme are toxic at high levels and particular systems are likely

beneficial at differing organ sites, it is advantageous for a bacterium to coordinate all iron uptake systems. It is probable that exploring cross-talk between siderophores and heme uptake will reveal interesting regulatory pathways that promote the most advantageous iron system expression.

Significant questions remain regarding how the ShlA hemolysin and heme uptake systems function in concert. It is assumed that ShlA releases heme from red blood cells which is then taken up by the heme systems; however, this relationship has not been empirically tested and also leads to questions around heme toxicity. If a deluge of heme is suddenly available to the bacterium, efficient degradation and storage systems must be employed to avoid toxicity. This makes the results of Chapter V even more interesting and physiologically relevant since the WT strain did have an extended lag phase in excess heme *in vitro* and may experience overwhelming levels of heme *in vivo*. It is currently unknown how toxic levels of heme kill bacteria. It is possible once heme is degraded, hydroxyl radicals accumulate from free iron and cause intracellular damage; however, studies speculate that toxicity is likely caused by DNA damage related to the heme itself [166, 167]. Bacteria do employ mechanisms of heme tolerance to avoid toxicity. These typically consist of actively effluxing heme, sequestering heme, or degrading it [168-172]. More work is needed to define Sm heme tolerance systems, but Sm does encode HemS, which has been identified and explored as a heme sequestration and degradation protein in *E. coli*, *Y. enterocolitica*, and *Y. pestis*, although its definitive function has not been described [173-175]. Additional research examining the functionality of Sm heme systems and how they contribute to heme tolerance is necessary to fully understand Sm heme uptake.

Serratia marcescens in polymicrobial infections

Serratia marcescens is commonly isolated from polymicrobial infections; therefore, it would also be interesting to study Sm in a polymicrobial context [176]. Sm encodes several "orphan" iron receptors that do not have characterized substrates. It is possible that these are additional receptors for its own siderophores; however, it is also likely that these are able to import siderophores made by other microbes. Evaluating if these receptors contribute to Sm fitness in a polymicrobial setting would provide insight on opportunistic infections. Additionally, possession of a hemophore also seems like an advantage in a polymicrobial context since hemophores are not ubiquitous across bacterial species. Similarly, the siderophore serratiochelin has not been identified in other Gram-negative pathogens outside of the *Serratia* genus, whereas yersiniabactin and aerobactin are found across several. Having unique iron uptake systems that cannot be "hijacked" by surrounding microbes is beneficial in polymicrobial environments. Although, while not yet documented, other pathogens could encode serratiochelin receptors. Studying how various iron uptake systems play a role when iron is being competed for, not just with the host but with other pathogens, would provide insightful perspectives on how microbes interact and equip themselves with virulence factors that are advantageous against other bacteria.

Drug Development Potential

A comprehensive understanding of iron acquisition in Sm, as well as *Enterobacterales*, could contribute to vaccine or drug development inhibiting iron uptake. From a high-level perspective, antibiotics that target iron acquisition have therapeutic potential. With iron being a critical nutrient, blocking bacterial uptake is a novel approach to antibiotic development.

However, targeting iron acquisition is complicated due to the arsenal of redundant uptake systems most bacteria possess. Targeting one system does not necessarily inhibit all iron uptake. However, because most iron transporters, importing both siderophores and heme, are TonB dependent, a universal iron-targeting antibiotic approach would be to inhibit the TonB protein that is responsible for energy transduction needed for proper receptor functionality [177, 178]. Additionally, a therapy that binds consensus sequences of the ferric uptake regulator (Fur) could block transcription of all iron uptake genes, and starve the bacterium of iron. While iron uptake systems are numerous and redundant in most bacteria, making iron uptake a difficult antibiotic or vaccine target, a broader approach to encompass them all may prove effective not just in a single bacterial species but to many that use the same uptake and regulatory mechanisms. For example, gallium compounds can disrupt ferric iron-dependent metabolic pathways and have shown antimicrobial activity against multi-drug resistant bacterial species [179].

A broad vaccine or antibiotic approach is beneficial to treat infections caused by many bacterial species or when pathogen identification cannot be done expediently. However, controlling Sm infections with a targeted therapeutic approach could be explored because of the uniqueness of the Sm iron acquisition systems. The advantage to identifying unique systems within a bacterial species is that these systems can be specifically targeted, leaving the host microbiome intact and avoiding unnecessary damage to the host. Antibiotics that target only particular pathogens also lessens the risk of antibiotic resistance developing among bacterial species. Therefore, identifying unique virulence factors or systems of pathogens could potentially be an approach to slowing the growing prevalence of antibiotic resistance.

Final Thoughts

Sm has been recognized as a significant human pathogen for several decades yet we are only beginning to understand its pathogenesis. Its rapid emergence from environmental pathogen to concerning human infection is clinically alarming and basic research examining virulence and fitness factors is crucial to vaccine or drug development. While studying virulence in humans is critical to understanding pathogenesis, there is an entire subdivision of research studying Sm in an environmental capacity. Not merging these two fields of study, human and environmental pathogenesis, would be a missed opportunity in the field. Studying Sm from an environmental comparator perspective would elucidate how Sm quickly became pathogenic in humans. One study compared a clinical Sm strain to a Sm strain isolated from a fly, and found that the clinical isolate had notably more insertional sequence transposases and integrases, and multidrug transport systems. Differences in virulence factors such as fimbriae, O-antigen, and secretion systems were also described between the clinical and environmental Sm isolates [88]. Continuing to examine environmental strains of Sm versus clinical isolates could provide valuable insights into the evolution of its virulence.

With antibiotic resistance to *beta*-lactams and polymyxins on the rise and outbreaks within hospitals becoming more frequent, Sm has the potential to pose a major threat to public health. Because Sm is a ubiquitous pathogen infecting plants, animals, humans, and residing in environmental reservoirs, this brings a broader, “One Health” perspective to studying Sm. By containing the environmental burden of Sm, this may limit infections and outbreaks in humans and contribute to balancing the other prongs of the One Health initiative that Sm affects.

Ultimately, this research informs the broader field of bacterial pathogenesis and how the virulence of an emerging pathogen fits into this narrative. Following the evolution of Sm from an

environmental bacterium thought to be harmless in mammals to where it is today, an antibiotic resistant and clinically problematic pathogen, we can be more aware of pathogens following a similar trajectory before they become a public health threat. Taking insights gained from this work, applying them to other pathogens and how virulence factors translate to human disease is an initial approach.

Appendix A

Supplemental Material for Chapters II-IV

Table A.1. Up-regulated genes under iron limitation

Gene	Description	Log_2FC	PValue
BVG96_RS11640	Sigma-70 family RNA polymerase sigma factor	8.33	1.92E-06
BVG96_RS07370	TonB-dependent hemin, ferrichrome receptor	7.77	4.92E-06
BVG96_RS14180	S9 family peptidase	7.66	7.94E-06
BVG96_RS21980	TonB-dependent receptor	7.62	6.94E-04
BVG96_RS07375	Hemin uptake protein, HemP	7.47	3.42E-06
BVG96_RS14185	Energy transducer, TonB	7.19	1.98E-05
BVG96_RS12820	TonB-dependent receptor	7.02	1.78E-05
BVG96_RS07365	Hemin transport protein, HmuS	6.88	5.83E-06
BVG96_RS08810	Enterochelin esterase	6.85	9.28E-06
BVG96_RS08805	MbtH family protein	6.74	7.28E-06
BVG96_RS09295	Hypothetical protein	6.66	3.08E-05
BVG96_RS21985	Condensation protein	6.65	5.03E-04
BVG96_RS01530	Hemophore, HasA	6.64	1.72E-04
BVG96_RS15325	Glutaredoxin-like protein, NrdH	6.54	2.55E-06
BVG96_RS07355	Iron ABC transporter permease	6.53	3.77E-06
BVG96_RS21990	Hypothetical protein	6.47	9.56E-04
BVG96_RS14190	Uncharacterized iron-regulated protein	6.42	4.39E-06
BVG96_RS08800	Non-ribosomal peptide synthetase	6.30	3.29E-05
BVG96_RS08815	TonB-dependent siderophore receptor	6.27	2.53E-05
BVG96_RS12825	Iron ABC transporter substrate-binding protein	6.26	3.33E-05
BVG96_RS07360	Hemin ABC transporter substrate-binding protein, HemT	6.25	7.12E-06
BVG96_RS11995	Hypothetical protein	6.21	4.41E-06
BVG96_RS07980	sigma-70 family RNA polymerase sigma factor, FecI	6.15	1.14E-05
BVG96_RS21975	Glutamate racemase	6.04	1.57E-04
BVG96_RS07975	Fec operon regulator, FecR	6.02	6.31E-04
BVG96_RS21970	Amino acid adenylation domain-containing protein	5.95	2.87E-04
BVG96_RS09295	Pyridoxamine 5'-phosphate oxidase	5.94	1.47E-04
BVG96_RS01485	TonB-dependent siderophore receptor	5.87	4.36E-05
BVG96_RS21965	Condensation protein	5.81	2.56E-04

BVG96_RS22005	MbtH family protein, chaperone	5.79	1.83E-05
BVG96_RS11995	Hypothetical protein	5.76	5.54E-06
BVG96_RS05215	Hypothetical protein	5.74	7.20E-05
BVG96_RS14175	TonB-dependent receptor	5.73	2.17E-05
BVG96_RS07350	Heme ABC transporter ATP-binding protein, HemV	5.70	7.36E-06
BVG96_RS11635	Hypothetical protein	5.64	7.64E-06
BVG96_RS22030	Isochorismatase	5.61	5.77E-05
BVG96_RS22025	DHB adenylate synthase-AMP ligase	5.58	8.18E-05
BVG96_RS22035	Hypothetical protein	5.54	1.17E-04
BVG96_RS14005	TonB-dependent siderophore receptor	5.54	5.95E-05
BVG96_RS22000	Enterochelin esterase	5.46	5.44E-05
BVG96_RS22020	Isochorismate synthase	5.32	4.71E-05
BVG96_RS01525	TonB-dependent receptor, HasR	5.25	7.58E-05
BVG96_RS17205	Biopolymer transporter, ExbB	5.08	4.29E-05
BVG96_RS14365	Hypothetical protein	5.03	1.54E-04
BVG96_RS23465	Putative inner membrane protein, hypothetical	4.81	6.33E-05
BVG96_RS01495	Shikimate kinase	4.72	6.57E-05
BVG96_RS22010	Enterobactin synthase subunit F	4.60	2.59E-04
BVG96_RS11645	TonB-dependent receptor	4.50	4.74E-05
BVG96_RS21995	TonB-dependent siderophore receptor	4.41	5.26E-04
BVG96_RS07430	Fe-S cluster assembly scaffold SufA	4.34	4.59E-05

Table A.2. Down-regulated genes under iron-limited conditions

Gene	Description	Log_2FC	PValue
BVG96_RS12895	Cytochrome C	-6.14	5.81E-05
BVG96_RS10870	Nitrate reductase subunit alpha	-5.95	1.23E-04
BVG96_RS12900	Trimethylamine-N-oxide reductase, TorA	-5.81	1.59E-05
BVG96_RS10865	Nitrate reductase subunit beta	-5.46	1.53E-04
BVG96_RS10860	Nitrate reductase molybdenum cofactor assembly chaperone	-5.25	7.09E-05
BVG96_RS12885	Hypothetical protein	-5.02	5.37E-04
BVG96_RS10935	NarK family nitrate/nitrite MFS transporter	-5.01	2.37E-04
BVG96_RS12880	Bifunctional PTS fructose transporter subunit IIA/HPr protein	-4.84	6.02E-04
BVG96_RS12875	1-phosphofructokinase	-4.59	3.33E-04
BVG96_RS22140	Succinate dehydrogenase/fumarate reductase iron-sulfur subunit	-4.55	1.65E-03
BVG96_RS20690	Sugar kinase	-4.45	1.01E-03
BVG96_RS09970	Sugar ABC transporter ATP-binding protein	-4.12	2.89E-04
BVG96_RS09965	Xylulokinase	-3.99	9.39E-04
BVG96_RS13225	2-succinyl-5-enolpyruvyl-6-hydroxy-3- cyclohexene-1-carboxylic-acid synthase	-3.97	9.25E-05
BVG96_RS06310	Non-heme ferritin	-3.96	8.23E-04
BVG96_RS00585	Histidine ammonia-lyase	-3.95	1.51E-03
BVG96_RS00290	3-isopropylmalate dehydratase small subunit	-3.77	3.94E-04
BVG96_RS13220	2-succinyl-6-hydroxy-2,4-cyclohexadiene-1-carboxylate synthase	-3.74	1.22E-04
BVG96_RS07905	Hypothetical protein	-3.70	2.47E-04
BVG96_RS20685	MFS transporter	-3.65	1.86E-04
BVG96_RS13355	Hypothetical protein	-3.64	2.90E-04
BVG96_RS12870	PTS fructose transporter subunit IIBC	-3.64	2.19E-04
BVG96_RS13350	Sugar phosphatase	-3.59	8.90E-05
BVG96_RS04485	Anaerobic C4-dicarboxylate transporter DcuC	-3.58	4.54E-04
BVG96_RS20025	phosphoglycerate mutase	-3.52	5.59E-04
BVG96_RS00580	Amino acid permease	-3.52	1.64E-04
BVG96_RS09690	Glycyl radical enzyme	-3.43	1.11E-03
BVG96_RS05830	Anaerobic C4-dicarboxylate transporter	-3.35	6.30E-04
BVG96_RS13210	o-succinylbenzoate synthase	-3.35	1.63E-04
BVG96_RS09975	ABC transporter permease	-3.22	5.54E-04
BVG96_RS13205	o-succinylbenzoate--CoA ligase	-3.19	1.91E-04
BVG96_RS13215	1,4-dihydroxy-2-naphthoyl-CoA synthase	-3.11	1.04E-03
BVG96_RS00160	Putative membrane protein	-3.04	4.88E-04
BVG96_RS22595	U32 family peptidase	-3.00	5.51E-04

BVG96_RS17660	TIGR01212 family radical SAM protein	-2.93	1.41E-03
BVG96_RS12925	Mannonate dehydratase	-2.88	4.10E-04
BVG96_RS18275	Maltose operon protein MalM	-2.88	7.01E-04
BVG96_RS22725	L-asparaginase	-2.80	1.52E-03
BVG96_RS10930	Undecapreyl-phosphate alpha-N-acetylglucosaminyl 1-phosphate transferase	-2.71	6.42E-04
BVG96_RS07530	Superoxide dismutase [Fe]	-2.71	8.39E-04
BVG96_RS00275	Transcriptional regulator, SgrR	-2.55	1.12E-03
BVG96_RS07910	MerR family transcriptional regulator	-2.48	8.42E-04
BVG96_RS10855	Respiratory nitrate reductase subunit gamma	-2.45	1.02E-03
BVG96_RS16055	Molecular chaperone	-2.31	1.65E-03
BVG96_RS12380	Beta-galactosidase	-2.30	1.45E-03

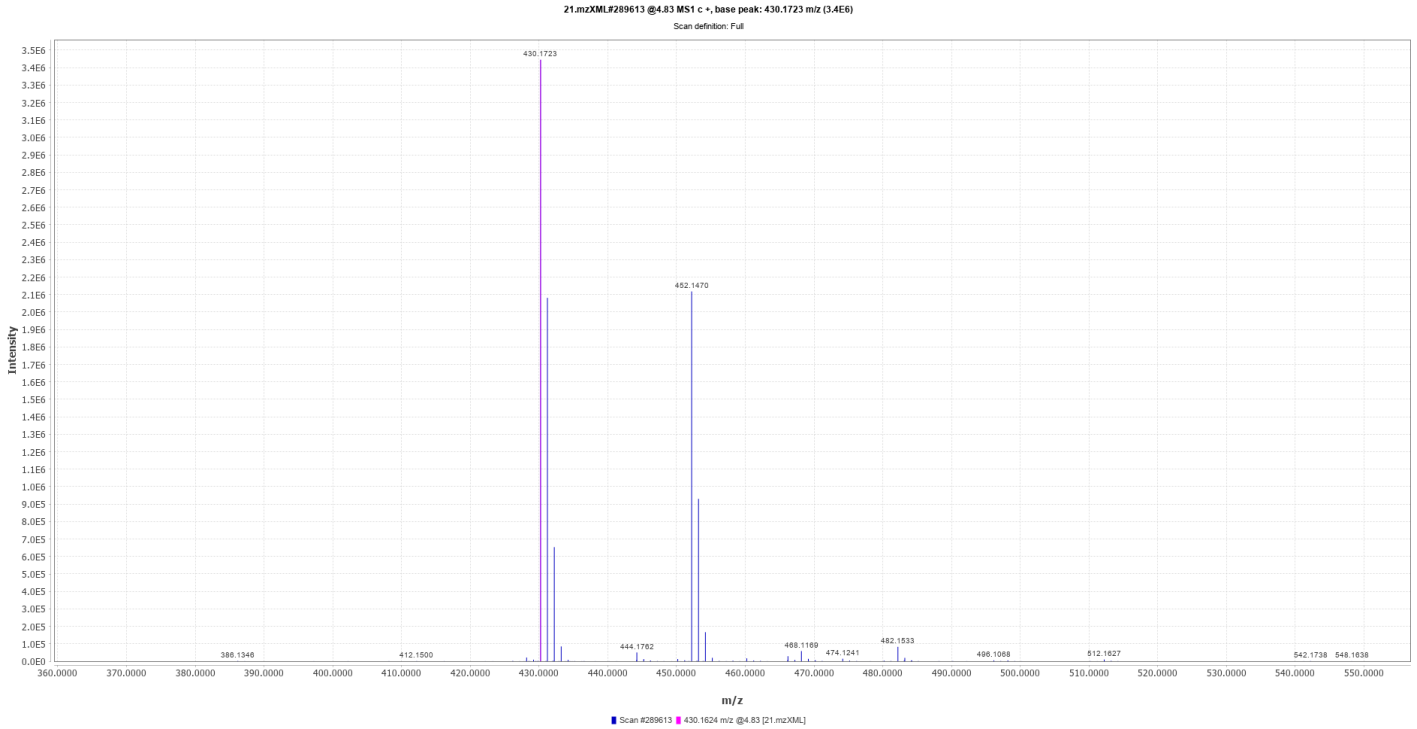

Figure A.1. Detection of serratiochelin A by mass spectrometry.

Spectra of serratiochelin A showed the presence of an $[M+H]^+$ ion at 430.1723 *m/z* and an $[M+Na]^+$ ion at 452.1470 *m/z* with molecular formula of $C_{21}H_{23}N_3O_7$ at a retention time of 4.84 minutes.

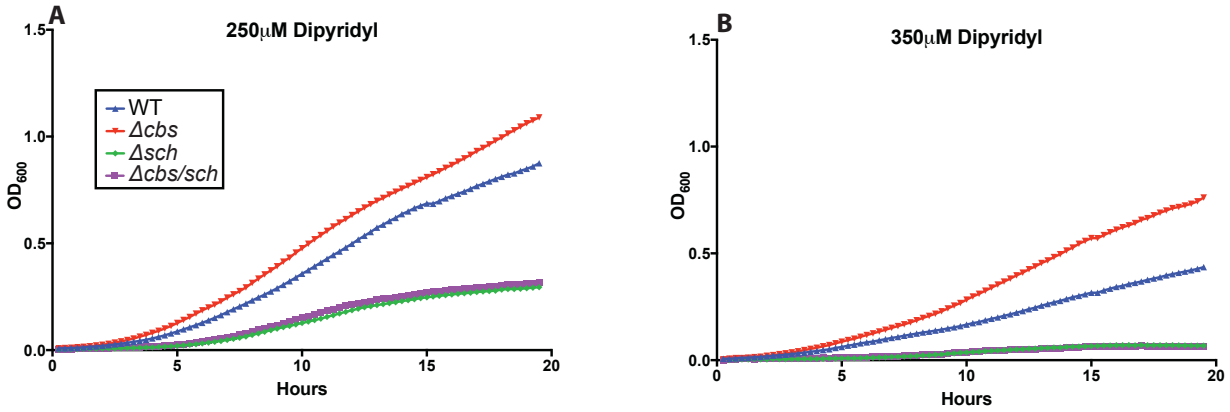

Figure A.2. UMH9 growth under iron-limitation is dependent upon presence of the *sch* locus.

S. marcescens UMH9 wild type, the *cbs* locus mutant (*Δcbs*), the *sch* locus mutant (*Δsch*), and the *cbs/sch* double loci mutant (*Δcbs/sch*) were inoculated into LB medium containing 250 μM (A) or 350 μM (B) dipyridyl after culture overnight in LB with 250 μM dipyridyl. Cultures were incubated with aeration at 37˚C and OD_{600} readings were taken every 15 minutes to measure bacterial growth. The mean of three independent replicates is shown.

Methods and Materials

RNA-seq analysis. RNA-seq analysis was performed by the University of Michigan Bioinformatics Core. Adapter sequences and low-quality ends were trimmed off the reads using Trimmomatic v0.36 [180]. EDGE-pro was used to align reads to the UMH9 reference genome (NCBI Reference Sequence: NZ_CP018923.1) and quantify differential expression [181]. Gene-level read count data were processed using the edgeR package in R for normalization and differential expression testing between the two groups [182]. By requiring a False Discovery Rate (FDR) ≤0.05 and Fold Change (FC) ≥1.5, differentially expressed genes were identified.

Supernatant Preparation for Mass Spectrometry. The supernatants from cultured microbial cells were transferred into vials and dried using Biotage® V10 Touch. The extracts were then brought up in a 1:1 mixture of HPLC grade methanol and milliQ water to achieve a concentration of 1 mg/mL. Each sample was centrifuged for 5 min at full speed and supernatant was transferred to MS vials prior to analysis using UHPLC-MS/MS.

Liquid Chromatography. Samples were analyzed using an Infinity II 1290 UHPLC from Agilent Technologies using Luna 5µ C18(2) 100 Å that was 50 mm in length and 1.0 mm in diameter. We used a flow rate of 0.3 mL/min at 25°C. The analytes were separated using a linear gradient with 0.1% formic acid in water (A) and in methanol (B); 0-1 minute at 30% B, followed by 6 minute gradient from 30-100% B, followed by 1 minute at 95% B and 1 minute of re-equilibration at 30% B.

Mass Spectrometry. The eluent from LC was followed by electrospray ionization (Dual AJS ESI) in positive mode and MS/MS detection on a 6545 quadrupole-time-of-flight (qTOF) mass spectrometer (Agilent Technologies). The ESI source parameters were: end plate offset, 500 V; capillary voltage, 3500 V; nebulizer, 35 psi (nitrogen gas); dry gas, 11.0 L/min; sheath gas temperature of 350°C and dry temperature, 320°C. The ion optics settings included: Oct 1 RF amplitude, 750 Vpp; fragmentor 175 V; skimmer 65 V; in-source collision-induced dissociation (isCID) energy, 30.0 eV and isolation width of 1.3 amu; quadrupole low mass cut-off, 50.0 m/z. Data were acquired both for molecular ions (MS1) and fragment ions (MS2) in data-dependent fragmentation (auto MS/MS). For MS1 acquisition, three spectra were collected per second (3 Hz).

MZmine 2 Data Preprocessing Parameters. The .mzXML data for all the samples were created using MSConvert and the obtained data sets were processed using MZmine 2 version 2.51 [183, 184]. The mass detection was realized using noise level at 10 complete data sets. The collected MS data point was connected to extracted ion chromatogram using the ADAP chromatogram builder with a minimum highest intensity of 2000, and an *m/z* tolerance of 10 ppm [185]. The isobaric peaks were de-convoluted using the chromatogram deconvolution feature of MZmine 2 with minimum peak height of 2000, baseline level of 1000, *m/z* range for MS2 scan pairing at 0.02 Da, and retention time (RT) range for MS2 scan pairing at 0.1 min. Isotopologues were grouped using the isotopic peak grouper algorithm with an *m/z* tolerance of 10 ppm and RT tolerance of 0.1 min. For the grouped data set, a peak alignment step was performed using the join aligner module [*m/z* tolerance of 0.004 (or 10 ppm), weight for *m/z* of 75, weight for RT of 25, and absolute RT tolerance of 0.1 min].

Appendix B

Insights into Citrate as a Chelator in the Absence of Serratiochelin

Summary

Chapter IV elucidated how the *sch* locus is necessary for UMH9 to compete with exogenous chelators such as dipyridyl or to strip iron from host proteins in serum. Results also revealed the significant contribution serratiochelin plays during murine infection. However, growth experiments in iron-depleted M9 minimal medium did not recapitulate the growth defect when the *sch* locus was deleted analogous to what was observed in medium supplemented with dipyridyl (Figure B.1). I hypothesized that an exogenous chelator was needed in the medium to necessitate the use of a siderophore. However, this prompted the hypothesis that another iron uptake system was transporting sufficient iron in M9 minimal medium conditions even when siderophores were deleted. Therefore, qPCR was performed in the full siderophore locus mutants to evaluate the expression of the other iron uptake systems identified by RNA-seq in Chapter II, including: heme uptake systems (*hem* and *has*), ferrous iron uptake systems (*efe* and *sit*), and citrate uptake (*fec*). qPCR revealed notably increased expression of both the *hem* and *fec* uptake systems when *sch* was deleted, but with no exogenous heme added to the culture, citrate transport through the *fec* system was particularly interesting (Figure B.2). I then wondered why the *Δsch* and *Δcbs/sch* mutants displayed no CAS activity in M9 conditions if citrate was able to chelate (Figure 4.2). I made a stock solution of 10% sodium citrate and ran a standard curve of

citrate in the CAS assay to evaluate at what concentration citrate shows CAS activity. Minimal CAS activity was seen at 3.4 mM, whereas bacteria produce nanomolar concentrations of citrate; thus explaining why citrate was undetectable by CAS assay (Table B.1). Citrate is a weak iron chelator; however, when there is no competition for iron, I hypothesize that it can sufficiently transport enough iron for the bacterium. However, during mammalian infection or in a polymicrobial context when iron is bound in host proteins or other siderophores, Sm needs a siderophore with high iron affinity to effectively compete for nutrients. It is possible that citrate plays a larger role in one of Sm environmental niches.

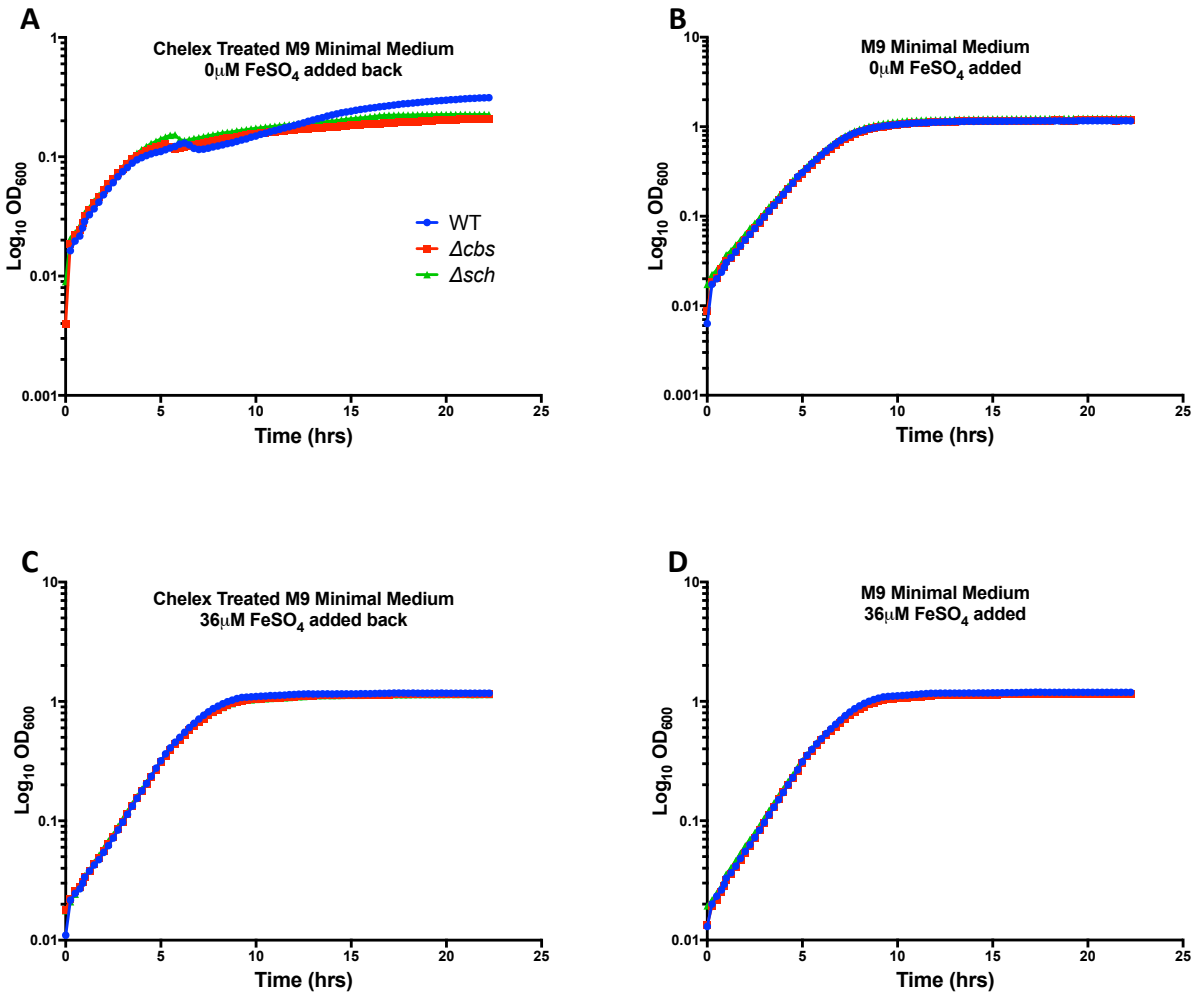

Figure B.1. The *Δcbs* and *Δsch* mutants grow comparably to WT in M9 minimal medium conditions.

The indicated strains were grown in either chelex treated (iron removed) (A, C) or normal M9 minimal medium (B, D). 36μM $FeSO_4$ was added to the cultures where indicated (C, D). Cultures were incubated with aeration at 37˚C and OD_{600} readings were taken every 15 minutes to measure bacterial growth.

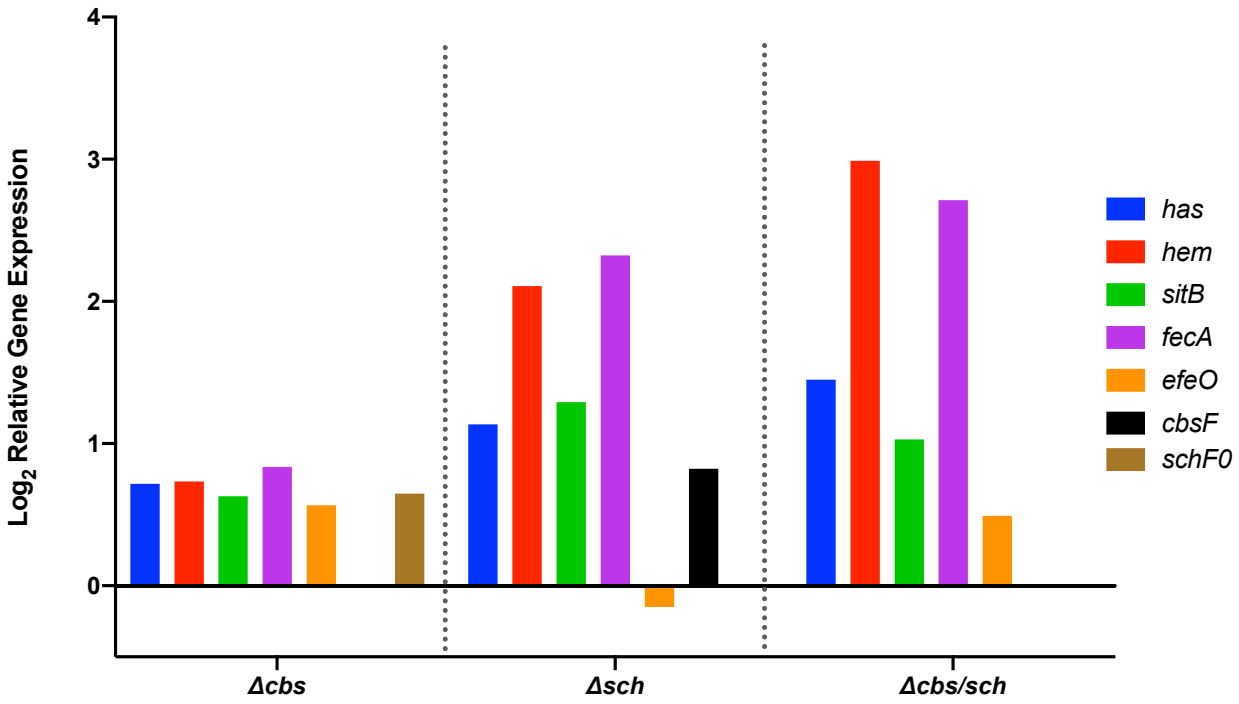

Figure B.2. Citrate transporter, *fecA*, is highly expressed in the absence of the serratiochelin locus, *sch*.

Strains were grown to mid-log phase in M9 minimal medium when RNA was harvested. cDNA was synthesized and qPCR was performed to compare iron system expression when the siderophore loci were deleted. *hem* and *has* represent heme acquisition systems, *sitB* and *efeO* represent ferrous iron uptake systems, *fecA* represents citrate transport. *cbsF* and *schF0* were included as controls. *gyrB* was used as an internal control.

Table B.1. Iron chelation associated with increasing citrate concentration

Citrate Concentration	CAS Activity
340 mM	+
3.4 mM	+/- (minimal activity)
34 μM	-
.34 μM	-
3.4 nM	-

Appendix C

The Role of Siderophores in UPEC Bacteremia

Summary

Uropathogenic *E. coli* (UPEC), the causative bacterium of most urinary tract infections (UTIs), encodes an arsenal of iron acquisition systems to import adequate iron for various cellular processes. Pyelonephritis *E. coli* strain CFT 073 encodes three siderophores (enterobactin, aerobactin, and salmochelin), two heme uptake systems, and 14 outer membrane transporters to bring in iron from these various sources. As such, these systems are redundant in their function, but potentially contribute unequally to UPEC virulence. For example, aerobactin and yersiniabactin mutants were frequently outcompeted in the urinary tract, and heme mutants were commonly outcompeted in the kidneys [19]. The importance of iron acquisition to UPEC has been well established in the context of UTIs with RNAseq experiments depicting significant upregulation of iron genes during active UTI [186]. However, if these UTIs are left untreated, bacteria can breach epithelial barriers in the urinary tract and infection can progress to the bloodstream. Almost 25% of sepsis cases occur from the urogenital tract, leading to mortality rates of 30-40% depending on the causative bacterium [187]. When infection reaches the bloodstream, it is unknown if a particular iron acquisition system is required for or contributes more significantly to establishing the infection.

In these experiments, asymptomatic bacteriuria strain ABU 83972 was used in addition to siderophore mutations made in CFT 073 and *E. coli* 536 to examine all siderophores in a common genetic background. CFT 073 and *E. coli* 536 express three of the four siderophores observed in UPEC strains; asymptomatic bacteriuria strains express all four siderophores although they do lack other UPEC virulence factors such as fimbriae [188]. The four siderophores of interest in this study and that UPEC strains can produce are the catecholate siderophores enterobactin and salmochelin, a hydroxamate aerobactin, and a mixed type siderophore called yersiniabactin. Enterobactin is produced and used by almost all *E. coli* strains; the host protein lipocalin-2 binds this molecule to inactivate it. Salmochelin is a glycosylated form of enterobactin and evades lipocalin-2 binding. Salmochelin, aerobactin, and yersiniabactin are considered stealth siderophores as they are typically found in pathogenic strains of *E. coli*.

Previous literature has described the importance of noncatecholate siderophores to establishing UTIs [19]; however, it is not known if similar or differing siderophores are important once the infection reaches the bloodstream. Therefore, we hypothesized that much like in the urinary tract, specific siderophores have a more significant contribution to bloodstream colonization.

This study used biosynthetic and receptor siderophore mutants in CFT 073, *E. coli* 536, and ABU 83972 in independent and mixed infections to determine if losing specific siderophore systems resulted in bacterial attenuation and/or a competitive disadvantage within the murine bloodstream. Initial experiments competing enterobactin, salmochelin, yersiniabactin, and aerobactin mutants against WT showed that an enterobactin biosynthesis mutant as well as yersiniabactin biosynthesis and receptor mutants had competitive disadvantages in the bloodstream (Figure C.1A, B). This suggests the importance of these siderophores during

infection. However, salmochelin and aerobactin mutants were equally as fit as the WT (Figure C.1C, D).

Because most UPEC strains encode only three of the four siderophore operons, requiring the use of both CFT 073 and *E. coli* 536 to examine all four siderophores, I explored using ABU 83972, a strain that encodes all siderophores, as a proxy for CFT 073 in order to evaluate all siderophores in one genetic background. I began by determining if the ABU strain could colonize the bloodstream to the same extent as CFT 073. Mice were independently challenged with either wild type CFT 073 or wild type ABU 83972. Infections were allowed to progress for one, two, and three days to determine an appropriate time point where CFT and ABU colonization levels were consistent. At one day post infection, the ABU strain colonized the bloodstream comparably to what was seen in the CFT infections in both the spleen and liver. Two days after the infection, bacterial counts between ABU and CFT were more variable and notably lower; however, not significantly different. Finally, after three days of infection, bacterial counts seemed to increase and were consistent between the ABU and CFT strains in both the spleen and liver (Figure C.2). Because bacterial counts were the most consistent between ABU 83972 and CFT 073 after one day, I proceeded with this time point for the following experiment.

ABU 83972 was a suitable proxy to examine the role of all four siderophores in one genetic background because it colonized the bloodstream to the same extent as CFT 073. Therefore, ABU siderophore mutants were acquired from Mark Schembri at the University of Queensland [189]. These strains had mutations in the siderophore biosynthesis machinery and contained single, double, and triple knockouts of the siderophore systems giving every possible combination of siderophore expression. The mutants used are listed in Table C.1. The table also

denotes the functional siderophores still expressed after the mutations were made. In the spleen, the single mutants, including *ΔybtS*, *ΔiroB*, and *ΔentB*, colonized the bloodstream similar to wild type levels with only a small decrease seen in the single *ΔiucABCD* mutant. This suggests potential overlapping roles between the intact siderophores systems. The mutant *ΔiucABCD*/*iroB* which still produces enterobactin and yersiniabactin saw comparable levels of wild type colonization. Interestingly, the mutant that does not make either enterobactin or yersiniabactin, *ΔentB*/*ybtS*, performed the worst in the bloodstream. Mutants that were able to produce only enterobactin or yersiniabactin, *ΔiucaABCD*/*iroB*/*ybtS* and *ΔentB*/*iucABCD*, respectively, had similar bacterial counts to WT. The *ΔiucABCD*/*ybtS* mutant which still produces enterobactin as well as salmochelin along with the *ΔiroB*/*ybtS* mutant which makes enterobacin and aerobactin did struggle slightly in the spleen. Surprisingly, the strain that did not produce any siderophores, *ΔentB*/*iucABCD*/*ybtS*, was able to colonize the bloodstream comparably to WT, potentially suggesting the importance of heme uptake in this model (Figure C.3A).

Similar trends seen in the spleen were also seen in the liver. The single mutants seemed to perform only slightly better than WT in the liver with the *ΔiroB* mutant doing the best. This may further emphasize the potential redundancy of the iron acquisition systems. In general, strains that produce either enterobactin, yersiniabactin, or both, performed as well as WT in the liver. The only mutant that didn't follow this trend was *ΔiucABCD*/*ybtS* which still produces enterobactin, but had only a slight decrease in bacterial counts (Figure C.3B). Taken together, these results generally suggest that yersiniabactin and enterobactin contribute more so to pathogenesis in the bloodstream after one day of infection corroborating our earlier results in CFT073 and *E. coli* 536.

Particular mutants did show decreased colonization one day after infection; however, it is possible that bacteria rely on different siderophores at different points in the infection. Therefore, I looked at bloodstream colonization at 2- and 3-days post infection to determine if the same mutants were consistently showing decreased bacterial counts. The *ΔentB*/*ybtS* mutant had comparable colonization to the wild type on day 2; however, it had significantly decreased bacterial burden on day 3. This result is consistent with the colonization seen with *ΔiucABCD*/*iroB* on day 3, which has intact enterobactin and yersiniabactin. After having decreased colonization on day 2, the *ΔiucABCD*/*iroB* mutant rebounded to wild type levels on day 3, the same time point when the *ΔentB*/*ybtS* mutant severely struggled. This suggests that enterobactin and yersiniabactin together may also play a role later in the infection (Figure C.4A).

In the liver, while the *ΔiucABCD* mutant did not show decreased colonization after one day, it had decreased bacterial burden two and three days after infection, consistent with what is seen in the spleen. The *ΔybtS* mutant had a similar level of colonization to wild type after two days; however, three days after infection, its bacterial burden dropped notably. *ΔentB* had consistently lower bacterial counts in the liver at 2 and 3 days post infection compared to WT while *ΔiroB* had levels comparable to WT. The *ΔiucABCD*/*iroB* and *ΔiroB*/*ybtS* mutants saw mild to moderate reduction in bacterial counts at two- and three-days post infection, which can be attributed to the loss of *ΔiucABCD* and *ΔybtS*, respectively, and not the loss of *ΔiroB* since the individual *ΔiucABCD* and *ΔybtS* single mutants had such notable decreases on their own and *ΔiroB* saw no such decrease alone (Figure C.4B).

Similar to what was seen in the spleen, mutants lacking *ΔentB* and *ΔybtS* had decreased burdens at day three in the liver, further suggesting the importance of enterobactin and

yersiniabactin throughout the infection while aerobactin seems to be important at later time points (2 and 3 days post infection). Salmochelin does not seem to play a significant role. To conclude, mutants having a colonization defect at one time point didn't necessarily have a defect at another time point, suggesting that particular siderophores may be important at different times during infections. Therefore, temporal requirement of individual siderophores may be necessary for bloodstream infection.

Table C.1. Siderophore mutants in ABU 83972[a]

Mutant	Functional Siderophores
WT	E Y S A
ΔiucABCD	E Y S
ΔybtS	E S A
ΔiroB	E Y A
ΔentB	Y A
ΔiucABCD/iroB	E Y
ΔiroB/ybtS	E A
ΔiucABCD/ybtS	E S
ΔiucABCD/iroB/ybtS	E
ΔentB/iucABCD	Y
ΔentB/ybtS	A
ΔentB/iucABCD/ybtS	None

[a]Mutants are single, double, and triple knockouts of the siderophore systems. Functional siderophores are those siderophores still expressed after mutation (E=enterobactin, Y=yersiniabactin, S=salmochelin, A=aerobactin).

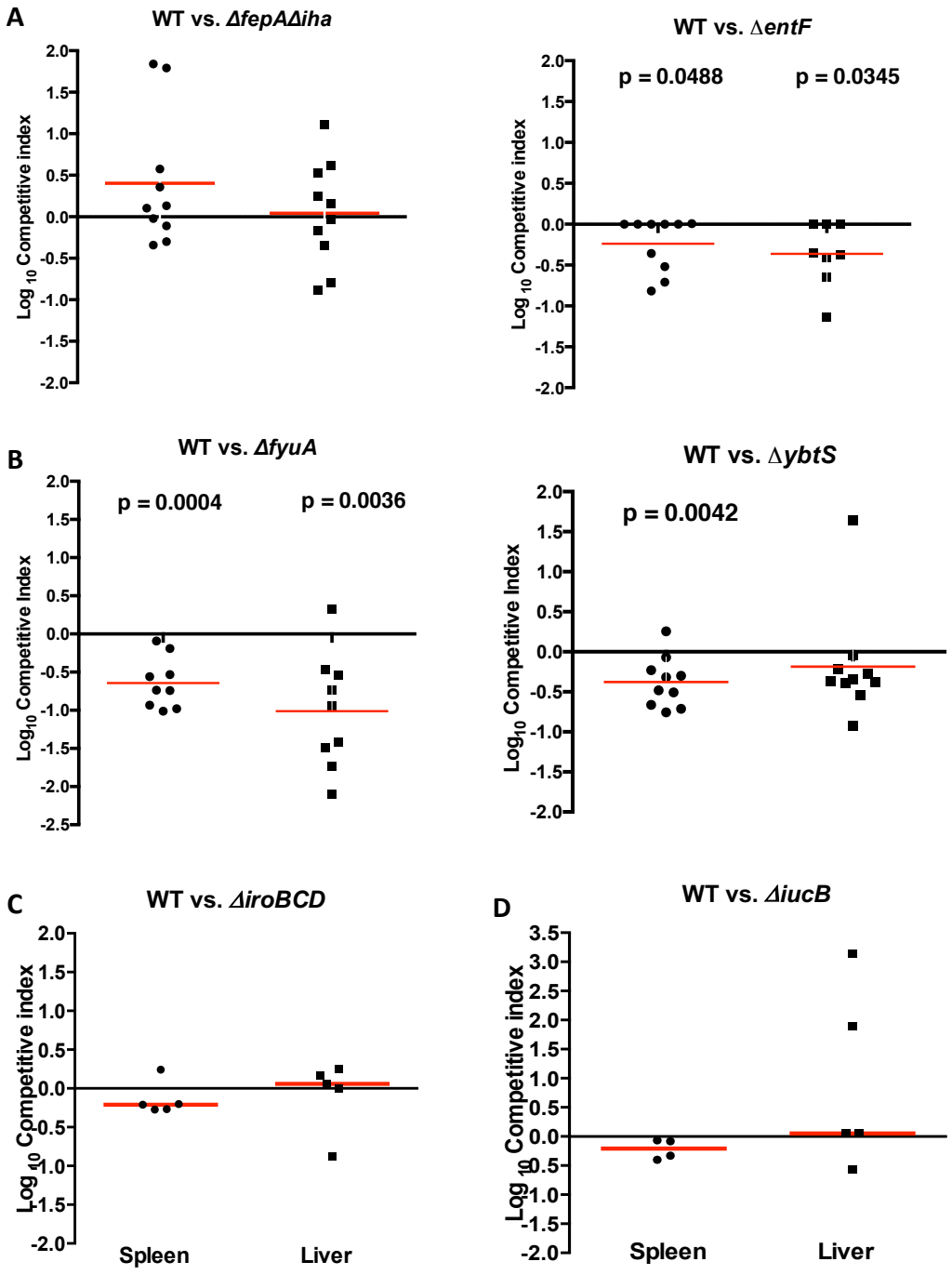

Figure C.1. Enterobactin and yersiniabactin significantly contribute to UPEC bacteremia. CBA/J mice were co-challenged via the tail vein with a 1:1 ratio of WT *E.coli* and the siderophore biosynthesis/receptor mutant. At 24 hours post infection, liver and spleen were collected to enumerate bacteria and then calculate competitive indices.

The solid black line represents a CI of 1.0, meaning the two strains compete equally. Solid red lines represent median CI. Statistics were calculated using the Wilcoxon Signed Rank Test with a theoretical median of 0.

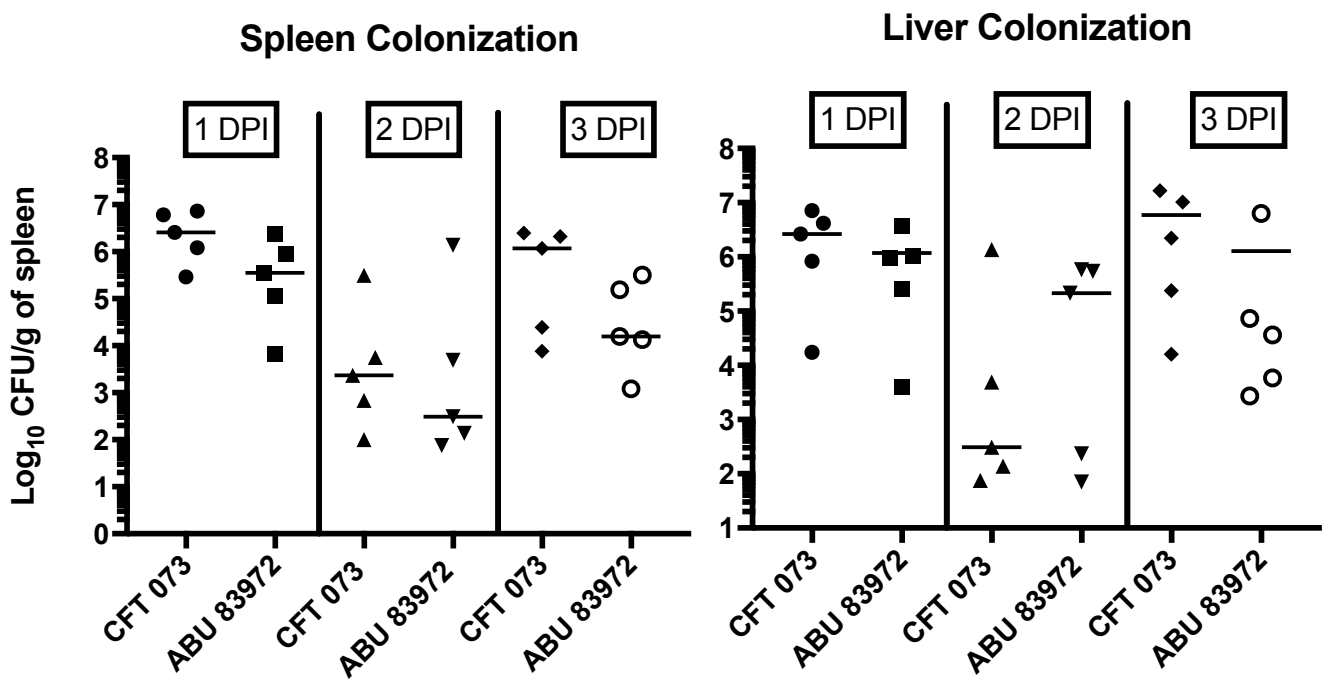

Figure C.2. ABU 83972 colonizes the bloodstream comparably to CFT073.

Mice were challenged independently with either CFT 073 or ABU 83972. After 1, 2, and 3 days post infection spleen and liver were collected. Recovered bacteria were counted to determine the relative bacterial burden at each time point between CFT 073 and ABU 83972.

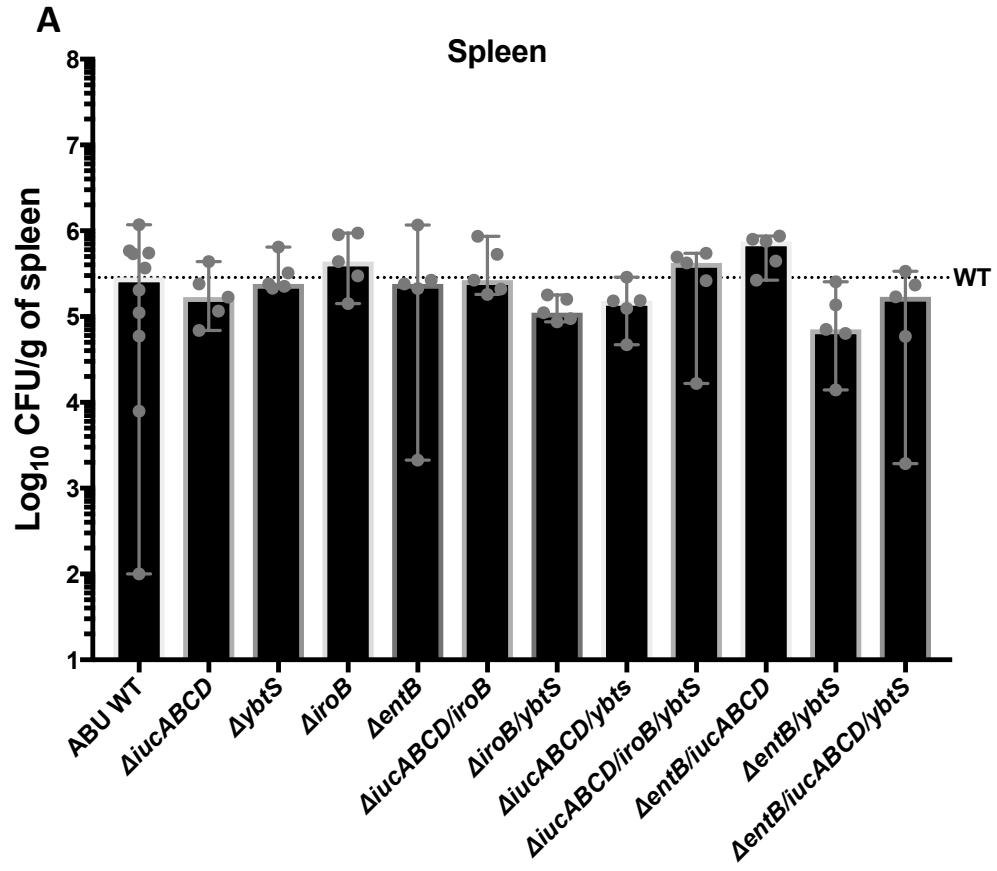
A
Spleen
Log10 CFU/g of spleen
8
7
6
5
4
3
2
1
WT
ABU WT
ΔiucABCD
ΔybtS
ΔiroB
ΔentB
ΔiucABCD/iroB
ΔiroB/ybtS
ΔiucABCD/ybts
ΔiucABCD/iroB/ybtS
ΔentB/iucABCD
ΔentB/ybtS
ΔentB/iucABCD/ybtS

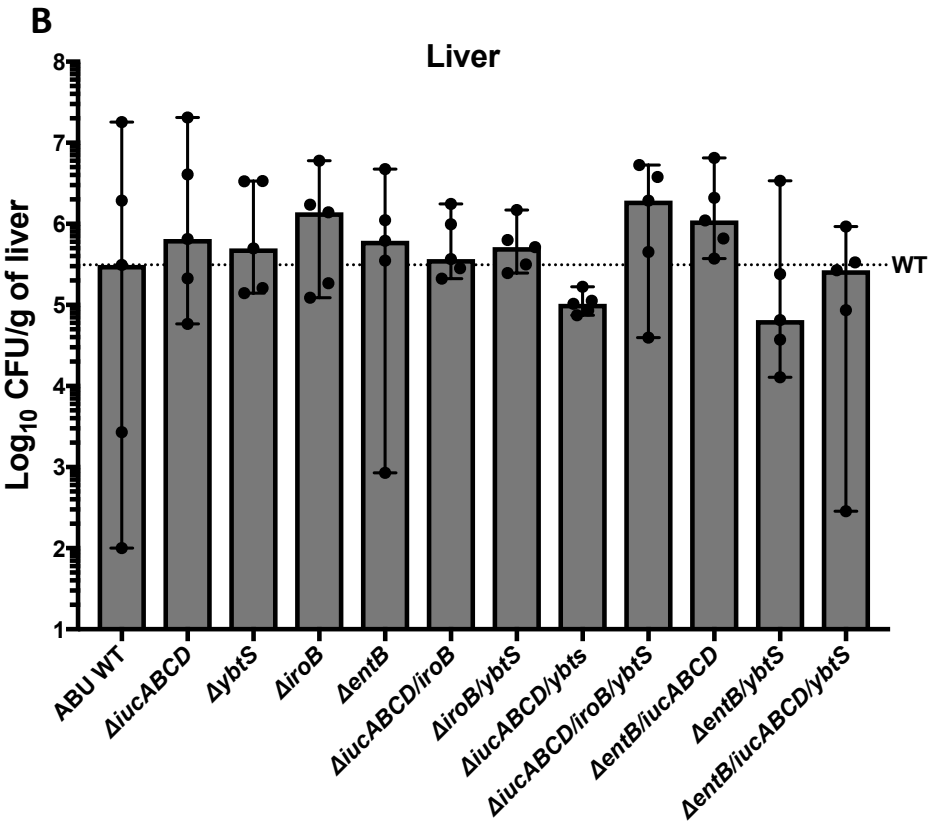
B
Liver
Log10 CFU/g of liver
8
7
6
5
4
3
2
1
WT
ABU WT
ΔiucABCD
ΔybtS
ΔiroB
ΔentB
ΔiucABCD/iroB
ΔiroB/ybtS
ΔiucABCD/ybts
ΔiucABCD/iroB/ybtS
ΔentB/iucABCD
ΔentB/ybtS
ΔentB/iucABCD/ybtS

Figure C.3. Yersiniabactin and various other siderophore mutants have decreased bloodstream colonization compared to wild type 24 hours post infection.

Mice were infected with each listed ABU mutant independently via the tail vein. After 24 hours, spleen and liver were harvested and homogenized. Recovered bacteria were counted to determine bacterial burden.

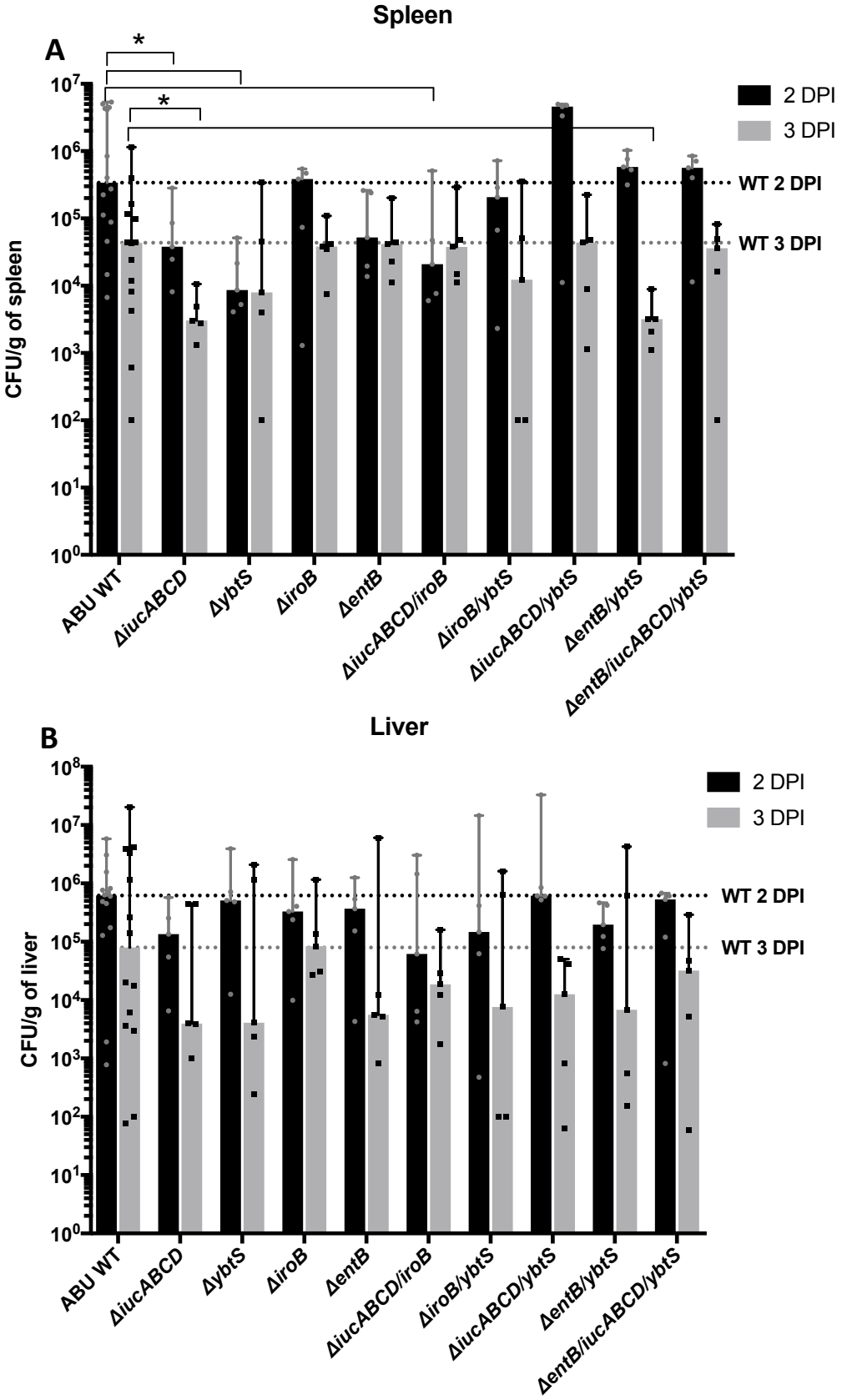
Spleen
A
*
*
2 DPI
3 DPI
WT 2 DPI
WT 3 DPI
CFU/g of spleen
10^0
10^1
10^2
10^3
10^4
10^5
10^6
10^7
ABU WT
ΔiucABCD
ΔybtS
ΔiroB
ΔentB
ΔiucABCD/iroB
ΔiroB/ybtS
ΔiucABCD/ybtS
ΔentB/ybtS
ΔentB/iucABCD/ybtS
Liver
B
2 DPI
3 DPI
WT 2 DPI
WT 3 DPI
CFU/g of liver
10^0
10^1
10^2
10^3
10^4
10^5
10^6
10^7
10^8
ABU WT
ΔiucABCD
ΔybtS
ΔiroB
ΔentB
ΔiucABCD/iroB
ΔiroB/ybtS
ΔiucABCD/ybtS
ΔentB/ybtS
ΔentB/iucABCD/ybtS

Figure C.4. Temporal differences in mutant colonization are seen at two and three days post infection.

Mice were independently challenged with the indicated ABU mutants. Spleen and liver were collected after two- and three-days post infection. Recovered bacteria were plated and enumerated.

References

1. Cassat, J.E. and E.P. Skaar, *Iron in infection and immunity.* Cell Host Microbe, 2013. **13**(5): p. 509-519.
2. Skaar, E.P. and M. Raffatellu, *Metals in infectious diseases and nutritional immunity.* Metallomics, 2015. **7**(6): p. 926-8.
3. Palmer, L.D. and E.P. Skaar, *Transition Metals and Virulence in Bacteria.* Annu Rev Genet, 2016. **50**: p. 67-91.
4. Tolosano, E., et al., *Heme scavenging and the other facets of hemopexin.* Antioxid Redox Signal, 2010. **12**(2): p. 305-20.
5. Richard, K.L., B.R. Kelley, and J.G. Johnson, *Heme Uptake and Utilization by Gram-Negative Bacterial Pathogens.* Front Cell Infect Microbiol, 2019. **9**: p. 81.
6. Troxell, B. and H.M. Hassan, *Transcriptional regulation by Ferric Uptake Regulator (Fur) in pathogenic bacteria.* Front Cell Infect Microbiol, 2013. **3**: p. 59.
7. Saito, T., M.R. Wormald, and R.J. Williams, *Some structural features of the iron-uptake regulation protein.* Eur J Biochem, 1991. **197**(1): p. 29-38.
8. Bagg, A. and J.B. Neilands, *Ferric uptake regulation protein acts as a repressor, employing iron (II) as a cofactor to bind the operator of an iron transport operon in Escherichia coli.* Biochemistry, 1987. **26**(17): p. 5471-7.
9. Hassett, D.J., et al., *Ferric uptake regulator (Fur) mutants of Pseudomonas aeruginosa demonstrate defective siderophore-mediated iron uptake, altered aerobic growth, and decreased superoxide dismutase and catalase activities.* J Bacteriol, 1996. **178**(14): p. 3996-4003.
10. Lam, M.S., et al., *Vibrio cholerae fur mutations associated with loss of repressor activity: implications for the structural-functional relationships of fur.* J Bacteriol, 1994. **176**(16): p. 5108-15.
11. Mey, A.R., et al., *Iron and fur regulation in Vibrio cholerae and the role of fur in virulence.* Infect Immun, 2005. **73**(12): p. 8167-78.
12. Rea, R.B., C.G. Gahan, and C. Hill, *Disruption of putative regulatory loci in Listeria monocytogenes demonstrates a significant role for Fur and PerR in virulence.* Infect Immun, 2004. **72**(2): p. 717-27.
13. Hider, R.C. and X. Kong, *Chemistry and biology of siderophores.* Nat Prod Rep, 2010. **27**(5): p. 637-57.
14. Carl J. Carrano, K.N.R., *Ferric ion sequestering agents. 2. Kinetics and mechanism of iron removal from transferrin by enterobactin and synthetic tricatechols.* J Am Chem Soc, 1979. **101**(18): p. 5401-5404.
15. Sheldon, J.R., H.A. Laakso, and D.E. Heinrichs, *Iron Acquisition Strategies of Bacterial Pathogens.* Microbiol Spectr, 2016. **4**(2).

16. Crosa, J.H. and C.T. Walsh, *Genetics and assembly line enzymology of siderophore biosynthesis in bacteria.* Microbiol Mol Biol Rev, 2002. **66**(2): p. 223-49.
17. Weakland, D.R., et al., *The Serratia marcescens Siderophore Serratiochelin Is Necessary for Full Virulence during Bloodstream Infection.* Infect Immun, 2020. **88**(8).
18. Choby, J.E., J. Howard-Anderson, and D.S. Weiss, *Hypervirulent Klebsiella pneumoniae - clinical and molecular perspectives.* J Intern Med, 2019.
19. Garcia, E.C., A.R. Brumbaugh, and H.L. Mobley, *Redundancy and specificity of Escherichia coli iron acquisition systems during urinary tract infection.* Infect Immun, 2011. **79**(3): p. 1225-35.
20. Mike, L.A., et al., *Siderophore vaccine conjugates protect against uropathogenic Escherichia coli urinary tract infection.* Proc Natl Acad Sci U S A, 2016. **113**(47): p. 13468-13473.
21. Sassone-Corsi, M., et al., *Siderophore-based immunization strategy to inhibit growth of enteric pathogens.* Proc Natl Acad Sci U S A, 2016. **113**(47): p. 13462-13467.
22. Miethke, M. and M.A. Marahiel, *Siderophore-based iron acquisition and pathogen control.* Microbiol Mol Biol Rev, 2007. **71**(3): p. 413-51.
23. Challis, G.L., *A widely distributed bacterial pathway for siderophore biosynthesis independent of nonribosomal peptide synthetases.* Chembiochem, 2005. **6**(4): p. 601-11.
24. Eisenhauer, H.A., et al., *Siderophore transport through Escherichia coli outer membrane receptor FhuA with disulfide-tethered cork and barrel domains.* J Biol Chem, 2005. **280**(34): p. 30574-80.
25. Chakraborty, R., E. Storey, and D. van der Helm, *Molecular mechanism of ferricsiderophore passage through the outer membrane receptor proteins of Escherichia coli.* Biometals, 2007. **20**(3-4): p. 263-74.
26. Pawelek, P.D., et al., *Structure of TonB in complex with FhuA, E. coli outer membrane receptor.* Science, 2006. **312**(5778): p. 1399-402.
27. Letoffe, S., P. Delepelaire, and C. Wandersman, *The housekeeping dipeptide permease is the Escherichia coli heme transporter and functions with two optional peptide binding proteins.* Proc Natl Acad Sci U S A, 2006. **103**(34): p. 12891-6.
28. Goetz, D.H., et al., *The neutrophil lipocalin NGAL is a bacteriostatic agent that interferes with siderophore-mediated iron acquisition.* Mol Cell, 2002. **10**(5): p. 1033-43.
29. Flo, T.H., et al., *Lipocalin 2 mediates an innate immune response to bacterial infection by sequestrating iron.* Nature, 2004. **432**(7019): p. 917-21.
30. Hantke, K., et al., *Salmochelins, siderophores of Salmonella enterica and uropathogenic Escherichia coli strains, are recognized by the outer membrane receptor IroN.* Proc Natl Acad Sci U S A, 2003. **100**(7): p. 3677-82.
31. Spurbeck, R.R., et al., *Escherichia coli isolates that carry vat, fyuA, chuA, and yfcV efficiently colonize the urinary tract.* Infect Immun, 2012. **80**(12): p. 4115-22.
32. Harrison, F., et al., *Optimised chronic infection models demonstrate that siderophore 'cheating' in Pseudomonas aeruginosa is context specific.* ISME J, 2017. **11**(11): p. 2492-2509.
33. Wintrobe, M.M., *The size and hemoglobin content of the erythrocyte. Methods of determination and clinical application. 1932.* J Lab Clin Med, 1990. **115**(3): p. 374-87.
34. Holland, I.B., M.A. Blight, and B. Kenny, *The mechanism of secretion of hemolysin and other polypeptides from gram-negative bacteria.* J Bioenerg Biomembr, 1990. **22**(3): p. 473-91.

35. Pramanik, A., et al., *Secretion and activation of the Serratia marcescens hemolysin by structurally defined ShlB mutants.* Int J Med Microbiol, 2014. **304**(3-4): p. 351-9.
36. Lu, Y., et al., *Uropathogenic Escherichia coli virulence factor hemolysin A causes programmed cell necrosis by altering mitochondrial dynamics.* FASEB J, 2018. **32**(8): p. 4107-4120.
37. Wandersman, C. and I. Stojiljkovic, *Bacterial heme sources: the role of heme, hemoprotein receptors and hemophores.* Curr Opin Microbiol, 2000. **3**(2): p. 215-20.
38. Stojiljkovic, I. and K. Hantke, *Hemin uptake system of Yersinia enterocolitica: similarities with other TonB-dependent systems in gram-negative bacteria.* EMBO J, 1992. **11**(12): p. 4359-67.
39. Stojiljkovic, I., et al., *The Neisseria meningitidis haemoglobin receptor: its role in iron utilization and virulence.* Mol Microbiol, 1995. **15**(3): p. 531-41.
40. Letoffe, S., J.M. Ghigo, and C. Wandersman, *Iron acquisition from heme and hemoglobin by a Serratia marcescens extracellular protein.* Proc Natl Acad Sci U S A, 1994. **91**(21): p. 9876-80.
41. Eakanunkul, S., et al., *Characterization of the periplasmic heme-binding protein shut from the heme uptake system of Shigella dysenteriae.* Biochemistry, 2005. **44**(39): p. 13179-91.
42. Ho, W.W., et al., *Holo- and apo-bound structures of bacterial periplasmic heme-binding proteins.* J Biol Chem, 2007. **282**(49): p. 35796-802.
43. Stover, C.K., et al., *Complete genome sequence of Pseudomonas aeruginosa PAO1, an opportunistic pathogen.* Nature, 2000. **406**(6799): p. 959-64.
44. LaMattina, J.W., D.B. Nix, and W.N. Lanzilotta, *Radical new paradigm for heme degradation in Escherichia coli O157:H7.* Proc Natl Acad Sci U S A, 2016. **113**(43): p. 12138-12143.
45. LaMattina, J.W., et al., *Anaerobic Heme Degradation: ChuY Is an Anaerobilin Reductase That Exhibits Kinetic Cooperativity.* Biochemistry, 2017. **56**(6): p. 845-855.
46. Ratliff, M., et al., *Homologues of neisserial heme oxygenase in gram-negative bacteria: degradation of heme by the product of the pigA gene of Pseudomonas aeruginosa.* J Bacteriol, 2001. **183**(21): p. 6394-403.
47. Laakso, H.A., et al., *A Heme-responsive Regulator Controls Synthesis of Staphyloferrin B in Staphylococcus aureus.* J Biol Chem, 2016. **291**(1): p. 29-40.
48. Verstraete, M.M., et al., *The heme-sensitive regulator SbnI has a bifunctional role in staphyloferrin B production by Staphylococcus aureus.* J Biol Chem, 2019. **294**(30): p. 11622-11636.
49. Hejazi, A. and F.R. Falkiner, *Serratia marcescens.* J Med Microbiol, 1997. **46**(11): p. 903-12.
50. Empel, J., et al., *Molecular survey of beta-lactamases conferring resistance to newer beta-lactams in Enterobacteriaceae isolates from Polish hospitals.* Antimicrob Agents Chemother, 2008. **52**(7): p. 2449-54.
51. Ishikawa, K., et al., *The nationwide study of bacterial pathogens associated with urinary tract infections conducted by the Japanese Society of Chemotherapy.* J Infect Chemother, 2011. **17**(1): p. 126-38.
52. Farmer, J.J., 3rd, et al., *Source of American Serratia.* Lancet, 1977. **2**(8035): p. 459-60.
53. Donowitz, L.G., et al., *Serratia marcescens bacteremia from contaminated pressure transducers.* JAMA, 1979. **242**(16): p. 1749-51.

54. Geiseler, P.J., B. Harris, and B.R. Andersen, *Nosocomial outbreak of nitrate-negative Serratia marcescens infections.* J Clin Microbiol, 1982. **15**(4): p. 728-30.
55. Mutton, K.J., L.M. Brady, and J.L. Harkness, *Serratia cross-infection in an intensive therapy unit.* J Hosp Infect, 1981. **2**(1): p. 85-91.
56. Ringrose, R.E., et al., *A hospital outbreak of Serratia marcescens associated with ultrasonic nebulizers.* Ann Intern Med, 1968. **69**(4): p. 719-29.
57. Rutala, W.A., et al., *Serratia marcescens nosocomial infections of the urinary tract associated with urine measuring containers and urinometers.* Am J Med, 1981. **70**(3): p. 659-63.
58. Sanders, C.V., Jr., et al., *Serratia marcescens infections from inhalation therapy medications: nosocomial outbreak.* Ann Intern Med, 1970. **73**(1): p. 15-21.
59. Traub, W.H., *Continued surveillance of Serratia marcescens infections by bacteriocin typing: investigation of two outbreaks of cross-infection in an intensive care unit.* Appl Microbiol, 1972. **23**(5): p. 982-5.
60. Whitby, J.L., J.N. Blair, and A. Rampling, *Cross-infection with Serratia marcescens in an intensive-therapy unit.* Lancet, 1972. **2**(7768): p. 127-9.
61. Lewis, A.M., et al., *A hospital outbreak of Serratia marcescens in neurosurgical patients.* Epidemiol Infect, 1989. **102**(1): p. 69-74.
62. Esel, D., et al., *Polymicrobial ventriculitis and evaluation of an outbreak in a surgical intensive care unit due to inadequate sterilization.* J Hosp Infect, 2002. **50**(3): p. 170-4.
63. Dorsey, G., et al., *A heterogeneous outbreak of Enterobacter cloacae and Serratia marcescens infections in a surgical intensive care unit.* Infect Control Hosp Epidemiol, 2000. **21**(7): p. 465-9.
64. Stephen, M. and M.K. Lalitha, *An outbreak of Serratia marcescens infection among obstetric patients.* Indian J Med Res, 1993. **97**: p. 202-5.
65. Cohen, A.L., et al., *Outbreak of Serratia marcescens bloodstream and central nervous system infections after interventional pain management procedures.* Clin J Pain, 2008. **24**(5): p. 374-80.
66. Khanna, A., M. Khanna, and A. Aggarwal, *Serratia marcescens- a rare opportunistic nosocomial pathogen and measures to limit its spread in hospitalized patients.* J Clin Diagn Res, 2013. **7**(2): p. 243-6.
67. Aronson, L.C. and S.I. Alderman, *The Occurrence and Bacteriological Characteristics of S. marcescens from a Case of Meningitis.* J Bacteriol, 1943. **46**(3): p. 261-7.
68. Rabinowitz, K. and R. Schiffrin, *A ward-contamination by Serratia marcescens.* Acta Med Orient, 1952. **11**(10): p. 181-4.
69. Gale, D. and A.C. Sonnenwirth, *Frequent human isolation of Serratia marcescens. Bacteriological and pathogenicity studies of twelve strains of S. marcescens recovered from nine patients during a six-month period.* Arch Intern Med, 1962. **109**: p. 414-21.
70. Lancaster, L.J., *Role of Serratia species in urinary tract infections.* Arch Intern Med, 1962. **109**: p. 536-9.
71. Taylor, G. and P.M. Keane, *Cross-infection with Serratia marcescens.* J Clin Pathol, 1962. **15**: p. 145-7.
72. Wheat, R.P., A. Zuckerman, and L.A. Rantz, *Infection due to chromobacteria; report of 11 cases.* AMA Arch Intern Med, 1951. **88**(4): p. 461-6.

73. Bernard, L.A. and W.C. Sutton, *Infection due to chromobacteria. Report of a case of pneumonia due to Chromobacterium prodigiosum successfully treated with kanamycin.* Arch Intern Med, 1960. **105**: p. 311-5.
74. Gurevitch, J. and D. Weber, *A strain of Serratia isolated from urine.* Am J Clin Pathol, 1950. **20**(1): p. 48.
75. Hawe, A.J. and M.H. Hughes, *Bacterial endocarditis due to Chromobacterium prodigiosum; report of a case.* Br Med J, 1954. **1**(4868): p. 968-70.
76. Patterson, R.H., Jr., G.B. Banister, and V. Knight, *Chromobacterial infection in man.* AMA Arch Intern Med, 1952. **90**(1): p. 79-86.
77. Campbell, J.R., T. Diacovo, and C.J. Baker, *Serratia marcescens meningitis in neonates.* Pediatr Infect Dis J, 1992. **11**(10): p. 881-6.
78. Livermore, D.M., T.G. Winstanley, and K.P. Shannon, *Interpretative reading: recognizing the unusual and inferring resistance mechanisms from resistance phenotypes.* J Antimicrob Chemother, 2001. **48 Suppl 1**: p. 87-102.
79. Stock, I., et al., *Natural antimicrobial susceptibilities of strains of 'unusual' Serratia species: S. ficaria, S. fonticola, S. odorifera, S. plymuthica and S. rubidaea.* J Antimicrob Chemother, 2003. **51**(4): p. 865-85.
80. Stock, I., T. Grueger, and B. Wiedemann, *Natural antibiotic susceptibility of strains of Serratia marcescens and the S. liquefaciens complex: S. liquefaciens sensu stricto, S. proteamaculans and S. grimesii.* Int J Antimicrob Agents, 2003. **22**(1): p. 35-47.
81. Champion, H.M., et al., *Cloning and characterization of an AAC(6') gene from Serratia marcescens.* J Antimicrob Chemother, 1988. **22**(5): p. 587-96.
82. Shimizu, K., et al., *Comparison of aminoglycoside resistance patterns in Japan, Formosa, and Korea, Chile, and the United States.* Antimicrob Agents Chemother, 1985. **28**(2): p. 282-8.
83. Yang, Y.J., P.J. Wu, and D.M. Livermore, *Biochemical characterization of a beta-lactamase that hydrolyzes penems and carbapenems from two Serratia marcescens isolates.* Antimicrob Agents Chemother, 1990. **34**(5): p. 755-8.
84. Diekema, D.J., et al., *The Microbiology of Bloodstream Infection: 20-Year Trends from the SENTRY Antimicrobial Surveillance Program.* Antimicrob Agents Chemother, 2019. **63**(7).
85. Control., E.C.f.D.P.a., *Annual Epidemiological Report on Communicable Diseases in Europe 2010.* Stockholm: ECDC; 2010, 2010.
86. Blossom, D., et al., *Multistate outbreak of Serratia marcescens bloodstream infections caused by contamination of prefilled heparin and isotonic sodium chloride solution syringes.* Arch Intern Med, 2009. **169**(18): p. 1705-11.
87. Su, J.R., et al., *Epidemiologic investigation of a 2007 outbreak of Serratia marcescens bloodstream infection in Texas caused by contamination of syringes prefilled with heparin and saline.* Infect Control Hosp Epidemiol, 2009. **30**(6): p. 593-5.
88. Iguchi, A., et al., *Genome evolution and plasticity of Serratia marcescens, an important multidrug-resistant nosocomial pathogen.* Genome Biol Evol, 2014. **6**(8): p. 2096-110.
89. Hertle, R., *Serratia marcescens hemolysin (ShlA) binds artificial membranes and forms pores in a receptor-independent manner.* J Membr Biol, 2002. **189**(1): p. 1-14.
90. Hertle, R., *The family of Serratia type pore forming toxins.* Curr Protein Pept Sci, 2005. **6**(4): p. 313-25.

91. Kurz, C.L., et al., *Virulence factors of the human opportunistic pathogen Serratia marcescens identified by in vivo screening.* EMBO J, 2003. **22**(7): p. 1451-60.
92. Lai, H.C., et al., *The RssAB two-component signal transduction system in Serratia marcescens regulates swarming motility and cell envelope architecture in response to exogenous saturated fatty acids.* J Bacteriol, 2005. **187**(10): p. 3407-14.
93. Lin, C.S., et al., *RssAB-FlhDC-ShlBA as a major pathogenesis pathway in Serratia marcescens.* Infect Immun, 2010. **78**(11): p. 4870-81.
94. Van Houdt, R., M. Givskov, and C.W. Michiels, *Quorum sensing in Serratia.* FEMS Microbiol Rev, 2007. **31**(4): p. 407-24.
95. del Pozo, J.L. and R. Patel, *The challenge of treating biofilm-associated bacterial infections.* Clin Pharmacol Ther, 2007. **82**(2): p. 204-9.
96. Liu, X., et al., *Characterisation of two quorum sensing systems in the endophytic Serratia plymuthica strain G3: differential control of motility and biofilm formation according to life-style.* BMC Microbiol, 2011. **11**(1): p. 26.
97. Shanks, R.M., et al., *A Serratia marcescens OxyR homolog mediates surface attachment and biofilm formation.* J Bacteriol, 2007. **189**(20): p. 7262-72.
98. Anderson, M.T., et al., *Capsule Production and Glucose Metabolism Dictate Fitness during Serratia marcescens Bacteremia.* mBio, 2017. **8**(3).
99. Mahlen, S.D., *Serratia infections: from military experiments to current practice.* Clin Microbiol Rev, 2011. **24**(4): p. 755-91.
100. Holden, V.I., et al., *Klebsiella pneumoniae Siderophores Induce Inflammation, Bacterial Dissemination, and HIF-1alpha Stabilization during Pneumonia.* mBio, 2016. **7**(5).
101. Benevides-Matos, N. and F. Biville, *The Hem and Has haem uptake systems in Serratia marcescens.* Microbiology, 2010. **156**(Pt 6): p. 1749-57.
102. Izadi-Pruneyre, N., et al., *The heme transfer from the soluble HasA hemophore to its membrane-bound receptor HasR is driven by protein-protein interaction from a high to a lower affinity binding site.* J Biol Chem, 2006. **281**(35): p. 25541-50.
103. Ghigo, J.M., S. Letoffe, and C. Wandersman, *A new type of hemophore-dependent heme acquisition system of Serratia marcescens reconstituted in Escherichia coli.* J Bacteriol, 1997. **179**(11): p. 3572-9.
104. Letoffe, S., P. Delepelaire, and C. Wandersman, *Free and hemophore-bound heme acquisitions through the outer membrane receptor HasR have different requirements for the TonB-ExbB-ExbD complex.* J Bacteriol, 2004. **186**(13): p. 4067-74.
105. Carbonell, G.V. and M.C. Vidotto, *Virulence factors in Serratia marcescens: cell-bound hemolysin and aerobactin.* Braz J Med Biol Res, 1992. **25**(1): p. 1-8.
106. Angerer, A., B. Klupp, and V. Braun, *Iron transport systems of Serratia marcescens.* J Bacteriol, 1992. **174**(4): p. 1378-87.
107. Ehlert, G., K. Taraz, and H. Budzikiewicz, *Serratiochelin, a New Catecholate Siderophore from Serratia marcescens*, in *Zeitschrift für Naturforschung C*. 1994. p. 11.
108. Seyedsayamdost, M.R., et al., *Mixing and matching siderophore clusters: structure and biosynthesis of serratiochelins from Serratia sp. V4.* J Am Chem Soc, 2012. **134**(33): p. 13550-3.
109. Rauscher, L., et al., *Chrysobactin-dependent iron acquisition in Erwinia chrysanthemi. Functional study of a homolog of the Escherichia coli ferric enterobactin esterase.* J Biol Chem, 2002. **277**(4): p. 2385-95.

110. Reitz, Z.L., M. Sandy, and A. Butler, *Biosynthetic considerations of triscatechol siderophores framed on serine and threonine macrolactone scaffolds.* Metallomics, 2017. **9**(7): p. 824-839.
111. Saha, R., et al., *Microbial siderophores: a mini review.* J Basic Microbiol, 2013. **53**(4): p. 303-17.
112. Furrer, J.L., et al., *Export of the siderophore enterobactin in Escherichia coli: involvement of a 43 kDa membrane exporter.* Mol Microbiol, 2002. **44**(5): p. 1225-34.
113. Horiyama, T. and K. Nishino, *AcrB, AcrD, and MdtABC multidrug efflux systems are involved in enterobactin export in Escherichia coli.* PLoS One, 2014. **9**(9): p. e108642.
114. Irina Khilyas, T.S., Lilia Matrosova, Alyona Sorokina, Margarita Sharipova, Lydia Bogomolnaya, *Production of Siderophores by Serratia marcescens and the Role of MacAB Efflux Pump in Siderophores Secretion.* BioNanoScience, 2016. **6**: p. 480-482.
115. Lee, J.Y., et al., *Regulation of petrobactin and bacillibactin biosynthesis in Bacillus anthracis under iron and oxygen variation.* PLoS One, 2011. **6**(6): p. e20777.
116. Tindale, A.E., et al., *Dual regulation of catecholate siderophore biosynthesis in Azotobacter vinelandii by iron and oxidative stress.* Microbiology (Reading), 2000. **146 (Pt 7)**: p. 1617-1626.
117. Peralta, D.R., et al., *Enterobactin as Part of the Oxidative Stress Response Repertoire.* PLoS One, 2016. **11**(6): p. e0157799.
118. Wandersman, C. and P. Delepelaire, *Bacterial iron sources: from siderophores to hemophores.* Annu Rev Microbiol, 2004. **58**: p. 611-47.
119. Wagegg, W. and V. Braun, *Ferric citrate transport in Escherichia coli requires outer membrane receptor protein fecA.* J Bacteriol, 1981. **145**(1): p. 156-63.
120. Khilyas, I.V., et al., *Genome Sequence of Pigmented Siderophore-Producing Strain Serratia marcescens SM6.* Microbiol Resour Announc, 2019. **8**(18).
121. Kliman, S., *The Importance of Ferrous Iron in Plants and Soils.* Soil Science Society Proceedings, 1937: p. 385-392.
122. Amari, T., et al., *Implication of citrate, malate and histidine in the accumulation and transport of nickel in Mesembryanthemum crystallinum and Brassica juncea.* Ecotoxicol Environ Saf, 2016. **126**: p. 122-128.
123. Hines, D.A., et al., *Genetic analysis of extracellular proteins of Serratia marcescens.* J Bacteriol, 1988. **170**(9): p. 4141-6.
124. Ratledge, C. and L.G. Dover, *Iron metabolism in pathogenic bacteria.* Annu Rev Microbiol, 2000. **54**: p. 881-941.
125. Institute, I.D. *How Much Iron is in the Body*. How Much Iron is in the Body 2009 02/05/2020 [cited 2020 02/05/2020]; Available from: http://www.irondisorders.org/how-much-iron-is-in-the-body/.
126. Crichton, R.R., *Inorganic biochemistry of iron metabolism: from molecular mechanisms to clinical consequences*. 2001, New York: John Wiley & Sons.
127. Faraldo-Gomez, J.D. and M.S. Sansom, *Acquisition of siderophores in gram-negative bacteria.* Nat Rev Mol Cell Biol, 2003. **4**(2): p. 105-16.
128. Ward, D.M. and J. Kaplan, *Ferroportin-mediated iron transport: expression and regulation.* Biochim Biophys Acta, 2012. **1823**(9): p. 1426-33.
129. Raymond, K.N., E.A. Dertz, and S.S. Kim, *Enterobactin: an archetype for microbial iron transport.* Proc Natl Acad Sci U S A, 2003. **100**(7): p. 3584-8.

130. Letoffe, S., P. Delepelaire, and C. Wandersman, *Functional differences between heme permeases: Serratia marcescens HemTUV permease exhibits a narrower substrate specificity (restricted to heme) than the Escherichia coli DppABCDF peptide-heme permease.* J Bacteriol, 2008. **190**(6): p. 1866-70.
131. Miller, J.H., *Experiments in molecular genetics*. 1972: Cold Spring Harbor Laboratory. 466.
132. Lautru, S. and G.L. Challis, *Substrate recognition by nonribosomal peptide synthetase multi-enzymes.* Microbiology (Reading), 2004. **150**(Pt 6): p. 1629-1636.
133. Weber, G., et al., *The peptide synthetase catalyzing cyclosporine production in Tolypocladium niveum is encoded by a giant 45.8-kilobase open reading frame.* Curr Genet, 1994. **26**(2): p. 120-5.
134. Wiest, A., et al., *Identification of peptaibols from Trichoderma virens and cloning of a peptaibol synthetase.* J Biol Chem, 2002. **277**(23): p. 20862-8.
135. Wang, M., et al., *Sharing and community curation of mass spectrometry data with Global Natural Products Social Molecular Networking.* Nat Biotechnol, 2016. **34**(8): p. 828-837.
136. Mohimani, H., et al., *Dereplication of microbial metabolites through database search of mass spectra.* Nat Commun, 2018. **9**(1): p. 4035.
137. Smith, S.N., et al., *Dissemination and systemic colonization of uropathogenic Escherichia coli in a murine model of bacteremia.* mBio, 2010. **1**(5).
138. Hantash, F.M. and C.F. Earhart, *Membrane association of the Escherichia coli enterobactin synthase proteins EntB/G, EntE, and EntF.* J Bacteriol, 2000. **182**(6): p. 1768-73.
139. Datsenko, K.A. and B.L. Wanner, *One-step inactivation of chromosomal genes in Escherichia coli K-12 using PCR products.* Proc Natl Acad Sci U S A, 2000. **97**(12): p. 6640-5.
140. Datta, S., N. Costantino, and D.L. Court, *A set of recombineering plasmids for gram-negative bacteria.* Gene, 2006. **379**: p. 109-15.
141. Schwyn, B. and J.B. Neilands, *Universal chemical assay for the detection and determination of siderophores.* Anal Biochem, 1987. **160**(1): p. 47-56.
142. Celine Herra, F.F., *Serratia marcescens*, in *antimicrobe*.
143. Koshland, F.H.D.E., *Protein*, in *Encyclopaedia Britannica*. Encyclopaedia Britannica, Inc.
144. Moradigaravand, D., et al., *Recent independent emergence of multiple multidrug-resistant Serratia marcescens clones within the United Kingdom and Ireland.* Genome Res, 2016. **26**(8): p. 1101-9.
145. Wattam, A.R., et al., *Improvements to PATRIC, the all-bacterial Bioinformatics Database and Analysis Resource Center.* Nucleic Acids Res, 2017. **45**(D1): p. D535-D542.
146. Bullen JJ, G.E., *Iron and infection: molecular, physiological, and clinical aspects*. 1999, New York: John Wiley and Sons.
147. Parrow, N.L., R.E. Fleming, and M.F. Minnick, *Sequestration and scavenging of iron in infection.* Infect Immun, 2013. **81**(10): p. 3503-14.
148. Thomason, L.C., et al., *Recombineering: genetic engineering in bacteria using homologous recombination.* Curr Protoc Mol Biol, 2014. **106**: p. 1 16 1-39.
149. White, D.C. and S. Granick, *Hemin Biosynthesis in Haemophilus.* J Bacteriol, 1963. **85**: p. 842-50.

150. Panek, H. and M.R. O'Brian, *A whole genome view of prokaryotic haem biosynthesis.* Microbiology (Reading), 2002. **148**(Pt 8): p. 2273-2282.
151. Morton, D.J., et al., *The heme-binding protein (HbpA) of Haemophilus influenzae as a virulence determinant.* Int J Med Microbiol, 2009. **299**(7): p. 479-88.
152. Lyles, K.V. and Z. Eichenbaum, *From Host Heme To Iron: The Expanding Spectrum of Heme Degrading Enzymes Used by Pathogenic Bacteria.* Front Cell Infect Microbiol, 2018. **8**: p. 198.
153. Schneider, S., et al., *An induced fit conformational change underlies the binding mechanism of the heme transport proteobacteria-protein HemS.* J Biol Chem, 2006. **281**(43): p. 32606-10.
154. Letoffe, S., J.M. Ghigo, and C. Wandersman, *Secretion of the Serratia marcescens HasA protein by an ABC transporter.* J Bacteriol, 1994. **176**(17): p. 5372-7.
155. Letoffe, S., et al., *Interactions of HasA, a bacterial haemophore, with haemoglobin and with its outer membrane receptor HasR.* Mol Microbiol, 1999. **33**(3): p. 546-55.
156. Letoffe, S., et al., *Activities of the Serratia marcescens heme receptor HasR and isolated plug and beta-barrel domains: the beta-barrel forms a heme-specific channel.* J Bacteriol, 2005. **187**(13): p. 4637-45.
157. Biville, F., et al., *Haemophore-mediated signalling in Serratia marcescens: a new mode of regulation for an extra cytoplasmic function (ECF) sigma factor involved in haem acquisition.* Mol Microbiol, 2004. **53**(4): p. 1267-77.
158. Choby, J.E. and E.P. Skaar, *Heme Synthesis and Acquisition in Bacterial Pathogens.* J Mol Biol, 2016. **428**(17): p. 3408-28.
159. Andrews, S.C., P.M. Harrison, and J.R. Guest, *Cloning, sequencing, and mapping of the bacterioferritin gene (bfr) of Escherichia coli K-12.* J Bacteriol, 1989. **171**(7): p. 3940-7.
160. Yao, H., et al., *The structure of the BfrB-Bfd complex reveals protein-protein interactions enabling iron release from bacterioferritin.* J Am Chem Soc, 2012. **134**(32): p. 13470-81.
161. Wang, Y., et al., *Characterization of the Bacterioferritin/Bacterioferritin Associated Ferredoxin Protein-Protein Interaction in Solution and Determination of Binding Energy Hot Spots.* Biochemistry, 2015. **54**(40): p. 6162-75.
162. Aich, A., M. Freundlich, and P.G. Vekilov, *The free heme concentration in healthy human erythrocytes.* Blood Cells Mol Dis, 2015. **55**(4): p. 402-9.
163. Chenault, S.S. and C.F. Earhart, *Organization of genes encoding membrane proteins of the Escherichia coli ferrienterobactin permease.* Mol Microbiol, 1991. **5**(6): p. 1405-13.
164. Grass, G., *Iron transport in Escherichia coli: all has not been said and done.* Biometals, 2006. **19**(2): p. 159-72.
165. Holt, K.E., et al., *Diversity and evolution of surface polysaccharide synthesis loci in Enterobacteriales.* ISME J, 2020. **14**(7): p. 1713-1730.
166. Nir, U., et al., *In vivo effects of porphyrins on bacterial DNA.* J Photochem Photobiol B, 1991. **11**(3-4): p. 295-306.
167. Lin, H. and J. Everse, *The cytotoxic activity of hematoheme: evidence for two different mechanisms.* Anal Biochem, 1987. **161**(2): p. 323-31.
168. Bozja, J., et al., *Porphyrin-based compounds exert antibacterial action against the sexually transmitted pathogens Neisseria gonorrhoeae and Haemophilus ducreyi.* Int J Antimicrob Agents, 2004. **24**(6): p. 578-84.

169. Fernandez, A., et al., *Two coregulated efflux transporters modulate intracellular heme and protoporphyrin IX availability in Streptococcus agalactiae.* PLoS Pathog, 2010. **6**(4): p. e1000860.
170. Hagman, K.E., et al., *Resistance of Neisseria gonorrhoeae to antimicrobial hydrophobic agents is modulated by the mtrRCDE efflux system.* Microbiology (Reading), 1995. **141 (Pt 3)**: p. 611-22.
171. Fitch, C.D., *Involvement of heme in the antimalarial action of chloroquine.* Trans Am Clin Climatol Assoc, 1998. **109**: p. 97-105; discussion 105-6.
172. Olliaro, P.L. and D.E. Goldberg, *The plasmodium digestive vacuole: metabolic headquarters and choice drug target.* Parasitol Today, 1995. **11**(8): p. 294-7.
173. Stojiljkovic, I. and K. Hantke, *Transport of haemin across the cytoplasmic membrane through a haemin-specific periplasmic binding-protein-dependent transport system in Yersinia enterocolitica.* Mol Microbiol, 1994. **13**(4): p. 719-32.
174. Suits, M.D., et al., *Identification of an Escherichia coli O157:H7 heme oxygenase with tandem functional repeats.* Proc Natl Acad Sci U S A, 2005. **102**(47): p. 16955-60.
175. Thompson, J.M., H.A. Jones, and R.D. Perry, *Molecular characterization of the hemin uptake locus (hmu) from Yersinia pestis and analysis of hmu mutants for hemin and hemoprotein utilization.* Infect Immun, 1999. **67**(8): p. 3879-92.
176. Shih, H.I., et al., *Serratia marcescens bacteremia at a medical center in southern Taiwan: high prevalence of cefotaxime resistance.* J Microbiol Immunol Infect, 2005. **38**(5): p. 350-7.
177. Hanson, M., et al., *High-Throughput Screening Assay for Inhibitors of TonB-Dependent Iron Transport.* J Biomol Screen, 2016. **21**(3): p. 316-22.
178. Yep, A., et al., *Inhibitors of TonB function identified by a high-throughput screen for inhibitors of iron acquisition in uropathogenic Escherichia coli CFT073.* mBio, 2014. **5**(2): p. e01089-13.
179. Hijazi, S., et al., *Antimicrobial Activity of Gallium Compounds on ESKAPE Pathogens.* Front Cell Infect Microbiol, 2018. **8**: p. 316.
180. Bolger, A.M., M. Lohse, and B. Usadel, *Trimmomatic: a flexible trimmer for Illumina sequence data.* Bioinformatics, 2014. **30**(15): p. 2114-20.
181. Magoc, T., D. Wood, and S.L. Salzberg, *EDGE-pro: Estimated Degree of Gene Expression in Prokaryotic Genomes.* Evol Bioinform Online, 2013. **9**: p. 127-36.
182. Robinson, M.D., D.J. McCarthy, and G.K. Smyth, *edgeR: a Bioconductor package for differential expression analysis of digital gene expression data.* Bioinformatics, 2010. **26**(1): p. 139-40.
183. Adusumilli, R. and P. Mallick, *Data Conversion with ProteoWizard msConvert.* Methods Mol Biol, 2017. **1550**: p. 339-368.
184. Olivon, F., et al., *MZmine 2 Data-Preprocessing To Enhance Molecular Networking Reliability.* Anal Chem, 2017. **89**(15): p. 7836-7840.
185. Myers, O.D., et al., *One Step Forward for Reducing False Positive and False Negative Compound Identifications from Mass Spectrometry Metabolomics Data: New Algorithms for Constructing Extracted Ion Chromatograms and Detecting Chromatographic Peaks.* Anal Chem, 2017. **89**(17): p. 8696-8703.
186. Brumbaugh, A.R., et al., *Blocking yersiniabactin import attenuates extraintestinal pathogenic Escherichia coli in cystitis and pyelonephritis and represents a novel target to prevent urinary tract infection.* Infect Immun, 2015. **83**(4): p. 1443-50.

187. Porat, A., B.S. Bhutta, and S. Kesler, *Urosepsis*, in *StatPearls*. 2020: Treasure Island (FL).
188. Roos, V., et al., *The asymptomatic bacteriuria Escherichia coli strain 83972 outcompetes uropathogenic E. coli strains in human urine.* Infect Immun, 2006. **74**(1): p. 615-24.
189. Watts, R.E., et al., *Contribution of siderophore systems to growth and urinary tract colonization of asymptomatic bacteriuria Escherichia coli.* Infect Immun, 2012. **80**(1): p. 333-44.